

Republic of Iraq
Ministry of Higher Education
And Scientific Research
University of Baghdad
College of Education of pure science Ibn Al-
Haitham
Department of Physics



Preparation of Barium Titante ($BaTiO_3$) Nano-Composites and Studying its some structural and dielectrical properties for it

By

Hala Hussein Ali Qasseim

(B.S physics 2012)

To the Department of Physics College of Education
(Ibn Al-Haitham) University of Baghdad as a Partial
Fulfillment of the Requirements for the Degree of
Master of Science in (Physics)

Supervised By

Ass.Prof.

Dr. Farouq Ibrahim Hussain

2017 AD

1439 AH

بِسْمِ اللَّهِ الرَّحْمَنِ الرَّحِيمِ

((وقل رب أدخل
صدق وأخرجني مخرج
صدق و اجعل لي من لدنك
سلطانا نصيرا))

صدق الله العظيم

Dedication

To My

Parents with my great love,

Brother and sister with my respect,

Dr. Shatha with respect, great love

and thankfulness.

Hala

Supervisor's certification

We certify that this thesis was prepared under my supervision at the University of Baghdad\College of Education for Pure Science (Ibn-AL Haitham) , Department of physics in partial fulfillment of the requirements for the degree of Philosophy Master of Science in physics.

Signature:



Name: Dr. Farouq Ibrahim Hussain

Title: Asst .Prof.

The Council of the Department of physics has approved the examining committee.

Signature:



Name: Dr. Kareem Ail Jasim

PDF Reducer Demo

Titel: Prof

Department of physics

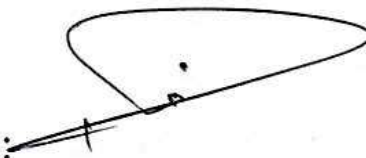
College of Education for Pure(Ibn-AL-Haitham),

University of Baghdad

Date:23/1/2017

Examining Committee Certification

certify that we have read this thesis entitled : " **Preparation of Barium Titante (TiO₃) Nano-Composites and Studying its some structural and dielectrical properties for it** " an examining committee , examined the student " **Hala Hussein** " in its content and what standing as a thesis for the degree Doctor of Philosophy of science in physics .

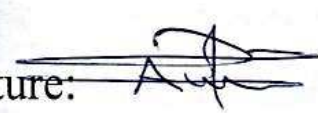
Singnature: 

Name: Dr. Khalid Hilal Harbi

Title: Professor

Date:

(Chairman)

Singnature: 

Namr: Dr. Anwar Hussein Ali

Title: Assistant Professor

Date:

(Member)

Singnature: 

Name: Dr. May Abdul Sattar Mohammed

Title: Lecturer

Date:

(Member)

Singnature: 

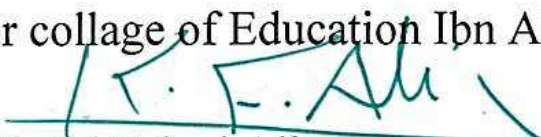
Name: Dr. Farouq Ibrahim Hussain

Title: Assistant Professor

Date: 29 / 10 / 2017

(Member, Supervisor)

proved for collage of Education Ibn Al-Haitham

gnature: 

me: Dr. Khalid Fahad Ali

le: Professor

te:

Acknowledgments

At first, I thank my God for helping me to complete this thesis. Then, I would like to express my sincere appreciation and deep gratitude to Ministry of Higher Education & Scientific Research /Research & Development Directorate / Pioneer Projects Department for providing the facilities and devices necessary for this work.

I'm grateful to the University of Baghdad, College of Education for Pure Science (Ibn-AL-Haitham), and to the Department of Physics.

I offer my deep gratitude to my family for their patience throughout this work.

Last, I would like to express my sincere appreciation and deep gratitude to my supervisors for their suggestion of the topic of this thesis (especially Dr.Shatha and Dr.Oday for helping and encouraging me throughout all the stages of this work) .

Abstract

In this work we prepared Barium titanate (BaTiO_3) hexacariumferrite, ($\text{Ba Fe}_{12} \text{O}_{19}$) and ($\text{Ni}_{0.7} \text{Zn}_{0.3} \text{Fe}_2 \text{O}_4$) soft-ferrite Nano-particles by using sol-gel auto combustion method. X-ray diffraction (XRD) studying for the above compound was done in order to obtain the structural and lattice parameters, crystallite size using scheirer equation and the x-ray density. In order to improve the electrical properties for (BT- $\text{BaFe}_{12}\text{O}_{19}$) with wt % of (80% BT20%BFO, 70%BT 30%BFO and 50%BT 50%BFO) and BT - $\text{Ni}_{0.7} \text{Zn}_{0.3} \text{Fe}_2 \text{O}_4$ with wt%(80%BT 20%NZF, 70%BT 30%NZF and 50%BT 50%NZF). A.C electrical properties were studied using LCR-meter.

Morphology studied for barium titanate, bariumhexu ferrite and soft – ferrite using (SEM, EDX and AFM) tests which showed that the compounds were in Nano-range with (20nm)-(30nm). In the present work we showed that the weight % of (50 %BT, 50% BFO) and (50% BT and 50% NZF) ferrite composite of best electrical properties then the other prepared composites.

As well as examine the (breakdown voltages), where the examination result shows durability of the insulation decreases with additions, compared with BaTiO_3 .

Content

<i>Title</i>	<i>Page</i>
<i>Chapter One(Introduction)</i>	
<i>1.1 Introduction</i>	<i>1</i>
<i>1.2 Ferro-electricity</i>	<i>1</i>
<i>1.3 Polarization</i>	<i>2</i>
<i>1.4 literature survey</i>	<i>2</i>
<i>1.5 The aim of work</i>	<i>7</i>
<i>Chapter two(Theoretical part)</i>	
<i>2.1 Dielectrics Materials</i>	<i>8</i>
<i>2.2 The principal conditions in insulators</i>	<i>9</i>
<i>2.3 Classification of Dielectric</i>	<i>9</i>
<i>2.4 Dielectric Strength</i>	<i>10</i>
<i>2.5 Polarization</i>	<i>11</i>
<i>2.5.1 Types of Polarization</i>	<i>13</i>
<i>2.5.1.1 Electronic polarization</i>	<i>13</i>
<i>2.5.1.2 Ionic polarization</i>	<i>13</i>
<i>2.5.1.3 Orientational polarization</i>	<i>14</i>

<i>2.5.1.4 Space charge or interfacial polarization</i>	<i>16</i>
<i>2.6 Electric properties study</i>	<i>17</i>
<i>2.7 Technology of Powder X-ray diffraction (XRD)</i>	<i>17</i>
<i>2.7.1 Structural parameters</i>	<i>19</i>
<i>2.7.1.1 Lattice parameters</i>	<i>19</i>
<i>2.7.1.2 ($\rho_{X\text{-ray}}$) Theoretical density</i>	<i>20</i>
<i>2.7.1.3 Grain size</i>	<i>20</i>
<i>2.8 Photovoltaic materials in general</i>	<i>21</i>
<i>2.9 BaTiO₃ BT</i>	<i>21</i>
<i>2.10 Formation of BT is from Perovskite group</i>	<i>21</i>
<i>2.10.1 Barium Titanate Structure (perovskite arrangement)</i>	<i>22</i>
<i>2.11 Structural transformations of barium titanate</i>	<i>23</i>
<i>2.12 Barium titanate synthesis methods</i>	<i>25</i>
<i>2.12.1 Conventional solid-state reaction</i>	<i>25</i>
<i>2.12.2 Chemical methods for barium titanate (BT) synthesis</i>	<i>26</i>
<i>2.12.2.1 Sol-Gel method</i>	<i>26</i>
<i>2.12.2.2 Hydrothermal Technique</i>	<i>26</i>
<i>2.12.2.3 Co-precipitation method</i>	<i>27</i>
<i>2.12.2.4 Polymeric precursor method</i>	<i>27</i>
<i>2.13 Properties of BaTiO₃</i>	<i>27</i>

<i>2.13.1 Electrical properties of (BaTiO₃)</i>	<i>27</i>
<i>2.13.2 Dielectric properties of (BaTiO₃)</i>	<i>29</i>
<i>2.13.3 The piezo-electric properties of (BaTiO₃)</i>	<i>29</i>
<i>2.14 Composite materials</i>	<i>30</i>
<i>2.15 Nano-materials</i>	<i>30</i>
<i>2.16 Ferrite materials (Ni_{0.7} Zn_{0.3}Fe₂O₄, Ba Fe₁₂O₁₉)</i>	<i>31</i>
<i>Chapter three (Experimental part)</i>	
<i>3.1 Introductions</i>	<i>34</i>
<i>3.2 Raw materials of prepared of BaTiO₃, BaFe₁₂O₁₉ and Ni_{0.7}Zn_{0.3}Fe₂O₄</i>	<i>34</i>
<i>3.3 Instrument</i>	<i>35</i>
<i>3.4 How to prepare</i>	<i>38</i>
<i>3.5 Prepare of (Ni_{0.7} Zn_{0.3} Fe₂O₄) ferrite</i>	<i>40</i>
<i>3.6 Prepare of (Ba Fe₁₂O₁₉) ferret</i>	<i>40</i>
<i>3.7 Prepare of (Ba TiO₃) ferret</i>	<i>41</i>
<i>3.8 Samples forming</i>	<i>41</i>
<i>3.9 Sintering process</i>	<i>42</i>
<i>3.10 Structure test</i>	<i>43</i>
<i>3.10.1 X-ray diffraction measurement</i>	<i>43</i>

<i>3.10.2 Scanning electron microscope measurement (SEM)</i>	<i>44</i>
<i>3.10.3 Energy – dispersive X-ray spectroscopy (EDX)</i>	<i>45</i>
<i>3.11 The electronic properties measurement</i>	<i>46</i>
<i>3.12 Measuring the Dielectric Strength</i>	<i>47</i>
<i>Chapter Four(Results and Discussions)</i>	
<i>4.1 Introduction</i>	<i>49</i>
<i>4.2 The properties of BaTiO₃, Ni_{0.7}Zn_{0.3}Fe₂O₄ and BaFe₁₂O₁₉Nanopowders</i>	<i>49</i>
<i>4.2.1 X-ray Diffraction</i>	<i>49</i>
<i>4.2.2 Indexing X-ray diffraction patterns</i>	<i>51</i>
<i>4.2.3 The lattice of BaTiO₃, BaFe₁₂O₁₉ and Ni_{0.7}Zn_{0.3}Fe₂O₄Nano compound and the length of ion</i>	<i>54</i>
<i>4.2.4 Theoretically calculate the lattice parameters, the unit cell size and density</i>	<i>56</i>
<i>4.2.5 Scanning Electron Microscopy (SEM)</i>	<i>57</i>
<i>4.2.6 Energy Dispersive X-Ray Spectroscopy (EDS)</i>	<i>61</i>
<i>4. 3 Dielectrically characteristic</i>	<i>63</i>
<i>4. 3. 1 Dielectric constant (ϵ'_r)</i>	<i>63</i>
<i>4.3.2 Dielectric loss factor (ϵ''_r)</i>	<i>66</i>
<i>4.3.3 Tangent loss ($\tan\delta$)</i>	<i>68</i>

<i>4.3.4 Alternating electrical conductivity ($\sigma_{a.c}$)</i>	<i>70</i>
<i>4.3.5 Dielectric strength</i>	<i>73</i>
<i>Chapter five</i>	
<i>Conclusions</i>	<i>75</i>
<i>Future Work</i>	<i>76</i>
<i>References</i>	<i>77</i>

The abbreviation

<i>AA1</i>	<i>20%BaFe₁₂O₁₉+80%BaTiO₃</i>
<i>AA2</i>	<i>50% BaFe₁₂O₁₉+50% BaTiO₃</i>
<i>BB1</i>	<i>20%Ni_{0.7}Zn_{0.3}Fe₂O₄+80%BaTiO₃</i>
<i>BB2</i>	<i>50% Ni_{0.7}Zn_{0.3}Fe₂O₄+50% BaTiO₃</i>
<i>BT</i>	<i>Barium Titanate</i>
<i>AA3</i>	<i>30%BaFe₁₂O₁₉+70%BaTiO₃</i>
<i>BB3</i>	<i>30%Ni_{0.7}Zn_{0.3}Fe₂O₄+70%BaTiO₃</i>

The definitions of the symbols that used

θ	Theta
ph	Potential of hydrogen
$R_p-R_{wp}-R_{exp}$	Reliability factors for Ratvlad
V	Volume
D	Particle size
ϵ_r'	Dielectric constant
ϵ_r''	Dielectric loss factor
Tan δ	Tangent loss
E_g	Energy gap
$\sigma_{a.c}$	Alternating electrical conductivity
f	Frequency
ϵ_0	Permilivity of vacuum
P_{x-ray}	Theoretical density
C.B	Conduction band
V.B	Valance band
ϕ	phi
$K_\alpha, K_\beta, K_\gamma$	Orbital atomic

XRD	X-ray diffraction
EDX	Energy-Dispersive X-ray spectroscopy
SEM	Scanning Electron Microscope
a, b, c	Lattice parameters constant
(meter)	Self Inductance Capacitor Resistance

List of figures

<i>Figure</i>	<i>Page</i>
<i>Fig.(2-1): Sketch energy bands in the absolute zero temperature</i>	<i>8</i>
<i>Fig.(2.2): (a) Electronic Polarization (b) Ion Polarization (C) Orientation Polarization (d)Space charge</i>	<i>15</i>
<i>Fig.(2.3): Interfacial Polarization</i>	<i>16</i>
<i>Fig.(2.4): Perovskite arrangement of ABO_3</i>	<i>22</i>
<i>Fig.(2.5): Unit cell of $BaTiO_3$ in deferent of phases</i>	<i>23</i>
<i>Fig.(2.6): Refers to the locations of ion in tetragonal system $BaTiO_3$</i>	<i>24</i>
<i>Fig.(2.7): Web constants of $BaTiO_3$ as purpose of hotness</i>	<i>24</i>
<i>Fig.(2.8): Field arrangements in plate (001) of tetragonal $BaTiO_3$. Arrows stand for the way of the glacial axis. The surface of the panel appears: (a) a "range" between domains C, (B) and A only fields</i>	<i>28</i>
<i>Fig.(2.9): Buffer constants of($BaTiO_3$) as a purpose of hotness</i>	<i>29</i>
<i>Fig.(3.1) Sensitive electronic balance</i>	<i>36</i>
<i>Fig.(3.2): Magnetic Stirrer</i>	<i>37</i>
<i>Fig.(3.3): Laboratory oven</i>	<i>37</i>
<i>Fig.(3.4): The shape special template for hydraulic piston</i>	<i>42</i>
<i>Fig.(3.5): Picture of the device (XRD) which is a type of (shimadZu XRD -6000)</i>	<i>44</i>

<i>Fig.(3.6): Picture of the scanning electron microscope (SEM)</i>	45
<i>Fig.(3.7): Picture of transferring (EDX)</i>	46
<i>Fig.(3.8): (LCR meter) device</i>	47
<i>Fig.(3.9): Dielectric strength equipment</i>	48
<i>Fig.(4.1): The XRD for(BaTiO₃ Nano powder)specimen</i>	49
<i>Fig.(4.2): The XRD for (BaFe₁₂O₁₉ Nano powder)specimen</i>	50
<i>Fig.(4.3): The XRD for (Ni_{0.7}Zn_{0.3}Fe₂O₄ Nano powder)specimen</i>	50
<i>Fig.(4.4):Riveted refinement for BaTiO₃ using Full-prof program</i>	52
<i>Fig.(4.5):Riveted refinement for BaFe₁₂ O₁₉ using Full-prof program</i>	52
<i>Fig.(4.6):Riveted refinement for Ni_{0.7}Zn_{0.3} Fe₂O₄ using Full-prof program</i>	53
<i>Fig.(4.7): Schematic of BaTiO₃ unit cell.</i>	54
<i>Fig.(4.8): Schematic of BaFe₁₂O₁₉ unit cell.</i>	55
<i>Fig.(4.9): Schematic of Ni_{0.7}Zn_{0.3}Fe₂O₄unit cell</i>	56
<i>Fig.(4.10): The SEM image of BaTiO₃ Nano powder</i>	58
<i>Fig.(4.11): The SEM image of BaFe₁₂O₁₉Nano powder</i>	58
<i>Fig.(4.12): The SEM image of BaFe₁₂O₁₉Nano powder</i>	59
<i>Fig.(4.13): The image j of BaTiO₃ Nano powder</i>	59
<i>Fig.(4.14): The image j of BaFe₁₂O₁₉Nano powder</i>	60

<i>Fig.(4.15): The image j of BaFe₁₂O₁₉Nano powder</i>	<i>60</i>
<i>Fig.(4.16): EDX patterns of the BaTiO₃Nano compounds</i>	<i>61</i>
<i>Fig.(4.17): EDX patterns of BaFe₁₂O₁₉Nano powder</i>	<i>62</i>
<i>Fig.(4.18): EDX patterns of Ni_{0.7}Zn_{0.3}Fe₂O₄Nano powder</i>	<i>62</i>
<i>Fig.(4.19): (ϵ'_r) of BaTiO₃specimens</i>	<i>64</i>
<i>Fig.(4.20): (ϵ'_r) for AA1, AA2, AA3, BB1, BB2& BB3 specimens</i>	<i>65</i>
<i>Fig.(4.21): Dielectric loss factor of theBaTiO₃specimens</i>	<i>66</i>
<i>Fig.(4.22): Dielectric loss factor for AA1, AA2, AA3, BB1, BB2& BB3 specimens</i>	<i>67</i>
<i>Fig.(4.23): $\tan\delta$forBaTiO₃ specimen</i>	<i>68</i>
<i>Fig.(4.24): $\tan\delta$ for AA1, AA2,AA3, BB1, BB2& BB3 specimens</i>	<i>69</i>
<i>Fig.(4.25): $\sigma_{a.c}$for BaTiO₃ specimens</i>	<i>71</i>
<i>Fig.(4.26): $\sigma_{a.c}$for AA1, AA2, BB1 & BB2 specimens</i>	<i>72</i>
<i>Fig.(4.27): Break down voltage for all specimens</i>	<i>73</i>
<i>Fig.(4.28): Dielectric strength for all specimens</i>	<i>74</i>

List of Tables

<i>Tables</i>	<i>Page</i>
<i>Table (3-1): Raw materials</i>	<i>35</i>
<i>Table (3-2): Quantities calculated to prepare ($Ni_{0.7}Zn_{0.3}Fe_2O_4$) ferrite by auto combustion sol-gel method</i>	<i>40</i>
<i>Table(3-3): Quantities calculated to prepare ($BaFe_{12}O_{19}$) ferrite by auto combustion sol-gel method</i>	<i>40</i>
<i>Table(3-4): Quantities calculated to prepare ($BaTiO_3$) ferrite by auto combustion sol-gel method</i>	<i>41</i>
<i>Table (3-5): Shows the symbols of Nano-composites in addition to the ratio(x %)</i>	<i>42</i>
<i>Table (4-1): The (R_p), (R_{wp}) and (R_{exp}) Reliability factors for Ratvlad, (Space group) and (phase) values for $BaTiO_3$, $BaFe_{12}O_{19}$ and $Ni_{0.7}Zn_{0.3}Fe_2O_4$ compounds prepared at sol-gel auto combustion technique</i>	<i>53</i>
<i>Table (4-2): Shows the atoms site in $BaTiO_3$ lattice</i>	<i>54</i>
<i>Table (4-3): Shows the atoms site in $BaFe_{12}O_{19}$ lattice</i>	<i>55</i>
<i>Table (4-4): Shows the atoms site in $Ni_{0.7}Zn_{0.3}Fe_2O_4$ lattice</i>	<i>56</i>
<i>Table (4-5): Shows lattice parameters, (c/a) ratio, the unit cell size, density of the $BaTiO_3$, $BaFe_{12}O_{19}$ and $Ni_{0.7}Zn_{0.3}Fe_2O_4$ Nano-compounds</i>	<i>57</i>

<i>Table (4-6): Shows practical size of the BaTiO₃, BaFe₁₂O₁₉ and Ni_{0.7}Zn_{0.3}Fe₂O₄ Nano-compounds</i>	57
<i>Table (4-7): Shows Weight% and Atomic% for BaTiO₃, BaFe₁₂O₁₉ and Ni_{0.7}Zn_{0.3}Fe₂O₄ Nano-compounds</i>	63
<i>Table (4-8): The (ϵ'_r), (ϵ''_r) and ($\tan\delta$) values at 50Hz and 1MHz for groups prepared at sintering temperature(1100°C), compaction(5.4 MPa) in room temperature</i>	70
<i>Table (4-9): The ($\sigma_{a.c}$) values at 50Hz and 1MHz for groups prepared at sintering temperature(1100°C), compaction(5.4 MPa) in room temperature</i>	72
<i>Table (4-10): The Dielectric strength and breakdown voltage values for groups prepared at sintering temperature(1100°C), compaction(5.4 MPa) in room temperature</i>	74

Chapter one
Introduction
and literature
Review

1.1 Introduction

Dielectric materials (BaTiO_3) is one of the best known Perovskite ferroelectric compounds [1- 4].

The technique of dopant incorporation into BaTiO_3 has been extensively investigated and the behavior of some transition metal ions as well as that of the larger rare earth ions has been well elucidated. The ionic radius is the main parameter that determines the substitution site [5]. BaTiO_3 are of great interest as capacitor materials because they combine high permittivity and high dielectric strength and can be solution processed on large and flexible substrates at low temperatures [6-11].

Among those spinel ferrites we are interested in Zn substituted mixed ferrites are useful for low and high frequency applications generally for power transformers, power inductors, microwave devices, read and write heads for high speed digital tape, etc. because of their high resistivity, low losses, mechanical hardness, high Curie temperature and chemical stability [12-17].

1.2 Ferro-electricity

The ferro-electric are single-Mono crystalline materials of Rochelle salt, there are two conditions for classifying materials as ferro-electrics spontaneous polarization and demonstrated are orienting polarization.

These materials have spontaneous electrical properties that can be reversed by applying an external electric field [18] and a permanent magnetic moment. This magnetic magnetism was already known as it was discovered in 1920 in the Rochelle salt by Valasic [19].

1.3 Polarization

In general, materials demonstrate Ferro electricity only below a specific phase critical temperature, T_C while Para electric has temperature above T_C . The spontaneous polarization vanishes, and the ferroelectric crystal transforms into the Para electric state. Many ferroelectrics lose their piezoelectric properties above T_C completely because their Para electric phase has Centro-symmetric crystallographic structure. [20].

1.4 literature survey

Feder, (2002), et. al. , have prepared series of ferrite format ($Ni_{0.35} Zn_{0.65} Fe_2O_4$) as well as ($Ni_{0.6} Cu_{0.2} Zn_{0.2} Fe_2O_4$) by using normal ceramic method , where they sintering ferrite that is output at different temperatures and concluded that the properties output ferrite relies heavily on chemical composition, and also depends on the sintering degree heat, and add an item (Cu) improves magnetic properties and reduces the degree of sintering temperature, in addition to all this, the increase adding the oxides to the Barium Titanate complex by 0.3 led to a decrease in electrical impedance [21] .

Mangalaraja, (2002), has prepared ferrite ($Ni_{0.8} Zn_{0.2} Fe_2O_4$) using the flash mode of combustion where sintering the ferrite with temperatures (1250 °C, 1150 °C) and studied magnetic hysteresis and Curie temperature degree where they found that the electrical dielectric constant of ferrite factory prepared by this way is much better than ferrite prepared by ceramic method, where concluded that ferrite who manufactured, suitable for use in high frequency applications [22].

Khasawinaha, (2008), et. al., have prepared composite materials (BaTiO_3) and ($\text{BaFe}_{12}\text{O}_{19}$) have been studied. The co-existence of magnetic hysteresis in the composite material has been observed in the temperature range (90-300) °K .The coercive field HC increases almost linearly with increasing the temperature and with increasing the concentration of BaTiO_3 in the system [23].

Liu, (2009), et. al. , have studied the Quasi-single magnetic domain M-type barium hexa-ferrite powders have been synthesized via sol–gel auto-combustion route, followed by secondary heating treatment at 800°C for 4 h, using barium nitrate, ferrite nitrate, ammonium nitrate, citric acid, and ammonia solution as the starting materials. The results indicated to chelation Ba and ferrite are the most important formulations by sol-gel technique, and change magnetic properties depended on change sintering, phase, adhesion of the grains and the crystalline regions [24].

Mojtaba, (2011), have prepared the $\text{Ba}_3\text{CO}_2\text{Fe}_{24}\text{O}_{24}$ Nano powders with Z-type structure by sol-gel method , and it heat treatment at 1270°C (4h) where the results of XRD, TEM , particle size for $\text{Ba}_3\text{CO}_2\text{Fe}_{24}\text{O}_{24}$ Nano powders with Z-type is less than 30nm . Also it has studied all from TG-DTA analysis to determine Tg.[25] .

Ahmed, (2012), et. al., have studied the Magneto electric bi-ferric Nano composite with $1/2\text{Ni}_{0.5}\text{Zn}_{0.5}\text{Fe}_2\text{O}_4 + 0.5\text{BaTiO}_3$ composition was synthesized by ceramic technique. The exact critical temperature and the thermal hysteresis (the area), depend on applied ac electric field. The delay between heating and cooling processes was estimated from the deceleration vs. frequency zone. The delivery mechanism in the samples was explained according to different models. This study enhances the use of this system in memory applications [26].

Ke Yu, (2013), et. al. , have prepared CPC Nano, where added BaTiO₃ to poly(vinylidene fluoride) polymer as fillers in 2012 Sundararajan et al , they were noticed enhanced dielectric permittivity and reduced loss tangent. The frequency and temperature dependencies of the dielectric permittivity and loss tangent of the Nano composites suggest that the introduced.

The consequences indicate that the presented ceramic fillers and interface areas have positive influences on the structure of the polymer matrix and contribute to the enhancement of the dielectric responses and energy storage properties of the Nano composites [27].

Avila, (2013), et. al., have prepared composite materials made of epoxy resin and (BaTiO₃) electro spun nanostructured fibers. BT fibers were synthesized from a sol based on barium acetate, titanium iso-propoxide, and poly (vinyl pyrrolidone). The fibers were heat-treated at different temperatures and characterized by X-ray , (SEM), and dielectric measurements were performed by means of dielectric spectroscopy. The dielectric permittivity and dielectric modulus of Epoxy resin/BT-fiber composites were measured for two types of samples: with the electrodes parallel and perpendicular to the BT fiber layers. Interestingly, composite spacemen's with electrodes perpendicular to the fiber layers and a BT content as low as 2 vol % led to dielectric permittivity's three times higher than that of pure epoxy resin[28] .

Bilge, (2014), et. al., Nano-BaTiO₃ powders have been manufactured using the hydrothermal method. During the synthesis, titanium iso-propoxide, iso-propanol and barium acetate were used as a major raw material. Reaction hydrothermally suspension in Teflon pot at 200°C in 1hour. These modified BaTiO₃ powders have been marked in several different ways,(FT- E, ZER, BIT, SIM), and (TG - DTA). The purity of the phase and crystal structure of BaTiO₃ was determined using (X-ray) diffract meter. According to (X-ray) diffraction

analysis, BaTiO₃ Nano powders have cubic stages at room temperature. SEM results revealed that the morphologies and sizes of BaTiO₃ molecules synthesized by Handan accelerate the voltage from 20 kV. The particle size of BaTiO₃ was calculated as 18.97 nm using (Scherer equation). The average pore diameter was measured using a house analysis and pore size was found to be 33.6424 nm [29].

Mujahid, (2015), et. al., have prepared powders of nanoparticles for BaTiO₃ tinged with ions La (Ba_{1-x} La_x TiO₃ or BLT) with percentages (x=0.005, 0.015, 0.02, 0.025) and non-tinged (Ba TiO₃ or BT) using technical semi-oxalates at room temperature with a PH adjustment function acid (PH) of the solution up to the value of 5.5, The researchers studied the crystallization and size particleboard for powders prepared using diffraction of X-ray (XRD) and electron microscopy scanner technology (SEM) where, they found granular size has reached about (65nm), as well as they study the properties of the insulation of the complexes (Polymer \ Barium Titanate) and complexes (Polymer \ Barium Titanate Lanthanum) and polymer resin polyester non-saturated as a function of frequency in the range (5-20 MHz) using the technique (LCR meter) where the dielectric constant theoretical calculation of the samples prepared using Brockmann Law for mixtures and also calculate the dielectric constant of the complexes and they found it decreases with increasing the proportion of tinged [30].

Dzunuzovic, (2015), et. al., have studied the rrite (NZF) and (BT) were prepared by auto-combustion synthesis.. Multi-ferroic composites with the general formula yNi_{1-x}Zn_xFe₂O_{4-(1-y)} BT (x= 0.3, 0.5, 0.7, y= 0.5) were prepared by mixing NZF and BT powders in a liquid medium in the ball mill.. The homogenous phase distribution in obtained composites was also confirmed. Impedance spectroscopy measurements were carried out in order to investigate

the electrical resistivity of materials, showing that grain boundaries have greater impact on the total resistivity than grains. Saturation magnetization and remnant magnetization continuously decrease with BT phase increase [31].

Aparna, (2016), et. al., have studied Ti-doped barium ferrite powders $\text{BaFe}_{(12-x)}\text{Ti}_x\text{O}_{19}$ for different 'x' value nano material has been synthesized using sol-gel method is presented in this article. As prepared nanomaterial is heat treated at 950°C temperature and characterized using XRD, FTIR and SEM techniques [32].

1.5 The aim of work

1-Preparation of (BaTiO₃), (Ni_{0.7}Zn_{0.3}Fe₂O₄) and (BaFe₁₂O₁₉) Nano powders, using (Sol-gel)-Auto combustion method, and study the dielectrical properties of powders prepared using mathematical methods, software and databases.

2- prepared nano composite's, with different wt. % of (BaTiO₃), (Ni_{0.7}Zn_{0.3}Fe₂O₄) and (BaFe₁₂O₁₉) Nano powders on dielectrically characteristic (Dielectric constant ϵ_r' , Dielectric loss factor ϵ_r'' , Tangent loss $\tan \delta$, Alternating electrical conductivity $\sigma_{a.c}$ and Dielectric strength).

Chapter two

Theoretical

part

2.1 Dielectrics Materials

These materials have low electrical conductivity. And use insulators to prevent the flow of the voltage to places that are undesirable or dangerous. The (Article dry wood, glass, plastics, rubber and ceramics.) are some examples of insulators. Also dry air and, oil to be used as Dielectric. Separation voltage passes with difficulty because the stick electrons to the nuclei to the extent they cannot move freely from one atom to another. So when connected to the separation electrical moves electrons through the barrier sufficient to produce the current.

According to the theory of energy bands for solids, a bundle valance band is completely filled in the absolute zero temperature. In addition to the (Energy gap) between the (Valance Band) and the (Conduction Band), as shown in the following fig. (2.1):

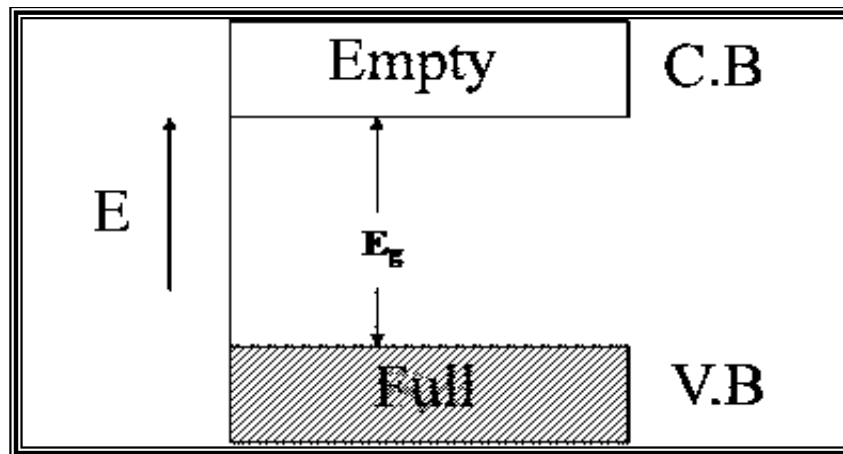


Fig. (2.1) Sketch energy bands in the absolute zero temperature.

The depth (energy difference) of this gap may be equal and above (10eV), where it even if it is to applied an electric field, the electrons do not move a large number in one direction, each electron is moving towards a certain to reverse invert another electron is moving in the opposite direction of movement because the band is completely filled, such as these materials are

called (Dielectrics). The energy gaps of insulators vary from material to material, In general, any material where the forbidden zone energy is equal to more than (6eV) be an insulator ,It is worth mentioning that the insulator is particles consists of a positive charge and the negative charge and often weight center of negative charges dregs on positive charge center of these molecules, but when there are these particles under the effect of an external electric field the positive charge will be brushed off area while supplanted negative charges of these molecules in the opposite direction, As a result, the weight center of positive charge is no longer above dregs on center negative charges, but separated by a small distance and then say that the molecule has become polarized [33]. But if the electric field is very large, this could lead to the acquisition of electrons of energy for conduction and so insulation broken.

2.2 The principal conditions in insulators are:

1-Having a high dielectric strength enough to withstand the electric field between the conductor poles.

2-Having good resistance to movement of the spark spin-off to prevent damage in the curved electric spark.

2.3 Classification of Dielectric.

Through the relationship between the electric field and polarization an insulating materials can be classified as insulating materials to:

1 - Permanent Polarization.

These are polarized in the absence of the electric field

2 - Linear Dielectric.

include on materials that do not change the ability of the material for electrification and permittivity with polarization and intensity of the electric field, and each of the permittivity and scalability electrifying function of the position and divided into: -

I. Linear Isotropic Dielectric.

Although the viability of electrifying and permittivity do not depend on polarization and the electric field, there is a similarity in the trends, the applicability of any asymmetric electrifying and permittivity of the corresponding directions are equal, but they can remain dependent on the position. [34]

II. Linear Isotropic Homogeneous Dielectric.

These materials have the same qualities of insulators in the category (I) these in addition; these materials do not depend on any position that the change in permittivity and electrifying scalability for the position is equal to zero [35].

3- Non Linear Dielectric.

Substances that have the existence of a functional relationship between electric field and electrical displacement and constants (the ability of the material forelectrifying and permittivity), and the relationship between them is sometimes complex, the ceramics are located within this category, and include insulation properties, including viroelectric, Bisoelectric property. [36-38]

2.4 Dielectric Strength.

The voltage that occurs then the breakdown is called (breakdown Voltage). when divided on the thickness of the specimens are called (Dielectric Strength). [39].

$$E_{br} = \frac{U_{br}}{d} \quad \dots(2-1)$$

E_{br} :- Dielectric strength

U_{br} :- Breakdown Voltage (volt or K volt)

d :- thickness of dielectric (cm or m)

E_{br} can be reduced by Cracks, impurities and holes [40] observe Dielectric Strength Correlation with Dielectric loss factor and electrical resistivity. Dielectric Strength increase when electrical resistivity increase and when

dielectric loss factor decrease [41,42] .This can be seen a breakdown in the material by watching one of the following .

- 1 - Void in the specimens, which occurs when you reach the real electrical durability of the insulation.
- 2 - Burn or melt, which occur when the material is heated locally and breakdown occurs. [43]

2.5 Electrical polarization

Electrical insulators have very few free electrons to take part in normal electrical conductivity. Such a material has interesting electrical properties because of the ability of an electric field to polarize the material to create electrical dipole, thus insulating material moleculars are called (Non polar molecules)[44]. As well as appearing dipole in a material in the presence of a field, dipoles may be present as a permanent feature of the molecular structure. Such dipoles are called (Permanent dipoles) in which the center of the positive charge does not coincide with the center of the negative charges such insulating material molecular are called (polar molecules). Induction of the dipoles is called electric polarization [45].

Phenomenon of polarization (P) down to the change in the arrangement of electrically charged particles of a dielectric in space, or is the surface charge density in a dielectric, equal to the dipole moment per unit volume of material being defined as follow:

$$P = Nm \quad \dots(2 - 2)$$

where:

N: is the number of dipoles per unit volume.

m: is the average dipole moment.

The electric dipole moment corresponds to two electric charges of opposite polarity $\pm q$ separated by the distance (d)[46]:

$$m = qd \quad \dots(2 - 3)$$

We can represent the electrical displacement (D) as the sum of the electric field (E) at a given point of dielectric and the polarization at the same point:

$$D = \varepsilon_0 E + P \quad \dots(2 - 4)$$

where:

ε_0 : is the permittivity of vacuum ($8.85 \times 10^{-12} \text{F/m}$)

The relationship between the electrical displacement and the electric field through a dielectric medium is:

$$D = \varepsilon_0 \varepsilon_r E \quad \dots(2 - 5)$$

ε_r : is called the relative permittivity or dielectric constant of the medium, for vacuum $\varepsilon_r=1$, so

$$D = \varepsilon_0 E \quad \dots(2 - 6)$$

By substitute equation (3-6) in (3-5) we get [47,48]:

$$P = \varepsilon_0 \varepsilon_r E - \varepsilon_0 E$$

$$P = \varepsilon_0 (\varepsilon_r - 1) E \quad \dots(2 - 7)$$

2.5.1 Mechanisms of polarization

Materials in which electric polarization occurs are called dielectrics. There are various possible mechanisms of polarization in dielectrics. Polarization can be categorized into several different types in terms of the displaced units.

2.5.1.1 Electronic polarization

The displacement under the action of an external electric field of the orbits in which negatively charged electrons move around a positively charged atomic nucleus leading to the formation of induced dipoles as shown in Fig. (2.2a). Electronic polarization occurs in all atoms, within every dielectric irrespective of other types of polarization. This type of polarization occurs during a very brief interval of time (of the order of 10^{-15} sec) i.e., the time of the period of oscillations of ultraviolet rays. It is temperature-insensitive, it is operative at most frequencies and drops off at very high frequencies ($\sim 10^{15}$ Hz). This type of polarization is frequently referred to as optical polarization[49].

2.5.1.2 Ionic polarization

Materials with ionic bonds may have ionic polarization. Ionic polarization is the displacement of negative and positive ions toward the positive and negative electrodes, respectively as in Fig. (2.2b). Like electronic polarization ionic polarization is induced, since the relative displacement of positive and negative ions occurs only when an external electrical field is present[50].

Being more massive than electrons, the ions cannot become polarization rapidly. A short time is required for the process of ionic polarization to set in, but longer than for electronic polarization, i.e., (10^{-13} - 10^{-12} sec). Ionic resonance occurs in the infrared frequency range (10^{12} - 10^{13} Hz), it is quite temperature insensitive[51].

2.5.1.3 Orientational polarization

This polarization arises in substance is built up of molecules possessing a permanent electric dipole moment. Under the influence of the applied field, these dipoles are aligned in the direction of the field, in consequence, orientation polarization takes place as in Fig. (2.2c). Such polarization is quite temperature sensitive[52], it occurs at low frequencies and is thus important because it can greatly affect the capacitive and insulative properties of glasses and ceramics in low frequency application.

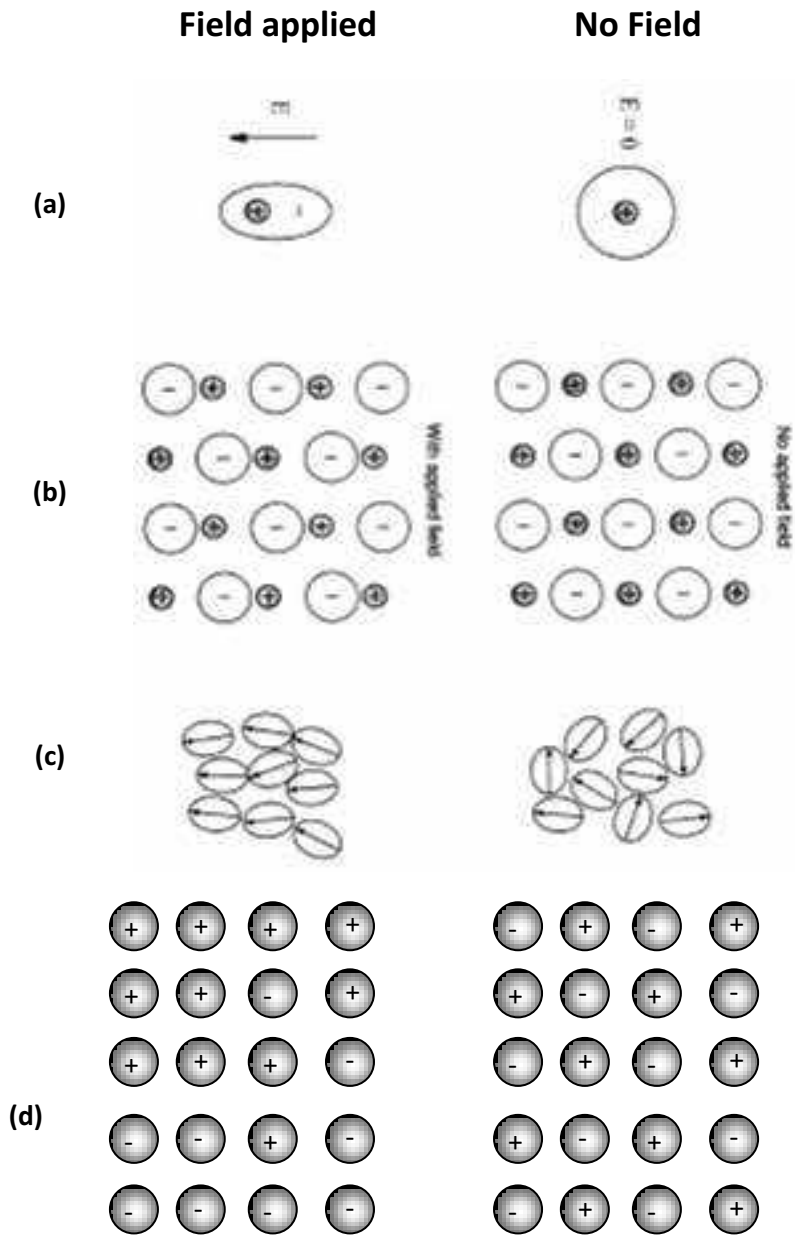


Fig.(2.2): Schematic representation of different mechanisms of polarization[53]

(a) Electronic polarization

(b) Ionic polarization

(c) Orientation polarization

(d) Space charge

2.5.1.4 Space charge or interfacial polarization

Interfacial polarization is of considerable practical interest because commercial insulating materials are usually heterogeneous.[54]

In heterogeneous materials there is usually an interfacial polarization arising from the accumulation of charge at structural interface where the application of an electric field may activate the movement of charge carriers, such as free electrons, ions, vacancies, impurity atoms, etc. as in Fig. (2.2d). However, the movement of charges through the material may be slowed down when the charge carriers-encounter another phase with lower electric conductivity. This causes the accumulation of charges at the interfaces. This interfacial polarization manifests itself to an outside observer as an increase in the permittivity[55].

The most frequent kind of inclusions of foreign phases in polycrystalline materials are pores, which constitute the most effective obstacle to movement of carriers.

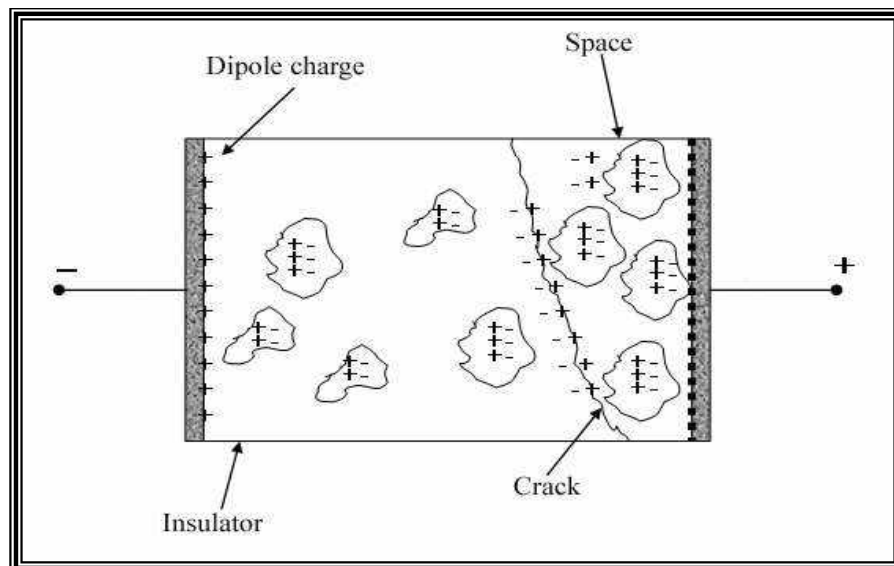


Fig. (2.3) Interfacial Polarization.[56]

2.6 Electric properties study

The study of the electrical properties of insulating materials help us to understand the behavior of charge or local charge shipments in insulating material when exposed to the influence of the electric field as to this matter of importance to know the polarization electrical insulator mechanisms and their impact on the properties of electrical insulation as well as the rest of the effect of some other factors, such as the electric field frequency inflicted on the insulating material content or replacement concentration in the composition of the insulation material.

2.7 Technology of Powder X-ray diffraction (XRD):

The technology X-ray diffraction is one of the key technologies and common use in the study of the structural properties of the material, as it provides basic information about the crystalline structure and material phase [57].

Using X-ray diffraction (XRD) of the powder to examine the structures of solids material and obtain information on the unit cell, such as the size of the unit cell, factorc, Brack's angle (Θ), crystal dimensions, the density of matter, particle size and other.

It can determine the shape of the unit cell by peaks sites in the pattern of diffraction, while the relative intensity of the peaks tell us an information about the order and type of atoms within the unit cell, while viewing peak at mid-intensity (FWHM) can gives us the granular size of the material under study [58].

It includes filtering program reliability factors or sometimes called the agreement factors, as the reliability factor the standard by which helps in judging the quality of the filtering process, by giving clear indications to follow the filtering process, and reliability factor factors are given as follows:

1. profile reliability factor

And it gives us the following relationship:

$$R_p = \frac{\sum_i l Y_{oi} - Y_{ci} l}{\sum_i Y_{ai}} \quad \dots (2-8)$$

As (Y_{oi}) and (y_{ci}): are the intensity of observation and calculated respectively.

2. (Weighted profile reliability)

And it gives us the following relationship.

$$R_{wp} = \frac{\sum_i (Y_{oi} - Y_{ci})^2 W_i}{\sum_i (Y_{ai})^2} W_i \quad \dots (2-9)$$

As (W_i): (Weighting factor) to the point (i)

It is calculated at that point by the following relationship:

$$W_i = \frac{1}{Y_{oi}} \quad \dots (2-10)$$

3. Expected reliability factor

If the background intensity high, the value of (R_{wp}) would be great automatically to obtain the ideal value (R_{wp}) should be close to the expected reliability factor (R_{exp}), which is expressed in the following relationship

$$R_{exp} = \left[(n - p) / \sum_i^n W_i Y_{oi}^2 \right]^{1/2} \quad \dots (2-11)$$

As the ((n): the number of points in the spectrum of the powder diffraction observed.

(p): the number of parameters that were being filtered.

The values of (R_{wp}) reflect the quality of the data used, so the ratio between (R_{wp}) and (R_{exp}) represents the quality of the Goofiness of dit (GOF) expressed by the following equation:

$$\chi^2 = R_{wp} / R_{exp} \quad \dots (2-12)$$

if there is a high-quality data, the value of (R_{exp}) will be small, and the value of (x^2) when the filtering process is complete, larger than the number (1), as during the filtering process begins value (x^2) large and decreases when the best deal for a specimen with data, but must not be less than the value of (x^2) of the number (1) or be equal to it, if the value of ($x^2 > 1$) at the end of the filtering process, this means that there are high quality in extracted in the filtering process data. [59-62].

2.7.1 Structural parameters

The study of the behavior of the structural parameters and measured it are great importance; because they contribute to interpretation of many of the physical properties of the material.

2.7.1.1 Lattice parameters

The networking parameters can be calculate (a, b, c) for the installation of quartet using surfaces space equation (d-spacing) X-ray installation for quartet with the help of the values of (hkl) that are extracted from the indexing process or from the global standard cards, according to the following equation: [63]

$$\frac{1}{d^2} = \frac{h^2+k^2}{a^2} + \frac{l^2}{c^2} \quad \dots (2-13)$$

We can also calculate the size of the unit cell of the tetragonal system by using the following equation [64]

$$V = ac^2 \quad \dots(2-14)$$

2.7.1.2($\rho_{x\text{-ray}}$) Theoretical density

We can calculate theoretical density ($\rho_{x\text{-ray}}$) from the spectrum and data of X-ray diffraction using the following relationship: [65]

$$\rho_{x\text{-ray}} = \frac{Z M_{wt}}{N_A V} \quad \dots (2-15)$$

As the (Z): the number of atoms in the unit cell.

(M_{wt}): molar mass (g / mol)

(N_A): Avogadro number 6.022×10^{23} (1 / mol)

2.7.1.3 (Crystallite size)

Calculated particle size of the powder nano scale using two methods, the first way: It is calculated using equation (Debye- Scherer), as in the following equation: [66]

$$D_{sh} = \frac{k \lambda}{\beta \cos \theta} \quad \dots (2-16)$$

As the (k): a constant value (about 0.9)

(λ): wavelength of X-ray unit ($^{\circ}\text{A}$)

(θ): angle of the fall of X-rays (deg)

β : maximum width of the summit for mid-intensity (FWHM), and measured in (rad)

D_{sh} : Particle size unit (nm)

In the second method is calculated particle size using equation (Williamson-Hall) (D_{w-H}), which take into account the Micro strain of the crystalline lattice, as in the following equation: [67]

$$\beta \cos \theta = k \lambda / D_{w-H} + [4 \varepsilon \sin \theta] \quad \dots (2-17)$$

As (ε): Micro Strain.

2.8 Photovoltaic materials in general

Electrolysis was detected in mono-crystalline materials in 1921. The material can be insulator and there was little insulation. Due to the excellent characters for barium titanate, therefore preferred for use in ceramic materials.

2.9 BaTiO₃ (BT)

BaTiO₃(BT) has a high chemical and mechanical stability, it can be synthesized and used to produce ceramic poly crystalline, due to excellent electrical insulation characteristics and little loss, allowing us to use it as a capacitors. BT has been widely applied in some devices.

2.10 Formation of BT is from Perovskite group.

The compositions of most of the commercial high dielectric constant ceramic materials used for disc or multilayer capacitor are based on BaTiO₃. Fine BaTiO₃ powder can be synthesized by conventional mixed oxide method [68-70], and a number of solution techniques such as oxalate co-precipitation Method [71-73], hydrothermal method [74, 75] and the Pechini process [76] etc. We present an analysis of BaTiO₃ formation via semi-oxalate method in which the precursor was prepared by precipitating barium oxalate at the surface of TiO₂ particles. TiO₂ powder is used instead of its organometallic salt, because of its easy availability and low cost. There has been no such oxalate-oxide reaction synthesis of BaTiO₃.

2.10.1 Barium Titanate Structure (perovskite arrangement)

The order of Perovskite is supported by several oxides containing the chemical formula ABO_3 . BT is one of the compounds that belong to the biophysical, its composition is subject to the formula ABO_3 (the coordination number for (A cation) equal 12 and 6 for B Cation while oxygen in the center of the facial edges). The pyro-physical structure has (3D) as shown in (Fig. 2.4A), also be seen as a closely packed cube arrangement of A and ions, with ions filling interstitial places as in (Fig. 2.4B) [77-84].

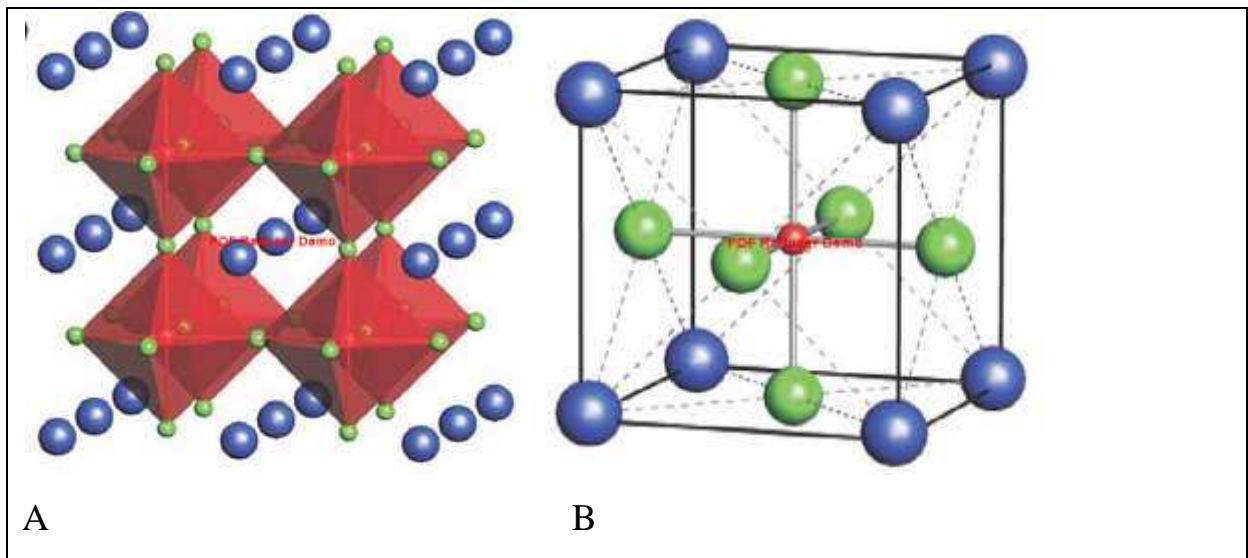


Fig .(2.4): perovskite arrangement of ABO_3 [84]

The perovskite groups include only vehicles with perfect cubic perovskite lattices, but besides all vehicles with configurations that can be resulting by the ideal one by small lattice distributions

2.11 Structural transformations of barium titanate

BaTiO₃ has been discovered as a transparent electrolyte pyrophosphate. Its properties are related to transparent electrode with a series of three structural transition phases. The T_c (Curie point) of BaTiO₃ is 120 °C. Above 120 °C the original cubic cell is stable up to 1460 °C. Above this temperature a hexagonal structure is stable [85]. When the temperature is lower than the Curie point, the crystalline changes occur in BaTiO₃, for the first time at about 120 °C. The translucent electrode transmission occurs between the cubic phase, the Para electric and the electrical insulator of the tetrahedral structure. Also happens at 5 °C transfer to the pyrophosphate phase and continues to -90 °C, where this phase has a three-dimensional structure at a low temperature phase. [86]. Titanium ions (Ti) possess equilibrium sites in the center of their octahedral at Curie as shown in Fig. (2.5), crystallographic changes of BaTiO₃ [77], but with a decrease of the temperature, Ti-ions jump between energetically favorable positions out of the octahedron center [79].

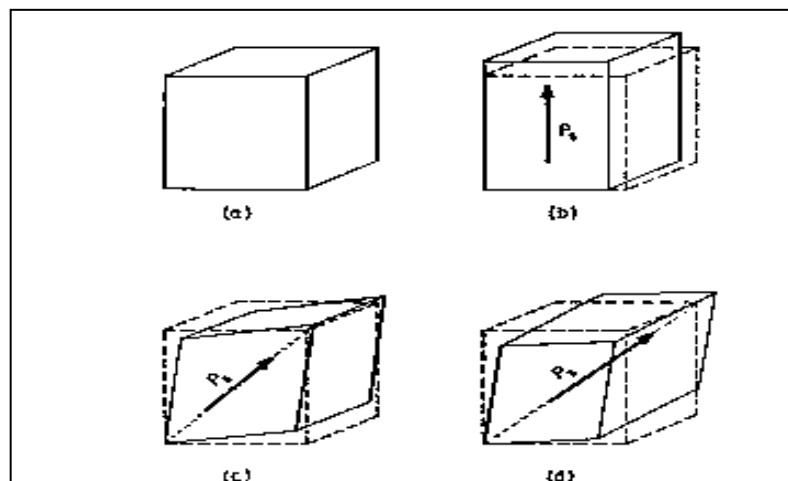


Fig.(2.5) Unit cell of BaTiO₃ in different phases.

[a] Cubic over 120 °C. [b] Quadrilateral between 120 °C and 5 °C.

[c] Orthorhombic between 5 °C and -90 °C. [d] octahedron under -90 °C [77].

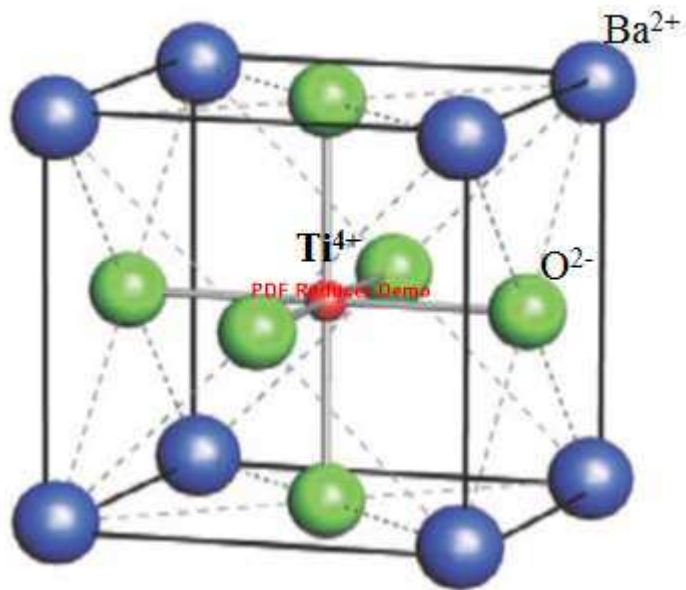


Fig.(2. 6) refers to the locations of ion in tetragonal system BaTiO_3 [79]

The changes can be due to defect in structural, bonds (include its shortening or lengthening), and dimensions of the lattice (Barium Titanate), relative to temperature [86].

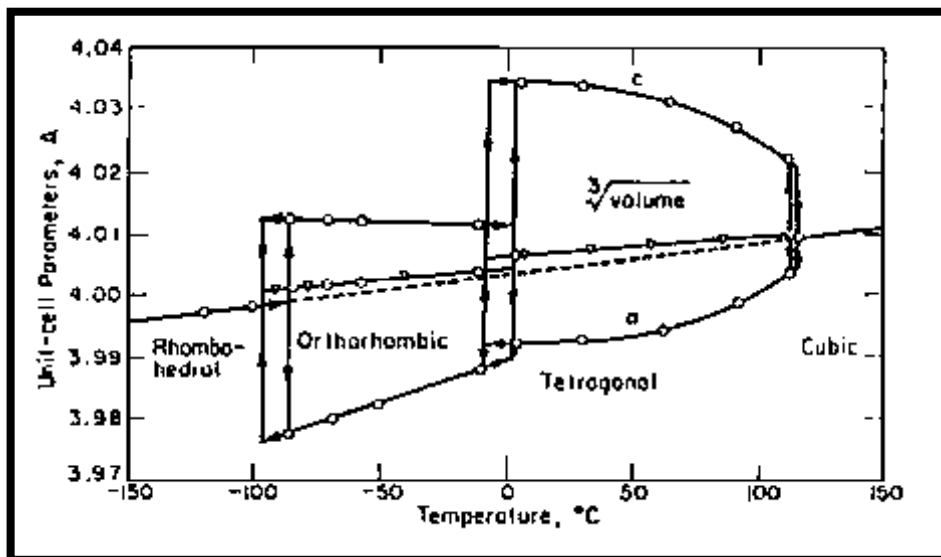


Fig. (2.7) web constants of BaTiO_3 as purpose of hotness[77]

2.12 Barium Titanate synthesis methods

BaTiO_3 installation techniques have been mentioned in much identification. The specific method of synthesis of barium titanate depends on the price, but most importantly is the end request. Excellence powders are not only affected by the synthesis but also by the materials used at first. Since plummeting electronic devices still requires smaller particle size powders with control morphology, the preferred properties of starting powder turn into a critical issue [87]. The successful synthesis of BT powder with unique insulating properties largely depends on cleanliness and crystal arrangement that significantly affect the last properties [88]. All methods have the advantages of getting BaTiO_3 ceramics with the desired properties.

2.12.1 Conventional solid-state reaction

Traditionally, barium titanate is prepared by a solid-state reaction that involves ball grinding of TiO_2 and BaO . The mixture is calcined at temperatures ranging from (800 to 1200 or 1300°C) depending on the researches [89-92]. The disadvantages of this technique, we obtain has a granular size of (2-5 μm) of the mixture (barium titanate) powder, in addition to the presence of impurities and heterogeneity during mixing leads to weakness in the electrical properties of the sintered [93]. Therefore, many modern chemical synthesis methods have been used to produce barium titanate powders with high purity and homogeneity at low temperatures [90].

2.12.2 Chemical methods for barium titanate (BT) synthesis

Modern chemical technique for (BT) preparation. Through the chemical techniques adopted in the preparation of the powder (barium titanate), the researchers were able from prepare (barium titanate) powder with high purity and particles size up to (nm) at low temperatures, it is these techniques are: sol-gel, hydrothermal, co-precipitation and polymeric precursor techniques [85-94].

2.12.2.1 Sol-Gel method

Sol-gel method one of the most important techniques in the preparation of Barium Titanate is the sol-gel, this technique is summarized in three main steps:

- 1- formation of the active monomer by partial metal degradation.
- 2- poly-condensation occurs to obtain colloid formation.
- 3- Additional decomposition occurs to configure oligomers and crosslinking, where increase viscosity of the sol gradually until reach to the transition point of the sol-gel and gelatin occurs.

After getting on the gel, heat treatment was used to get the powder. Gel technology was also developed in a similar process, where it does not require long heat treatment for product, which can produce of the powder with a limit of (20 nm) at a low heat temperature (80 °C) and an alkaline state [95].

2.12.2.2 Hydrothermal Technique

Recently, a microwave- hydrothermal method was developed and shown some advantages over the conventional hydrothermal route [96]. One of the main reasons for the increasing interest in the use of microwaves for the collection of ceramic materials is low costs due to rapid (time and energy), rapid internal heating and installation of new materials [97].

2.12.2.3 Co-precipitation method

These technique simple and a widely studied and under special controlled conditions used to obtain the chemical homogeneity from mixing ions at the molecular level. The disadvantage this technique is that optimum conditions cannot be achieved where precipitation for both (Ba) and (Ti) occurs at one time[98].

2.12.2.4 Polymeric precursor method

It is one of the most widely used technologies. The process of polymerization of glycolic acid and methane with stearic acid is used to form polycarbonate resin. There is no any segregation between the mineral and the polymeric chains during the degradation of organic matter fig.(2.8); illustrations for (BaTiO₃) depending on the pechini method [99].

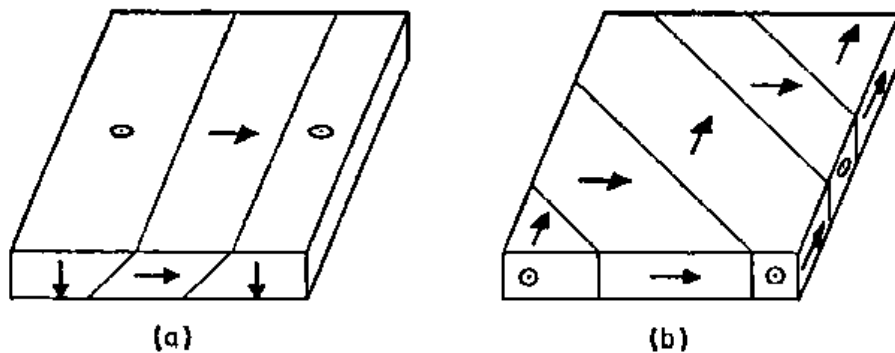
2.13 Properties of BaTiO₃

2.13.1 Electrical properties of (BaTiO₃)

Barium titanate is the initial known see-through electrode ceramic and is a good sift for a variety of application due to its outstanding insulating properties, transparent electrolyte and piezoelectric. Ferro-electricity is mainly connected with domain structure and domain movement. The structure of the field during the phase (para-electric phase) cube to the stage of (tetragonal) (phase is related to the translucent electrical insulation) the shift in the temperature of Curie. The work and kind of domains depend on the turnout of additions and the microstructure obtained during the sintering procedure. Homogeneous and little microbial granules with a single field structure en-abling a transparent and uniform electrode behavior of BaTiO₃ ceramics. In the case of granular microstructure of course apart from a single sphere, the band is the dominant structure that affects the properties of the translucent electrode,

becoming heterogeneous permutations within the crystal [77]. Besides the modification of the crystals, the outside strain in the grain as well have a significant effect on the arrangement of the field, where grain size(microstructure) is an extremely important limit which has an effect on the field thickness and energy area.

In The quadrilateral phase there are two types of space walls. The primary kind of transparent electrode fields draws vertically on every other and the kind of wall area that separates this type of sphere is called the "90°C wall". When the polar axis is at right angles to the plate level, the field is called "c", and when it is at the stage of the cover, the field is called "a" area (with similar extinction).The next kind of scopes polarizes parallel to each other; these fields are called 180°C spheres, and the wall is called separated by the "180° wall." Figs. (2.8) show area arrangements in a quadrilateral cover (BaTiO_3) [78].



Fig; (2.8) Field preparations in plane (001) of tetragonal BaTiO_3 .

Arrows stand for the way of the glacial axis. (a) a "range" between domains C, (B) and A only fields.

2.13.2 Dielectric properties of BaTiO_3

(BaTiO_3) The main material used to produce ceramic dielectric capacitors, multilayer capacitors etc. It is used for this request due to steady static insulator and low dielectric loss. The values of the dielectric steady depend on the synthesis pathway, which means purity, density, grain size, etc. [82] Static insulation also depends on temperature, frequency.

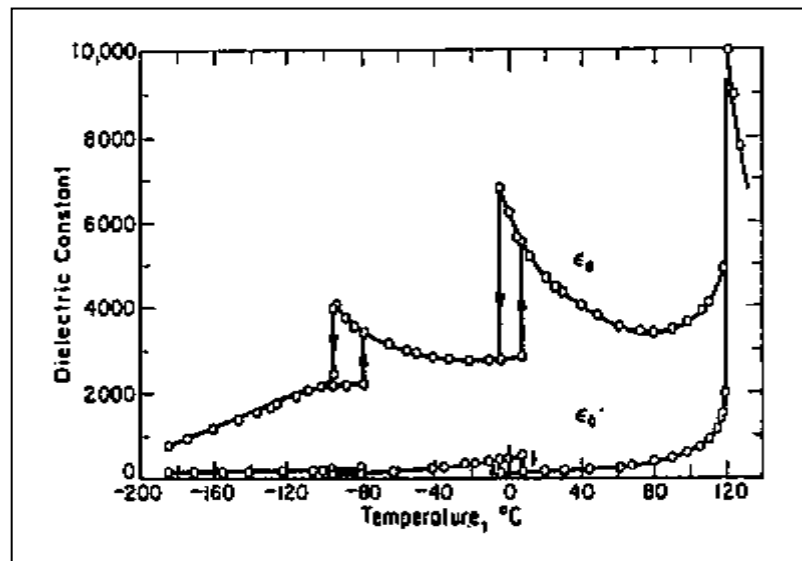


Fig. (2.9) Buffer constants of(BaTiO_3) as a purpose of hotness [78]

2.13.3 The piezo-electric properties of (BaTiO_3)

Barium titanate is the most extensively used for physically power full piezo-electric properties. The word "piezoelectric" is resulting as of the Greek "pesine", which income pressure; therefore, piezoelectric is generating electrical energy as an effect of automatic force. An essential state for the piezoelectricity is its presence asymmetry in the gemstone. Two of the effects are applied in piezo-electric crystals, in universal, and in ceramic electrolyte transparent, in exacting. The straight result (intended as a producer) is determined by the observable fact in which the electrical charge (polarization) is generate as of the automatic pressure , whereas the opposite effect (chosen as a motor) is related

to the automatic group resulting from the request of an electric field. Evaluation of piezo-electric ceramics used for their aptitude to produce great amount of (V (m/n)) High-hard ceramic objects are typically ferroelectric solid Material that do not easily polarize and have relatively low abrasive principles. They are use in devices Such as movable gas igniters and litter girls. Polarization in order to obtain optimal competence as piezoelectric rudiments. Since the curie temperature of Barium Titanate is relatively high, maintaining piezo-electric property, BaTiO₃ be able to use for these purpose, at temperatures up to 70 °C.

2.14 Composite materials

Composite is combined two materials or more to enhance of the properties such as mechanical properties Recently composite materials containing phases (ferroelectric and ferromagnetic) have attracted considerable attention because of their potential applications. It is known that Barium titanate is an excellent ferroelectric material, and it has been used in capacitors, and Barium ferrite is known as ferromagnetic material and has been used in the production of multi-layer chip inductors [100-105].

2.15 Nano-materials

Among magnetic materials, ferrite ceramics are currently the focus of considerable interest. Hexagonal ferrite ceramics are generally applied as permanent magnets, high-density magnetic recording media, and microwave devices because of their unique properties including large magneto crystalline anisotropy, high saturation magnetization, coercively, and corrosion resistivity [106-111].

2.16 Ferrite materials ($\text{Ni}_{0.7}\text{Zn}_{0.3}\text{Fe}_2\text{O}_4$, $\text{Ba Fe}_{12}\text{O}_{19}$)

Magnetic ceramics are of great importance for the production of electronic components called Ferrites. It has wide applications ranging from simple functional devices, such as small mini magnets, and advanced devices to electronic electrical industry such as recording devices and magnetic cards. Ni-Zn ferrite is an important member of these magnetic materials due to its wide range of applications as the result of its high resistivity, high magnetic permeability, low dielectric loss, high Curie temperature, high mechanical hardness, low porosity, reasonable cost and chemical stability.[112-114]. Materials, which are piezoelectric and magneto astrictive at the same time, are generally called magneto-electric (ME) or ferro-ferroic (FE) materials. These materials become magnetized when placed in an electric field, and electrically polarized when placed in a magnetic field [115-121]. The term “composite” broadly refers to a material system that is composed of a discrete constituent (reinforcement) distributed in a continuous phase (matrix), and which derives its distinguishing characteristics from the properties of the constituents and their geometry. Composite materials are usually classified based on the physical or chemical nature of the matrix phase such as polymer, metal and ceramic. In addition, there are some reports to indicate the emergence of intermetallic-matrix and carbon-matrix composites. Composite materials are practically used in all branches of industry. Ferrite-based materials are the most widely used as magnetic materials with excellent chemical stability and their production is relatively cheap. Barium ferrites have very important applications such as accumulating and processing of information. Ferrite is a material of great importance because it use in of large number from technological applications , as it can be used as a model material, thus providing an opportunity of a better understanding of the magnetic interactions at Nano scale [122-128]. Ferrites are a magnetic material widely used in microwave and electrical industries, where

showing high electrical resistance, in addition to its magnetic behavior. One of the most interesting applications of materials is the use of computers, recording devices, magnetic cards, and other advantages are the possibility of preparing different structures and thus modify the magnetic properties. One of the challenges of recent times, one of the challenges is to improve the magnetic properties of soft ferrite such as de-magnetization power and anisotropic energy [129-133].

Nowadays, many microwave absorption materials were developed to reduce the pollutions from microwaves in the GHz range increasingly used in wireless communication tools, local area networks and so on. Because ferrites have higher efficiency and lower cost, they are considered as promising radar absorption material (RAM). Ferrites are divided into three families: spinel, hexagonal ferrites and garnets, Barium hexagonal ferrites was paid more attention as RAM for its plate structure. Recently, various techniques have been developed to prepare barium ferrite, e. g. , the conventional ceramic method, the citrate precursor method, and a variety of wet chemical methods such as co-precipitation, hydrothermal synthesis, and so on. Now new manufacturing techniques of sol-gel method can prepare ultrafine particles with perfect crystallography and narrow size distribution, stimulate an increased interest to prepare Ba ferrite ultrafine particle [134-145]. The formation reaction of hex ferrites has been studied by many researches. Barium hex ferrites ($\text{BaFe}_{12}\text{O}_{19}$) are magnetic material that has great advantages (scientific and technological), in addition to its chemical stability and corrosion resistance. In the past decade, there has been an increasing interest in ways to prepare fine particles of barium hex ferrites, because of their excellent magnetic applications, furthermore the production of the particles of this compound sensitive to the methods of manufacturing in terms of grinding and mixing, especially when manufactured as ceramics at the degree of sintering ($1200\text{ }^{\circ}\text{C}$), generally yields non-

homogeneous mixtures on a microscopic scale and induces lattice strains in the material [146-148]. In order to achieve highly homogeneous ultrafine particles of barium hex-ferrite and to avoid using the milling process, various techniques, such as chemical co-precipitation, hydrothermal, sol–gel, glass crystallization, micro-emulsion, citrate precursor and salt melt methods, have been developed. However, a number of difficulty in obtain high purity, ultrafine and homogeneous particle of barium hex-ferrite with thin size distribution have been pointed out via more than a few investigators [149-156].

The composition of Barium hex-ferrite powder by Sol-Gel combustion technology is the focus of current work. This process has the advantages of inexpensive precursors, simple preparation method, and powder Nano-sized output. This work is aimed at investigating the evolution of the phase during combustion and subsequent calcification of Nano-sized particles prepared by the Sol-Gel combustion method.

Barium hex-ferrite, with its chemical formula $\text{BaFe}_{12}\text{O}_{19}$ (denoted as BF), is the best-known representative of the hex-ferrite family which is used extensively as a relatively low cost ceramic permanent magnet. BF is one of the most important hard magnetic materials, widely used in permanent magnets, magnetic recording media, and microwave applications, due to its fairly large magneto crystalline anisotropy, high Curie temperature, relatively large magnetization, as well as excellent chemical stability and corrosion resistance.

Chapter three
Experimental
part

3.1 Introductions

The work includes two step

- 1-The first phase of the three basic components preparing (BaFe₁₂O₁₉, Ni_{1-x}Zn_x Fe₂O₄,BaTiO₃) as Nano components .
- 2-Include preparing Nano composite.

In this chapter we present a detail explanation for all the laboratory operation which have been done in this research and prepare for generate these equations:

Hard ferrite	Ba Fe ₁₂ O ₁₉
Nickel Zinc Ferrite	Ni _{1-x} Zn _x Fe ₂ O ₄
Pure Barium Titanate	BaTiO ₃

When x=0.3, all that using " sol-gel auto combustion method " From the raw materials used in the preparation of samples and how calculate the weights ,the method of preparation , a calcinations process ,pressing ,sintering and the study of the electrical properties and electrical histera explain with photo for the instrument used in each step of the research.

3.2 Raw materials of prepared of BaTiO₃, BaFe₁₂O₁₉ and Ni_{0.7}Zn_{0.3}Fe₂O₄.

In this research we have been used sol-gel auto combustion method for preparation the samples and we chose the raw materials that used in the reaction , below a table have full describe with detail for each raw materials used in the reaction .

Table(3-1): raw materials

materials	Chemical formula	molar mass g/mol	purity	Country product	The company
Eisen Nickel	$\text{Fe}(\text{NO}_3)_3 \cdot 9\text{H}_2\text{O}$	403.999	99%	Germany	E.Merck
Nickel Nitrate	$\text{Ni}(\text{NO}_3)_2 \cdot 6\text{H}_2\text{O}$	290.79	99%	Germany	Riedel
Zinc Nitrate	$\text{Zn}(\text{NO}_3)_2 \cdot 6\text{H}_2\text{O}$	297.51	98.5%	Spain	Scharlah
Citric Acid	$\text{C}_6\text{H}_8\text{O}_7 \cdot \text{H}_2\text{O}$	210.14	99%	Switzerland	Fluka
Ammonia	$\text{NH}_3 \cdot \text{OH}$	34.03	99%	India	Lobachemie
Titanium Dioxide	TiO_2	79.866	99%	England	GCC
Barium Nitrate	$\text{Ba}(\text{NO}_3)_2$	261.35	99%	Germany	Merck

3.3 Instrument

We used a several number of instruments to prepare all the ferrite powder some of the instrument that we already used:

1. Sensitive electronic balance

It is an instrument has a high accuracy which allow to as to calculate the white in accuracy of (10^{-4} deg), it is very important instrument as shown in the Fig. (3.1) specially used in scientific laboratory, we should use it carefully and maintain it from inside and outside, and it is better to use the same electronic balance all the time of the research to avoid the mistake.



Fig. (3.1) Sensitive electronic balance

2. Magnetic Stirrer

It is an instrument used in scientific laboratory which the principle of his work is rotated the magnetic field which led to effect on the moving column inside the liquid , that is led to rotate it very fast around itself which eventually led to full mix for the liquid located in the beaker .The magnetic field that generate from the rotating is put inside the instrument that has a thermal spectrum or another way to overheat the liquid, we prefer the magnetic mixer vs. mechanic mixer because it is less noise and more efficiency and does not need extra moving Colum except the one small moving Colum in the bottom of the liquid and this one Colum is easy to maintain, clean, contemned and used again look Fig. (3.2) show the magnetic mix.



Fig. (3.2) Magnetic Stirrer

3. Laboratory oven

It is one of the important laboratory instrument which used in the preparing procedure of the ferrite, this instrument has an advantage of thermal insulation by saving the heat inside him and control it through thermostat preparer for this purpose, Where the oven is working on the heating and drying and sintering samples and all this is made by using (electric oven) device UK made as shown in Fig. (3.3).

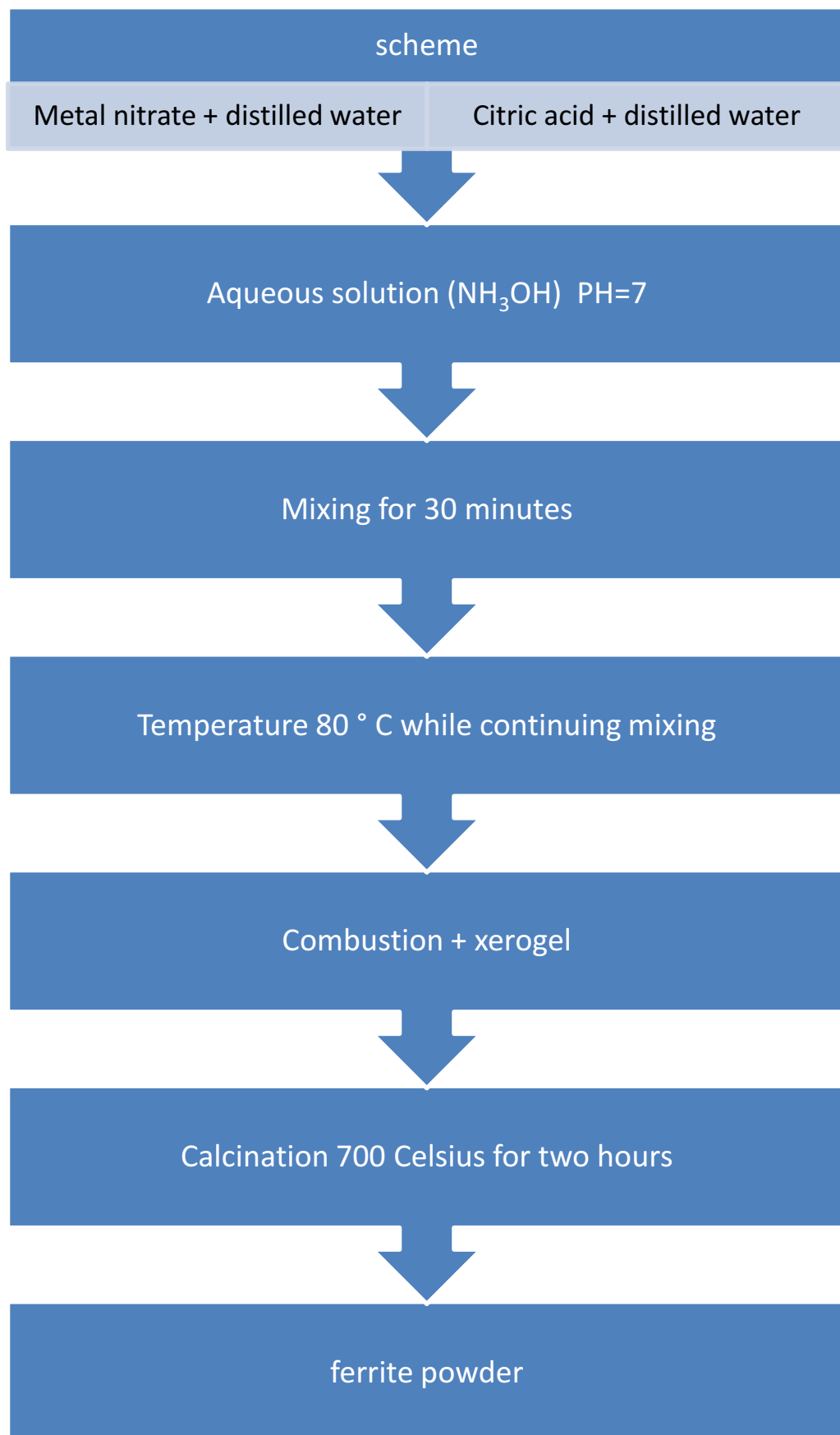


Fig. (3.3) Laboratory oven

3.4 How to prepare

Sol-gel auto combustion method includes with automatic combustion number of steps are summarized as follows:

1. The processing done by melting each of citric acid and nitrates (Metal nitrate) in distilled water separately by molar ratios calculated for each sample.
2. After it became mix all of the acid with water and nitrate with water is a solution that is placed in a large beaker and a suitable heat-resistant (Pyrex), Where the ingredients mix together well by magnetic stirrer during this we adjusted acid (PH) until it become approximately 7 by adding ammonia in the form of drops .
3. Leaves the solution to ensure homogeneity of the components with each other for 30 minutes, where are the good homogeneity and distribution of the solution at room temperature.
4. It is raising the temperature to 80 °C and installed at this point, stirring constantly until the gas starts escalated until a gel form.
5. After a half-hour the gel begins to reignite to form after that xerogel which are milled using a mortar of agate.
6. The resulting powder is placed in a bowl of porcelain (each sample placed in a special container), where we put the samples in an oven at a temperature (700 °C) for the purpose of a calcination process, For two hours at a rate of (5°C /min) upward where they are during calcination to get rid of the remnants of the interaction may be still stuck, such as the remnants of the water and the remnants dioxide resulting from the combustion that occurs during the preparation process so as to get a nutritious phase required, below scheme (1-3) shows the auto combustion sol-gel method .



scheme No. (3-1) auto combustion sol-gel method.

3.5 Prepare of (Ni_{0.7} Zn_{0.3} Fe₂O₄) ferrite

We prepare (Ni_{0.7} Zn_{0.3} Fe₂O₄) by auto combustion sol-gel method when (X=0.3) which is the best value because it gave us best result as shown in the table(3.2) below for the weight ratios of the materials that go into the interaction of the sample preparation and it's (100 g) of metal nitrate

Table (3-2):Quantities calculated to prepare (Ni_{0.7} Zn_{0.3} Fe₂O₄) ferrite by auto combustion sol-gel method

Sample	X	MassOfNiNitrate(g)	MassOfZnNitrate(g)	MassOfFeNitrate(g)	Total MassOfNitrate(g)	ValueOfDistilled water(ml)	MassOfCitric acid(g)	MassOfDistilled water(ml)	Moller ratio(M)
A1	0.3	19.9185	7.9656	72.1158	100	100	17.1430	100	1:1

3.6 prepare of (Ba Fe₁₂O₁₉) ferrite

By using auto combustion sol-gel method for the value (x=0.3). Table (3-3):quantities calculated to prepare (Ba Fe₁₂O₁₉) ferrite by auto combustion sol-gel method

Sample	X	MassOfBaNitrate(g)	MassOfFeNitrate(g)	Total MassOfNitrate(g)	ValueOfDistilled water(ml)	MassOfCitric acid(g)	MassOfDistilled water(ml)	Moller ratio(M)
A1	0.3	5.1165	94.8834	100	100	4.1116	100	1:1

3.7 Prepare of(BaTiO₃)

We prepare (BaTiO₃) by using auto combustion sol-gel method , table

(3-4)

Sample	MassOfHNO ₃ (g)	MassOfTiO ₂ (g)	ValueOfDistilled water(ml)	MassOfCitric acid(g)	MassOfDistilled water(ml)	Moller ratio(M)
BT	30	43.029	100	69.72	100	1:1

3.8 Samples forming

After preparing basic components (BaTiO₃, BaFe₁₂O₁₉& Ni_{0.7}Zn_{0.3}Fe₂O₄) and make all tests have been added to the two compounds(Ba Fe₁₂O₁₉& Ni_{0.7}Zn_{0.3}Fe₂O₄)to (BaTiO₃) with percentages are 20%, 30% and 50% to determine the effect of these compounds on the properties of the insulating compound (BaTiO₃) an operation preparations were obtained as follows (AE) special electrical measurements has been established sampled manner dry pressing where the powders mode weighing (3)g for each sample and the push of a Hydraulic compressor (local made) using the template of a material (stainless steel) Diameter (1.7 cm) , thickness (0.85 cm) and presses (5,4 Mpa)to term period of 5 minutes . We prepare complexes of basic compounds which have been prepared by adding nanoparticles component (Ni_{0.7}Zn_{0.3}Fe₂O₄ and BaFe₁₂O₁₉) by 20%, 30% and 50% to the compound (BaTiO₃) following table represents a ratios and added symbols complexes.



Fig. (3.4) the shape special template for hydraulic piston

Table (3-5): shows the symbols of Nano composites in addition to the ratio(x %)

Samples	Ratio(x %)	Symbols
BaTiO₃	0	BT
20% BaFe₁₂O₁₉+80% BaTiO₃	20	AA 1
30% BaFe₁₂O₁₉+70% BaTiO₃	30	AA 2
50% BaFe₁₂O₁₉+50% BaTiO₃	50	AA 3
20%Ni_{0.7}Zn_{0.3}Fe₂O₄+80%BaTiO₃	20	BB1
30%Ni_{0.7}Zn_{0.3}Fe₂O₄+70%BaTiO₃	30	BB2
50% Ni_{0.7}Zn_{0.3}Fe₂O₄+50% BaTiO₃	50	BB 3

AC - electrical properties Templates

3.9 sintering process

It is the last stage of preparation ferrite after pressing process where the samples are placed (AC) in a British-made electric furnace (carbolite) under normal atmospheric pressure, heating rate 5°C /min and sintered temperature 1100°C, and kept the samples at these temperature for 4 hours, after the completion of the sintering process and extinguish the furnace to the next day where left in the furnace to cool, because direct them out and exposed to air leads to cracking and thus damage to the sample.

3.10 structure test

3.10.1 X-ray diffraction measurement

Is nondestructive analytical technique gives information about the crystal structure and properties of synthetic materials and the device used in this type of search (shimadzu XRD _6000) with the following specifications?

Target Type Cu-K α

The current 30 mA

Voltage difference 40 Kv

Wave length 1.5418 \AA

This device is in the laboratory service of the College of Education, Ibn al-Haytham Pure Sciences where checking this device X-ray diffraction pattern and sites section that appear when we shine X-rays to a range of angles ($2\theta = 10^\circ - 80^\circ$) on the surface of the powder as a result of reflections from crystalline surfaces that gets then overlapping construction of the waves of X-rays of cards (ICDD) International Centre for Diffraction Data this could be ascertained from ferrite output accuracy, also provides us with device information included in the table showing the angles of diffraction and the distance between the crystalline levels and relative intensity of each summit and a maximum width at mid-intensity (FWHM) This information is important for the physical calculation and Fig. (3.5) shows the device used in this research.



Fig. (3.5) a picture of the device (XRD) which is a type of (shimadzu XRD -6000)

3.10.2 Scanning electron microscope measurement (SEM)

This technique provides us with more three-dimensional surface of the sample and by exploiting electronics counter, not the window as a result of a collision with a sample this way we can see the unseen world of minute objects Particularly with regard to installation Nano scale by image in black and white for them zoom power up to 100,000 times and that the light source is a fuse element is made of a product for electronics counting heated up. This was called the microscope scanner because it is based not filmed the sample once, but the concentration of electronics beam, on a small spot of the sample and captures the image and then moves to the neighboring spot and picked it up and so on, that is, it does not get the image of the sample completely, but picked up point by point, and then combines comic dots to form the final image on a computer screen [157] in our research is the use of the microscope type (Inspect S 50) as in Fig. (3.6) [158].



Fig. (3.6) is a picture of the scanning electron microscope (SEM)

which has been taking the picture of the samples and analysis (analysis of the resulting image) using the program (Image-j), it is special program used for image analysis in two and three-dimensional and also provides us with a summary of the area distribution calculated after the analysis process, which includes a number of granules in the picture (count) and smaller (Min) and largest (Max) dots on the image area.

3.10.3 Energy – dispersive X-ray spectroscopy (EDS)

Is an analytical technique used to determine the type of items or chemical analysis of the samples, where the principle of this technique depends on the X-rays resulting from the mutual impact between charged particles, such as a package of electrons with the sample material and the resulting X-ray shall be distinct of the constituent elements of the sample so you can figure out the chemical composition of the sample. chemical element distinguished group in the spectrum of X-rays. For X-rays characteristic of the sample, should excite the atoms first, and this happens when the sample ejected beam of electrons as in (SEM) scanning electron as a result, liberated electron from the inner orbital of the atom this leads to the occurrence of irritation and instability operation and process, due to the occurrence of a vacancy electronic that fills the orbits of

atomic highest and when the electrons move from the orbits of atomic highest to the orbits of atomic lowest it sends an X-ray with energy equal to the energy difference between the orbits and the difference between the energy is unique for each element and there are a number of allowable transitions between atomic orbitals, which symbolized by (K_{α} , K_{β} , K_{γ}), as shown in the Fig. (3.7) [159].

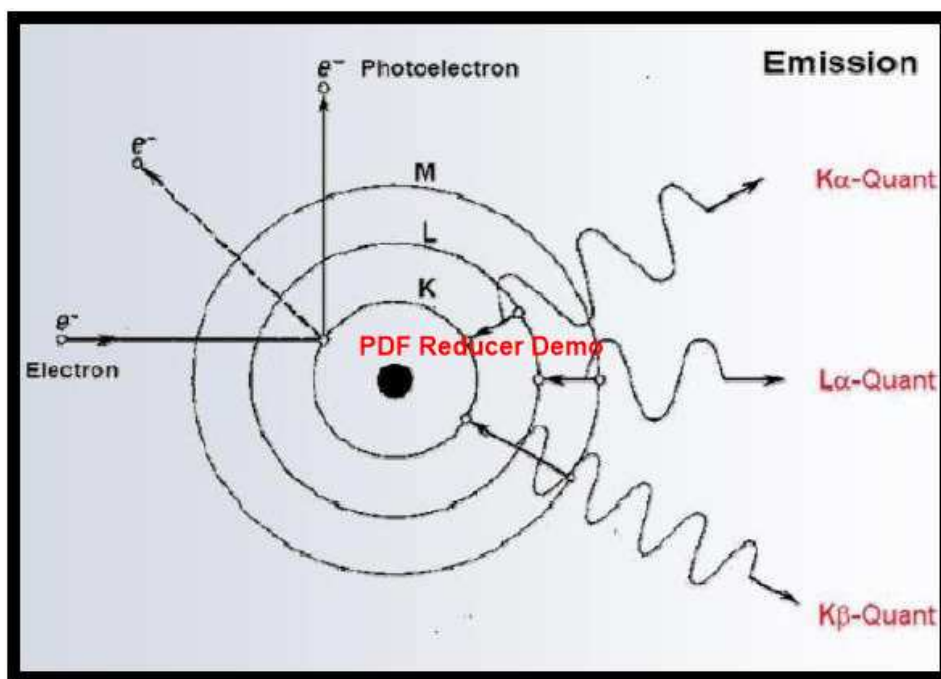


Fig. (3.7) picture of transferring (EDS) [159]

3.11 The electronic properties measurement

Were prepared polarities special for electrical tests (AE) and through coating the opposite surfaces with material (silver paste), in order to be connected to the device electrodes (LCR meter) used to measure the electrical properties of this type of device (50 Hz -1 MHz) GPIB , RS ,232 ,Taiwan Gwinstek ,LRC -8105 (2050), and connected to their computer to show the results directly on the screen, where it is by this device measuring the amplitude (C_p) remained loss angle ($\tan \delta$) and resistance alternating as a function of frequency for a frequency range of (50 Hz - 1 MHz), as well as measuring continuous resistance as a function of difference voltage change and its use can

get (Dielectric constant ϵ_r , Dielectric loss factor ϵ_r'' , Alternating electrical conductivity ($\sigma_{a.c}$) and Fig. (3.8) shows the device (LCR meter) user [160].



Fig. (3.8) (LCR meter) device

3.12 Measuring the Dielectric Strength.

High Voltage supplier was used with a range (0-60 kV) and frequency (50 HZ) of the type (BAUR-PGO-S-3) Germany origin. Where they are measuring the development of samples in a liquid with a high dielectric strength (transformer oil 40 kV/mm) to overcome the problem of transmission of the spark catch (Flashover) There is another reason to use this liquid is the elevation of it is burning temperature, so that used in the study of change dielectric strength with temperature and the rang of (35-110°C) by heating the oil, and poles from brass to insurance good conductivity and the sample touch point with the pole spherical (2mm) in diameter, and the measuring is madding by putting the sample between the poles, which is embedded in oil, and applicate voltage on the sample surface until the breakdown insulator is happened and the current pass through the sample, and the breakdown effect ion on the sample appear then breakdown voltage for the sample measured and sample thickness measured from the breakdown point by micrometer, the dielectric strength is

calculated, and the transforming oil was changed after finishing from several measurements, to insure that no ionization in transforming oil is happened which leads to inaccuracy in measurement, as shown in the Fig. (3-9)[161].



Fig. (3-9) dielectric strength equipment [161].

Chapter four
Results and
Discussions

4.1 Introduction.

This chapter includes a two-step, the first-step is explain results of manufacturing of BaTiO_3 , $\text{Ni}_{0.7}\text{Zn}_{0.3}\text{Fe}_2\text{O}_4$ and $\text{BaFe}_{12}\text{O}_{19}$ Nano powders by sol-gel auto combustion technique, and treated at 900°C . While second-step explanation dielectrically properties for composite samples, disc form with a diameter of (1.7) cm and (0.85 cm) thickness and treated at (1100°C).

4.2 The properties of BaTiO_3 , $\text{Ni}_{0.7}\text{Zn}_{0.3}\text{Fe}_2\text{O}_4$ and $\text{BaFe}_{12}\text{O}_{19}$ Nanopowders.

4.2.1 X-ray Diffraction.

The XRD patterns of the BaTiO_3 , $\text{Ni}_{0.7}\text{Zn}_{0.3}\text{Fe}_2\text{O}_4$ and $\text{BaFe}_{12}\text{O}_{19}$ Nano powders after calcinations at 700°C , they were formed at $\text{pH} = 7$, shown in Figs. (4.1), (4.2) and (4.3) respectively.

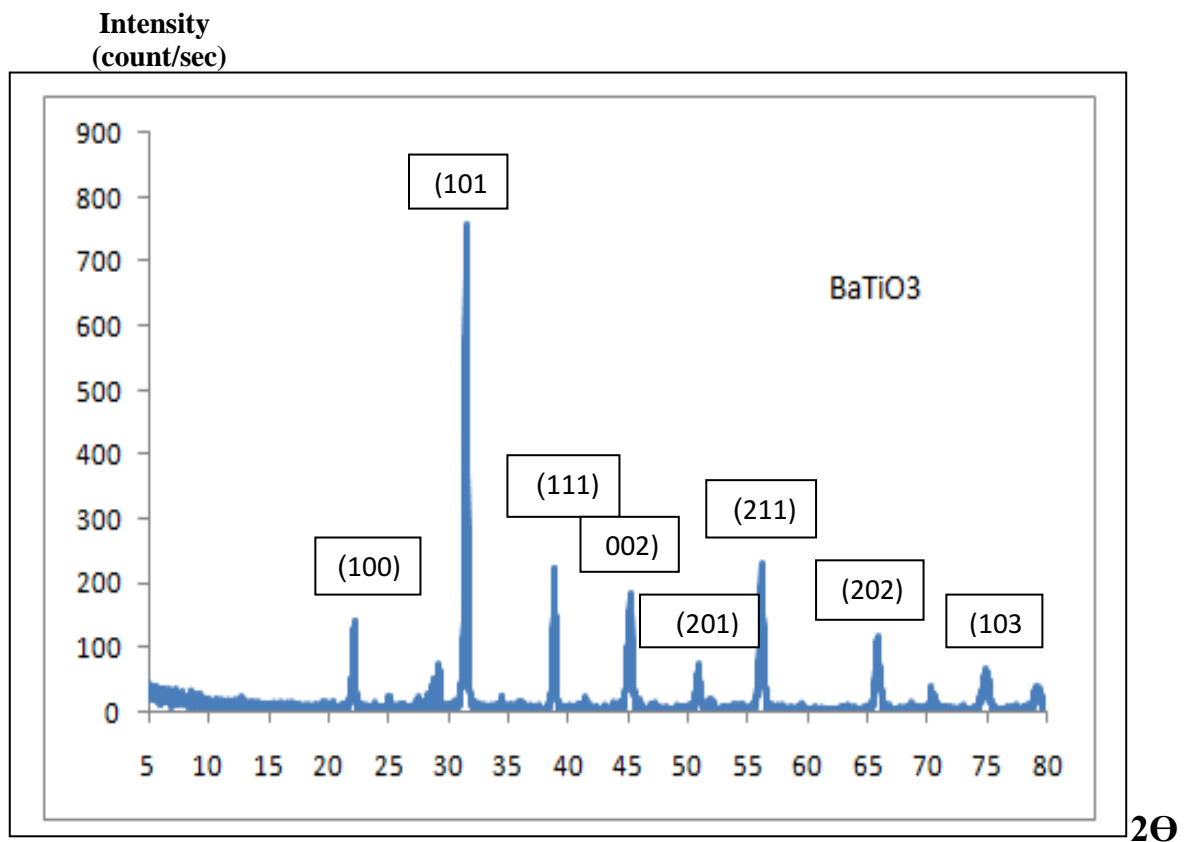


Fig.(4.1) The XRD for(BaTiO_3 Nano powder)specimen.

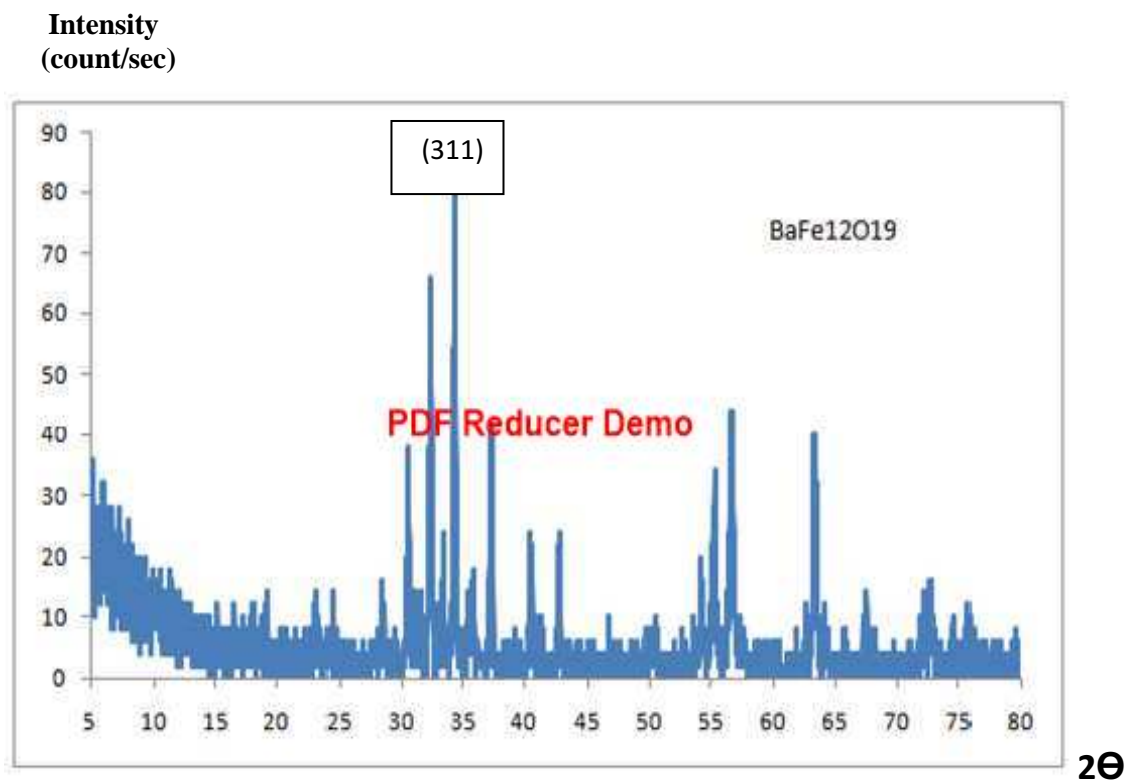


Fig.(4.2) The XRD for (BaFe₁₂O₁₉ Nano powder)specimen.

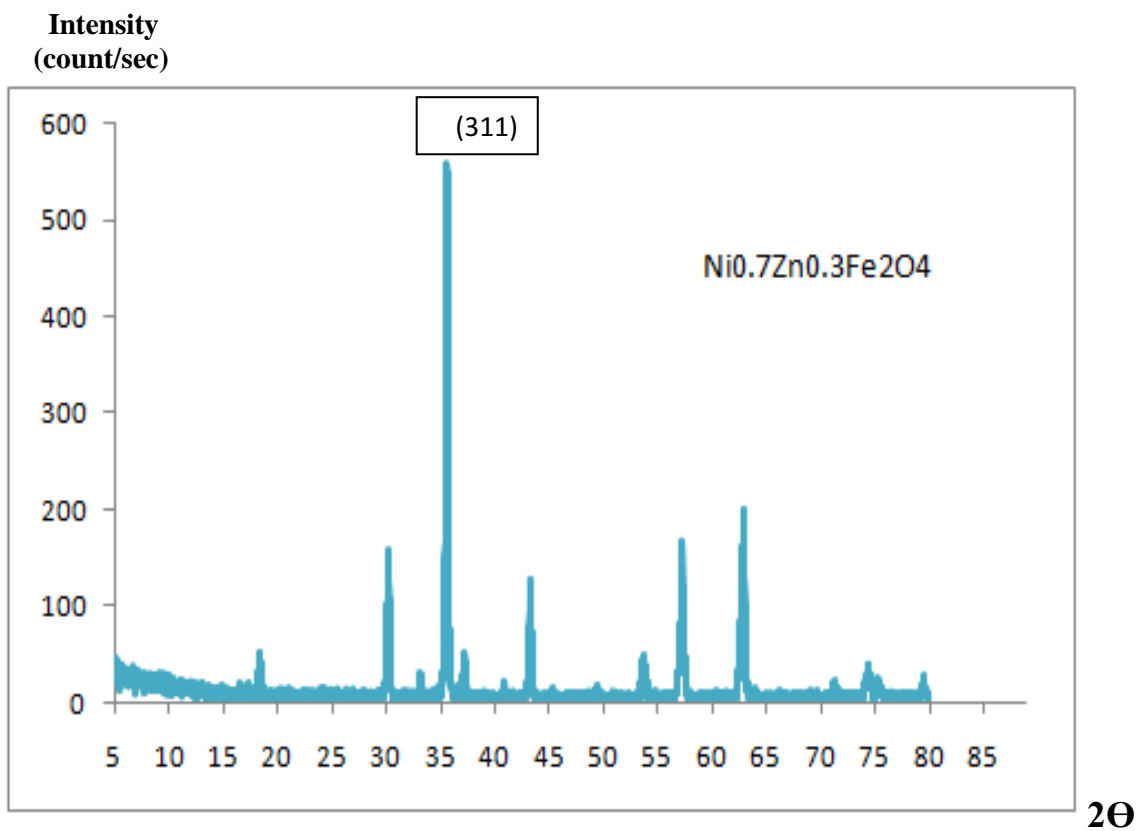


Fig.(4.3) The XRD for (Ni_{0.7}Zn_{0.3}Fe₂O₄ Nano powder)specimen.

After comparing the (X-ray) diffraction pattern of the(BaTiO₃), (BaFe₁₂O₁₉) and (Ni_{0.7}Zn_{0.3}Fe₂O₄)Nano powders, prepared in sol-gel auto combustion technique with standard tetragonal (no intermediate phases are present here) BaTiO₃ phase (JCPDS No.31-0174) [162]. This implies that the particles are apparently stabilized in the cubic form at room temperature, but with decreased (~100 nm) crystal size. This phenomenon shows that the transformation of barium titanate is a function of temperature and crystal size, the cubic form of BaTiO₃ is non-polar [163].

4.2.2 Indexing X-ray diffraction patterns.

Indexing of spectra X-ray diffraction was used for BaTiO₃, BaFe₁₂O₁₉ and Ni_{0.7}Zn_{0.3}Fe₂O₄Nano powders prepared in sol-gel auto-combustion technique .using (Dicvol 91)program, we obtained the X-ray diffraction in the range of (2θ from 5 to 80) for each sample. Then the output indexing data was analysis by using (Full prof) program, which the depends on Ratvld analyzes crystal structure after that the results were lasted the calculated (R_p),(R_{wp})and(R_{exp}) factors by the program .

The Ratvld analyzes crystal structure is shown in Fig. (4.4),(4.5) and (4.6) respectively. Table (4.1): The(R_p),(R_{wp})and(R_{exp}) Reliability factors for Ratvld analyzes crystal structure, (Space group) and (phase) values for BaTiO₃, BaFe₁₂O₁₉ and Ni_{0.7}Zn_{0.3}Fe₂O₄Nano powders prepared at sol-gel auto combustion technique.

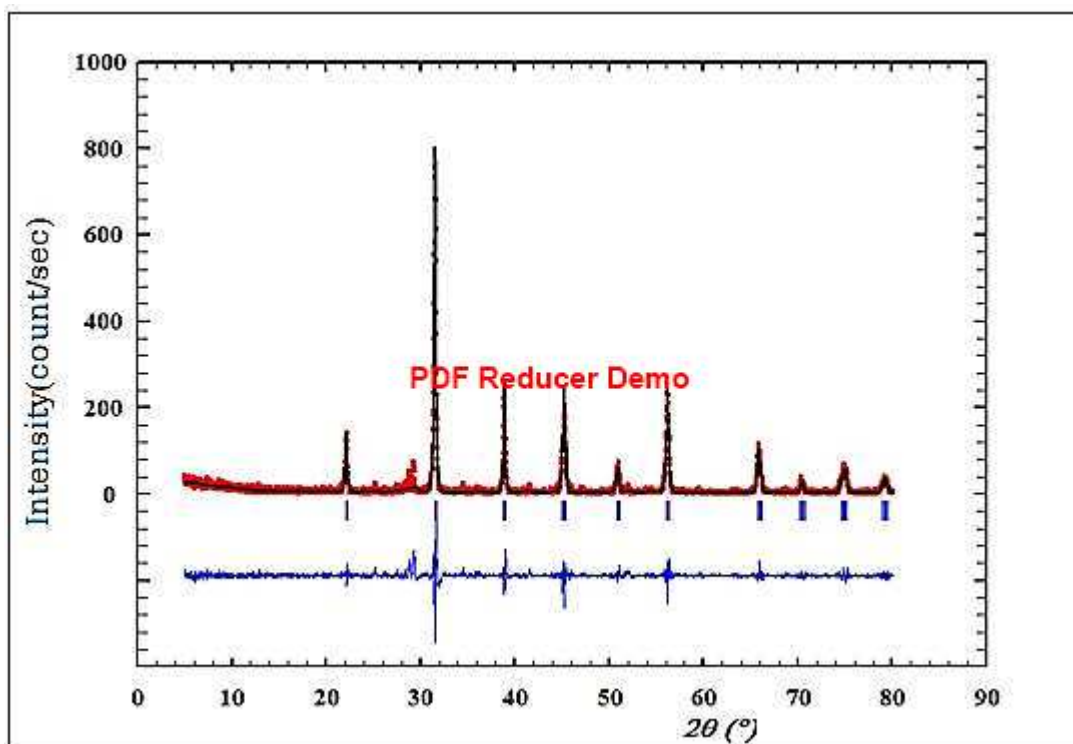


Fig. (4.4) Rietveld refinement for BaTiO₃ using Fullprof program

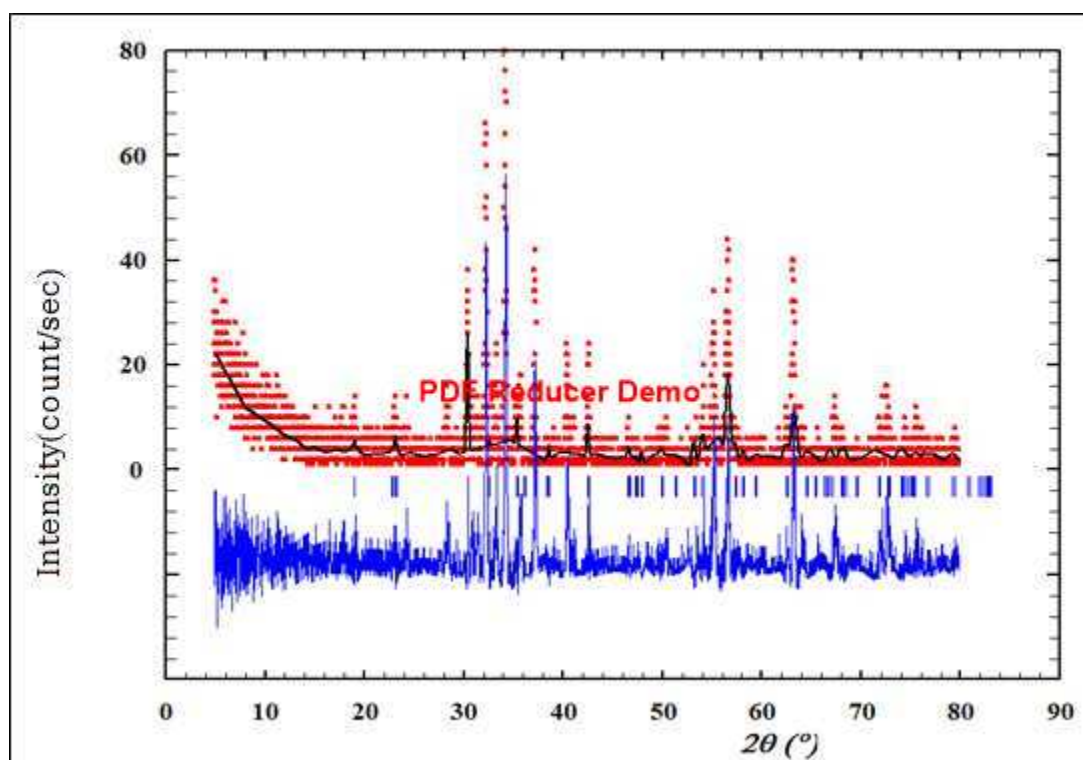


Fig. (4.5) Rietveld refinement for BaFe₁₂O₁₉ using Fullprof program

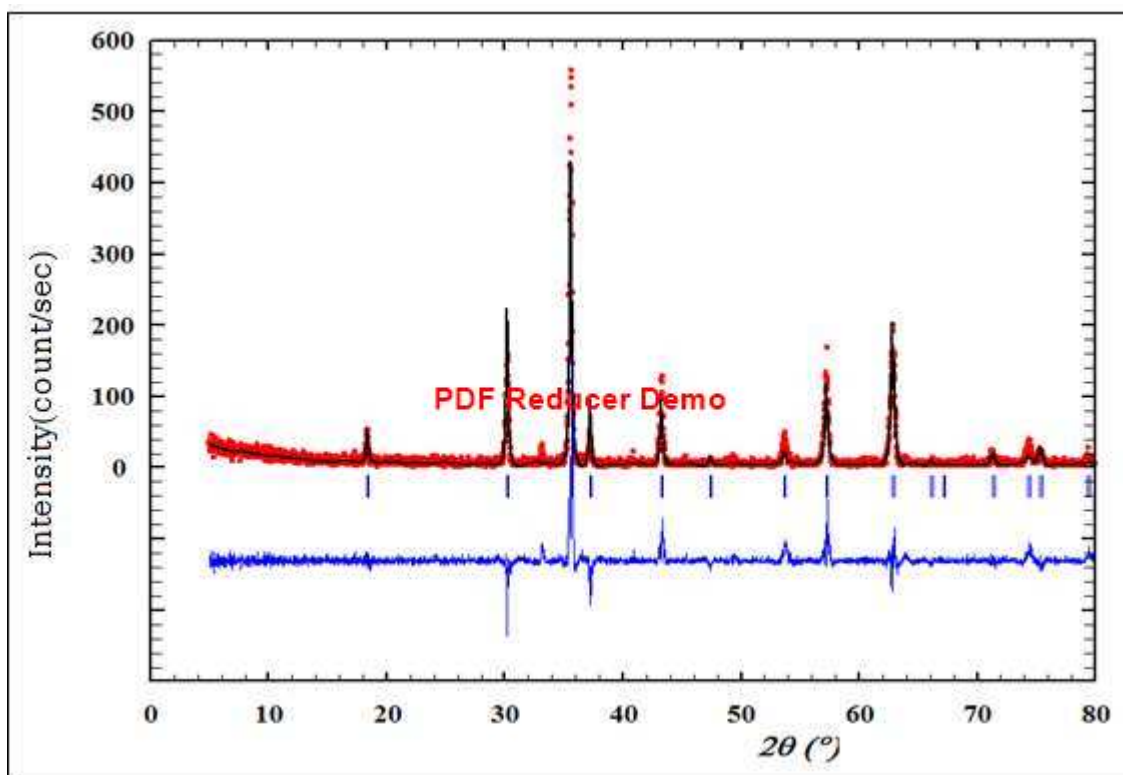


Fig. (4.6) Rietveld refinement for $\text{Ni}_{0.7}\text{Zn}_{0.3}\text{Fe}_2\text{O}_4$ using Fullprof program

Table (4-1): The (R_p), (R_{wp}) and (R_{exp}) Reliability factors for Ratvlad, (Space group) and (phase) values for BaTiO_3 , $\text{BaFe}_{12}\text{O}_{19}$ and $\text{Ni}_{0.7}\text{Zn}_{0.3}\text{Fe}_2\text{O}_4$ compounds prepared at sol-gel auto combustion technique

Sample	R_p	R_{wp}	R_{exp}	Space group	Phase
BaTiO_3	22.2	30	31.5	P4mm	Tetragonal
$\text{BaFe}_{12}\text{O}_{19}$	46.4	51.7	1.23	P63mm	Hexagonal
$\text{Ni}_{0.7}\text{Zn}_{0.3}\text{Fe}_2\text{O}_4$	46.4	51.7	1.23	FD3m	Cubic

4.2.3 The lattice of BaTiO_3 , $\text{BaFe}_{12}\text{O}_{19}$ and $\text{Ni}_{0.7}\text{Zn}_{0.3}\text{Fe}_2\text{O}_4$ Nano compound and the length of ion.

It was painted crystal lattice of the BaTiO_3 , $\text{BaFe}_{12}\text{O}_{19}$ and $\text{Ni}_{0.7}\text{Zn}_{0.3}\text{Fe}_2\text{O}_4$ Nano compounds by (Full prof) program, as well as it has been identified lattice parameters as illustrated Fig. (4.7) – (4.9) . Table (4.2),(4.3) and (4.4) shows the atoms site in BaTiO_3 , $\text{BaFe}_{12}\text{O}_{19}$ and $\text{Ni}_{0.7}\text{Zn}_{0.3}\text{Fe}_2\text{O}_4$ lattice .

Table (4-2): shows the atoms site in BaTiO_3 lattice

Atom	X	Y	Z
Ti	0.50000	0.50000	0.51000
O.	0.50000	0.00000	0.47900
O	0.50000	0.50000	-0.02200
Ba	0.00000	0.00000	0.00000

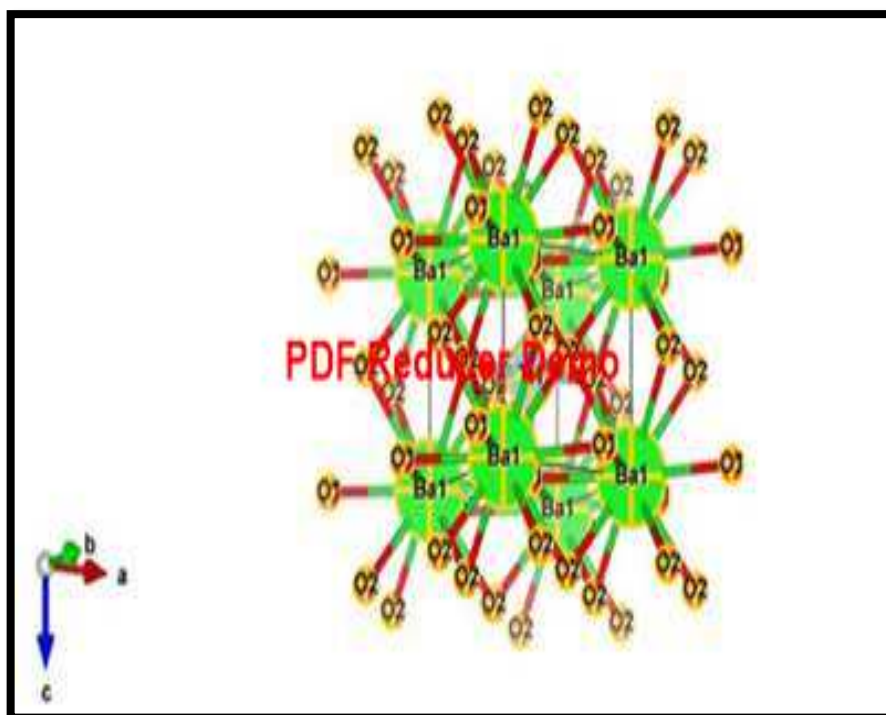


Fig. (4.7) schematic of BaTiO_3 unit cell.

Table (4-3): shows the atoms site in BaFe₁₂O₁₉ lattice

Atom	X	Y	Z
Ba	0.66667	0.33333	0.28312
Fe1	0.00000	0.00000	0.02210
Fe2	0.00000	0.00000	0.25000
Fe3	0.33333	0.66667	0.02710
Fe4	0.33333	0.99970	0.19030
Fe5	0.17130	0.34260	-0.10840
O1	0.00000	0.00000	0.14500
O2	0.33000	0.66667	-0.05450
O3	0.18640	0.37290	0.25000
O4	0.15830	0.31660	0.05140

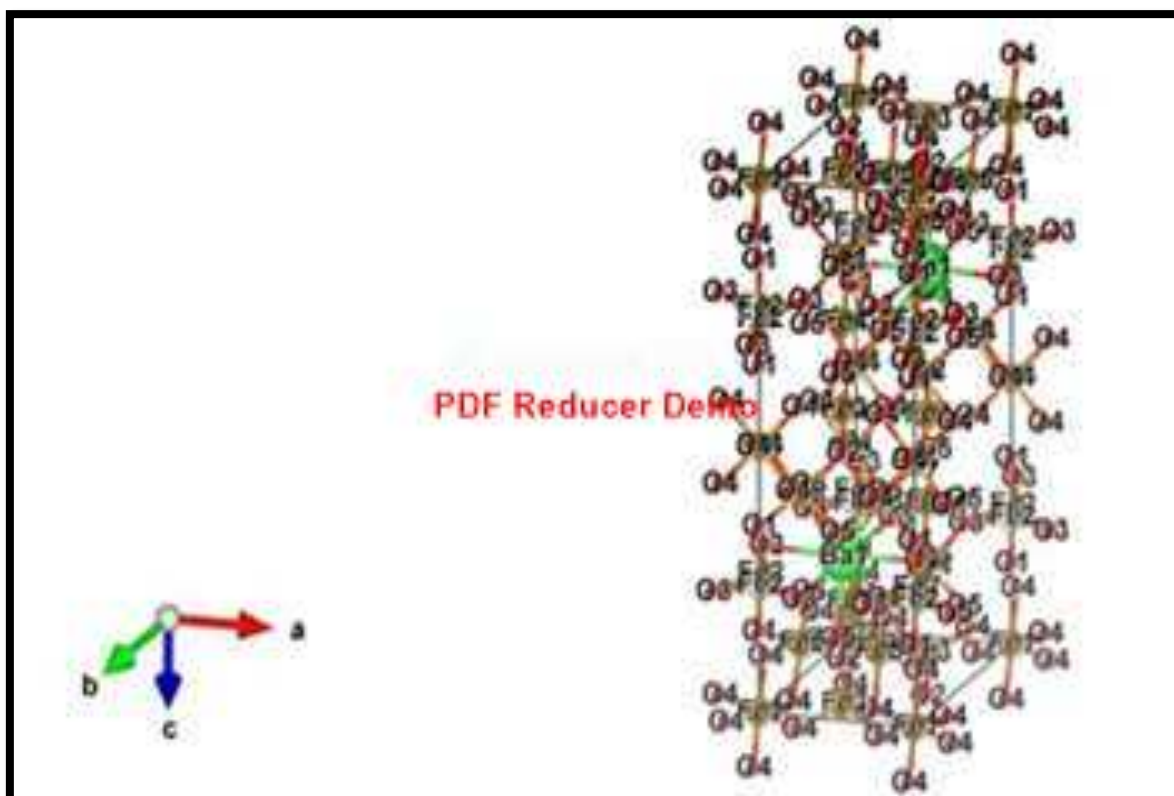
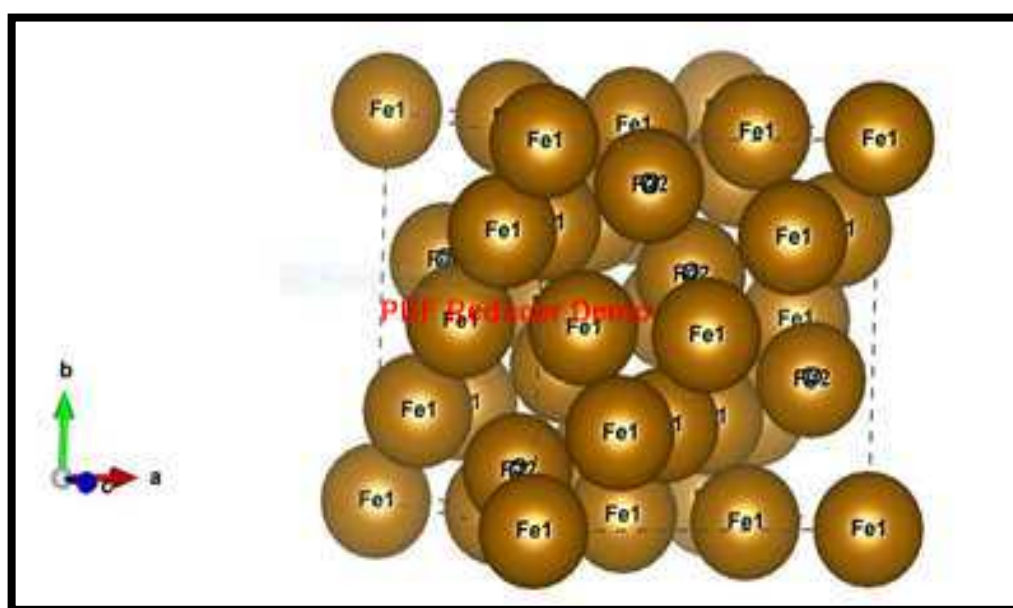
Fig. (4.8) schematic of BaFe₁₂O₁₉ unit cell.

Table (4-4): shows the atoms site in $\text{Ni}_{0.7}\text{Zn}_{0.3}\text{Fe}_2\text{O}_4$ lattice

Atom	X	Y	Z
Fe1	0.00000	0.00000	0.00000
Fe2	0.62500	0.62500	0.62500
Ni	0.62500	0.62500	0.62500
Zn	0.00000	0.00000	0.00000
O	0.38000	0.38000	0.38000

Fig. (4.9) schematic of $\text{Ni}_{0.7}\text{Zn}_{0.3}\text{Fe}_2\text{O}_4$ unit cell.

4.2.4 Theoretically calculate the lattice parameters, the unit cell size and density.

It was calculated the lattice parameters, (c/a) ratio, the unit cell size, density of the BaTiO_3 , $\text{BaFe}_{12}\text{O}_{19}$ and $\text{Ni}_{0.7}\text{Zn}_{0.3}\text{Fe}_2\text{O}_4$ specimens prepared in sol-gel auto combustion technique, by using the following equations (2.8), (2.9) and (2.10). Table (4.5) shows lattice parameters, (c/a) ratio, and the unit cell size, density of the BaTiO_3 , $\text{BaFe}_{12}\text{O}_{19}$ and $\text{Ni}_{0.7}\text{Zn}_{0.3}\text{Fe}_2\text{O}_4$ Specimens.

Table (4-5): shows lattice parameters, (c/a) ratio, the unit cell size, density of the BaTiO_3 , $\text{BaFe}_{12}\text{O}_{19}$ and $\text{Ni}_{0.7}\text{Zn}_{0.3}\text{Fe}_2\text{O}_4$ Nano compounds

Sample	a(Å)	b(Å)	c(Å)	c/a	V(Å ³)	$\rho_{x\text{-ray}}$ (g/cm ³)
BaTiO_3	3.9915 0	3.9915 0	4.02500	1.00839 3	64.6647	6.007
$\text{BaFe}_{12}\text{O}_{19}$	5.8790 0	5.8790 0	23.4030 0	3.98077 9	3219.9307	5.389
$\text{Ni}_{0.7}\text{Zn}_{0.3}\text{Fe}_2\text{O}_4$	8.4170	8.4170	8.4170	1.0000	596.3098	5.345

Table (4-6): shows practical size of the BaTiO_3 , $\text{BaFe}_{12}\text{O}_{19}$ and $\text{Ni}_{0.7}\text{Zn}_{0.3}\text{Fe}_2\text{O}_4$ Nano compounds

Samples	D(nm)
BaTiO_3	10.46
$\text{BaFe}_{12}\text{O}_{19}$	12.7
$\text{Ni}_{0.7}\text{Zn}_{0.3}\text{Fe}_2\text{O}_4$	19

4.2.5 Scanning Electron Microscopy (SEM).

As shown in the surface topography results (SEM). Surface micrographs for the (BaTiO_3 , $\text{BaFe}_{12}\text{O}_{19}$ and $\text{Ni}_{0.7}\text{Zn}_{0.3}\text{Fe}_2\text{O}_4$ Nano powders) specimens are shown in Figs. (4.10, 4.11 and 4.12), the results show a cubic BaTiO_3 which forms sphere like particles [164].

The grain size as shown from (SEM) results is around (20,36 and 19) nm for BaTiO_3 , $\text{BaFe}_{12}\text{O}_{19}$ and $\text{Ni}_{0.7}\text{Zn}_{0.3}\text{Fe}_2\text{O}_4$ Nano powders, which are agree with the particle size obtained from x-ray data using Scherer's formula which gave average particle size around (10.46, 12.7 and 19) nm. As shown from SEM image the particles have different sizes and possible agglomerations also some particles appear larger than originally size in x-ray scan .This is because of the upper limit of Scherer's about 100 nm [165].

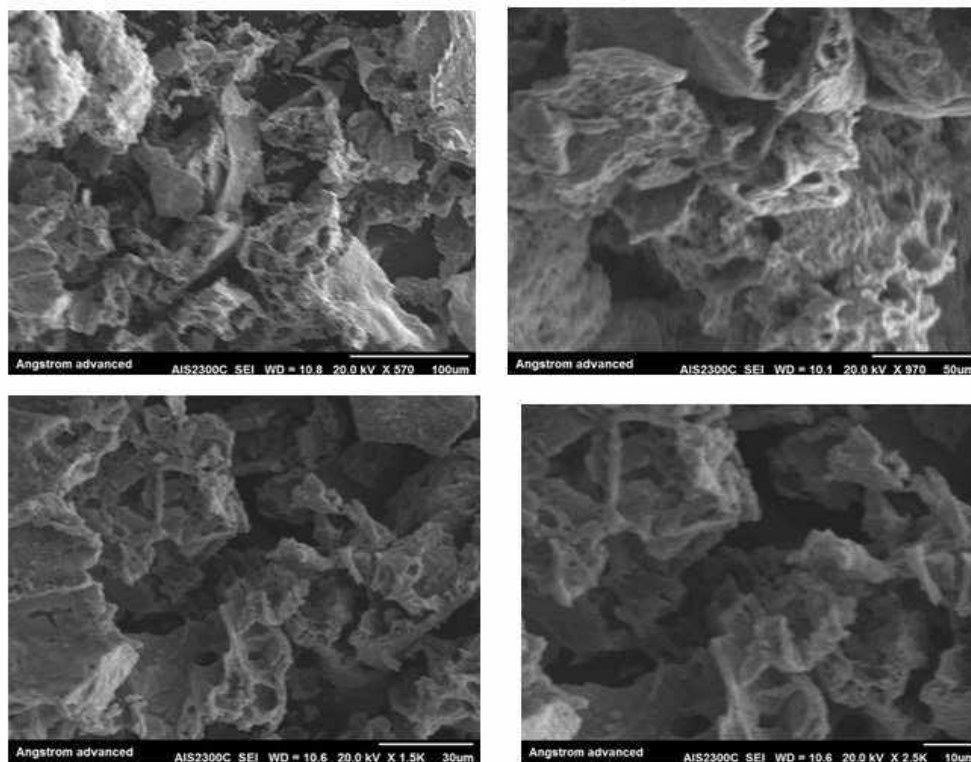


Fig. (4.10) The SEM image of BaTiO₃ Nano powder.

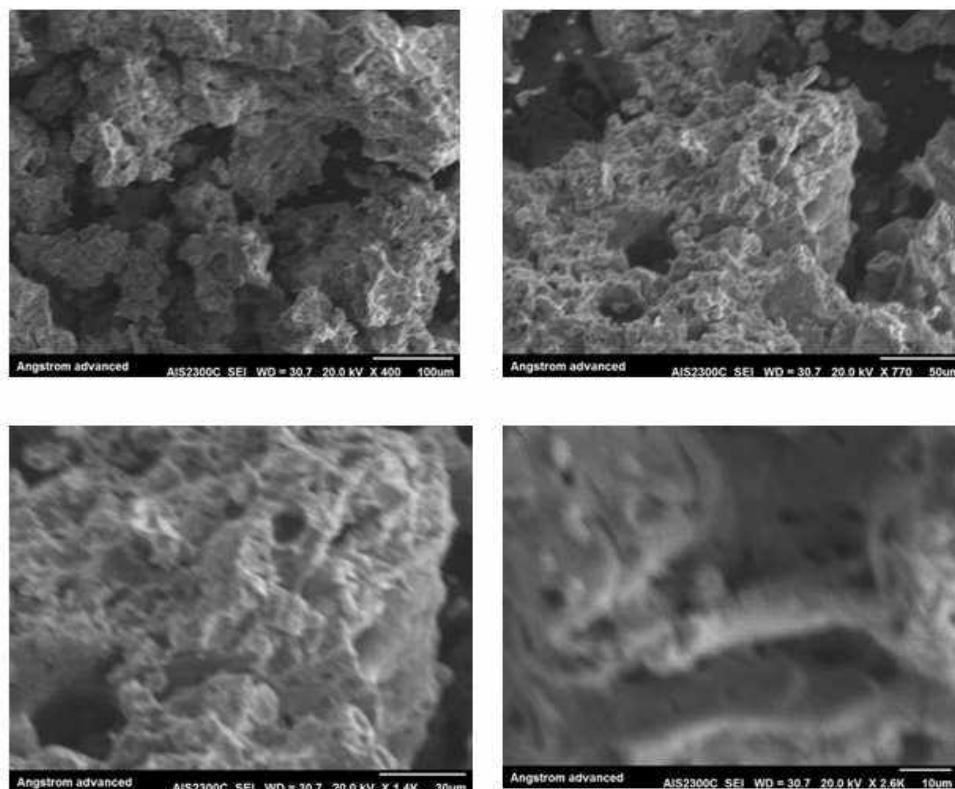


Fig. (4.11) The SEM image of BaFe₁₂O₁₉ Nano powder.

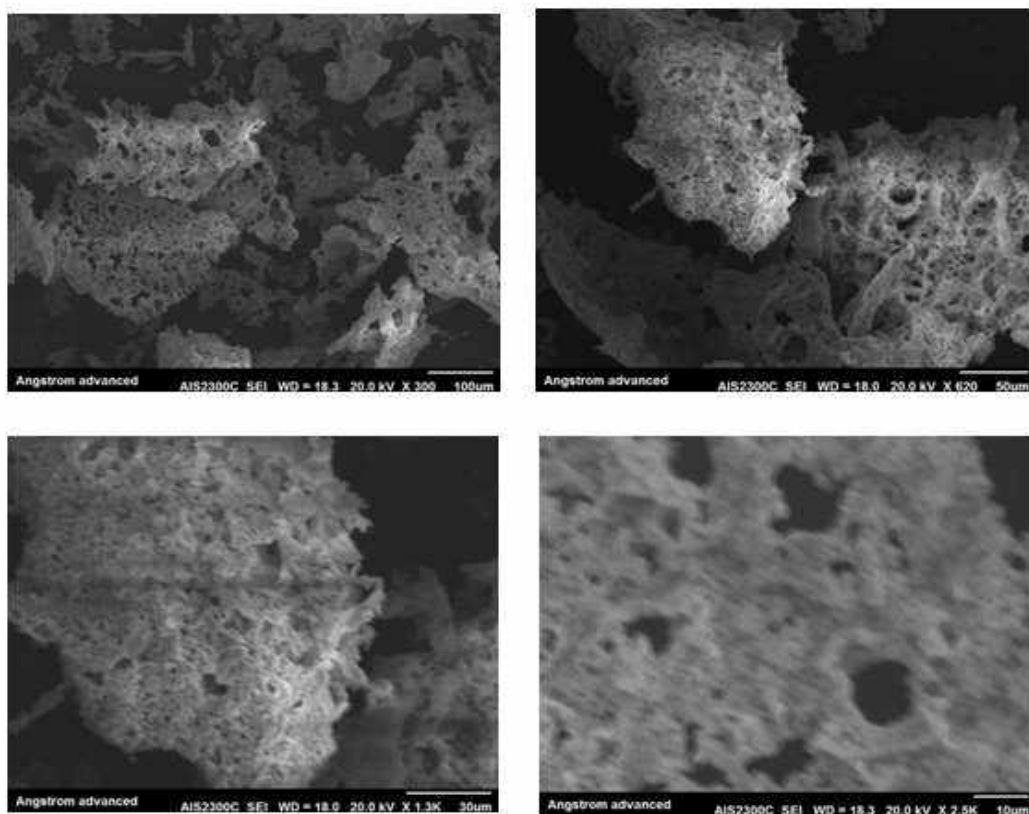


Fig. (4.12) The SEM image of BaFe₁₂O₁₉Nano powder

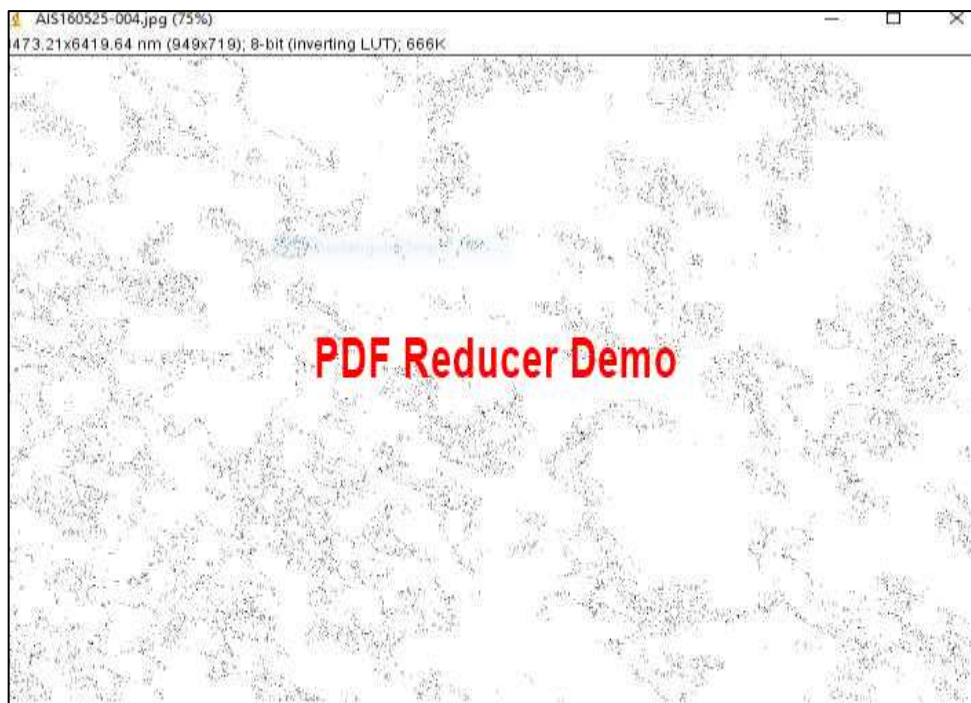


Fig. (4.13) the image j of BaTiO₃ Nano powder

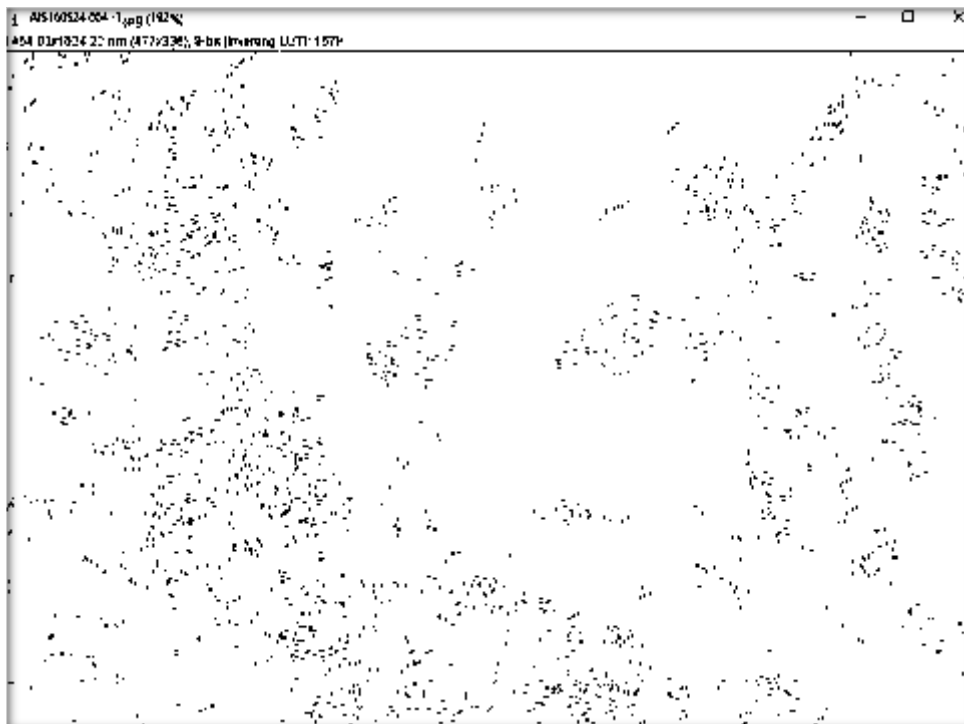


Fig. (4.14) the image j of $\text{BaFe}_{12}\text{O}_{19}$ Nano powder



Fig. (4.15) the image j of $\text{Ni}_{0.7}\text{Zn}_{0.3}\text{Fe}_2\text{O}_4$ Nano powder

4.2.6 Analysis of the Results of EDS

The Figs. (4.18 - 4.20) are shown analysis of the results for (BaTiO_3 , $\text{BaFe}_{12}\text{O}_{19}$ and $\text{Ni}_{0.7}\text{Zn}_{0.3}\text{Fe}_2\text{O}_4$ Nano powders) specimens by EDS.

EDS analysis of the BaTiO_3 compound shows that the ratio of Ba: Ti: O is about [56.52:14.23:29.25] as shown in Fig. (4.18). While the EDS results for $\text{BaFe}_{12}\text{O}_{19}$ specimen in figure (4.19) shows that the percentage of [Ba: Fe: O] is about 11.00:41.24:47.76. The third $\text{Ni}_{0.7}\text{Zn}_{0.3}\text{Fe}_2\text{O}_4$ compound from figure (4.20) we can find the ratio of Ni: Zn: Fe: O is [15.80:3.86:58.87: 21.48]. These results .Notes through these results show that the elements are blended to prepare BaTiO_3 , $\text{BaFe}_{12}\text{O}_{19}$ and $\text{Ni}_{0.7}\text{Zn}_{0.3}\text{Fe}_2\text{O}_4$ specimens have maintained lineage after sintering.

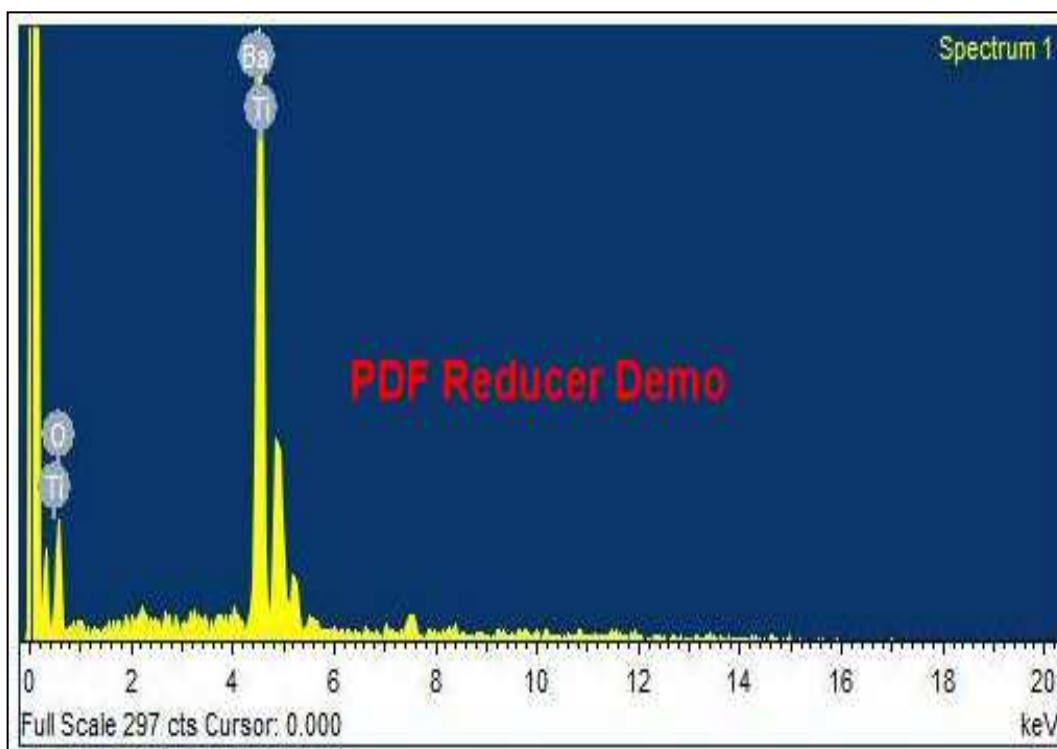


Fig. (4.16) EDX patterns of the BaTiO_3 Nano compounds.

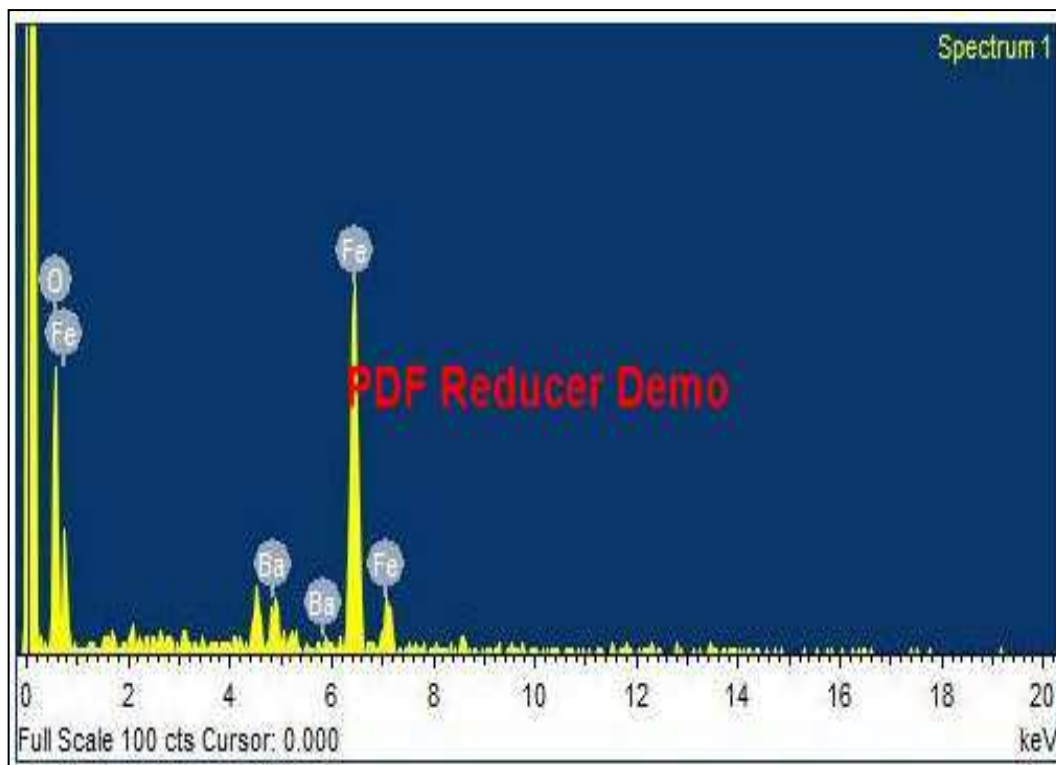


Fig. (4.17) EDX patterns of BaFe₁₂O₁₉ Nano powder.

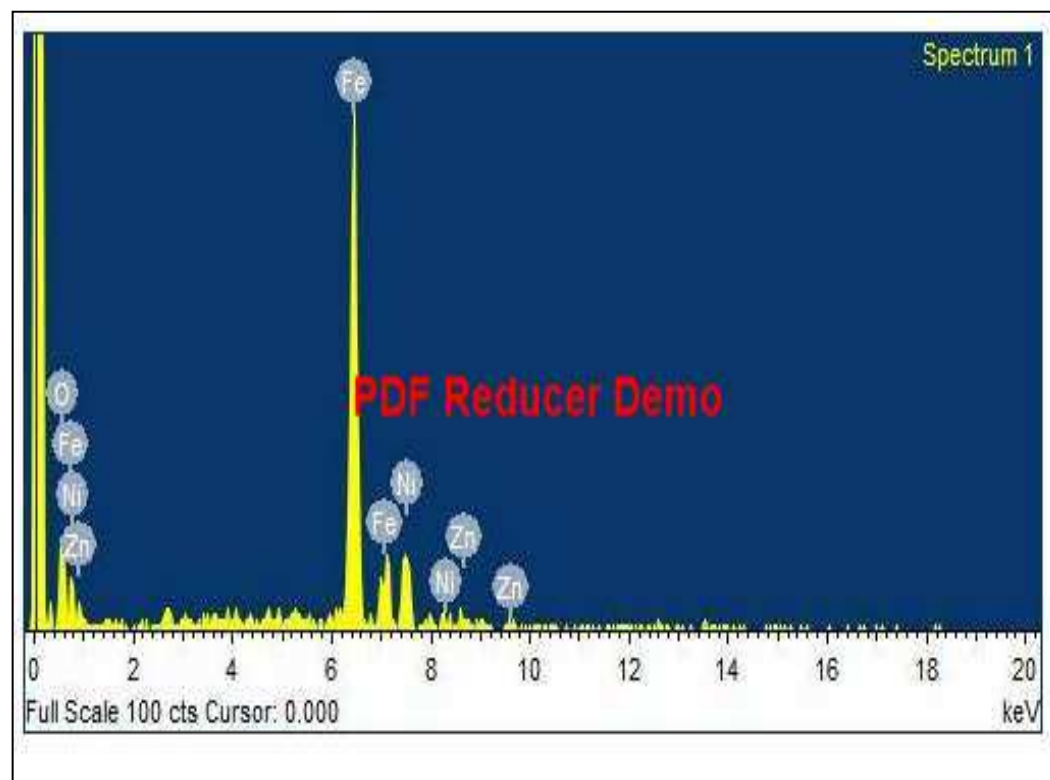


Fig. (4.18) EDX patterns of Ni_{0.7}Zn_{0.3}Fe₂O₄ Nano powder.

Table (4-7): shows Weight% and Atomic% for BaTiO₃, BaFe₁₂O₁₉ and Ni_{0.7}Zn_{0.3}Fe₂O₄ Nano compounds

BaTiO ₃			BaFe ₁₂ O ₁₉			Ni _{0.7} Zn _{0.3} Fe ₂ O ₄		
Element	Weight %	Atomic %	Element	Weight %	Atomic %	Element	Weight %	Atomic %
O	29.25	72.07	O	47.76	78.48	O	21.48	49.27
Ti	14.23	11.71	Fe	41.24	19.41	Fe	58.87	38.69
Ba	56.52	16.22	Ba	11.00	2.11	Ni	15.80	9.87
						Zn	3.86	2.17

4. 3 dielectrically characteristic.

4. 3.1:- Dielectric Constant (ϵ'_r)

The dielectric characteristics can vary widely between solids, which are a function of frequency of field and other external factors, and the response can nonlinear or linear [166].

The electrical properties include, the frequencies special effects on the (ϵ'_r), (ϵ''_r), ($\tan\delta$), and ($\sigma_{a.c}$) at the range (50-10⁶)Hz, in the (RT), also involve Breakdown voltage and dielectric strength measurements . Figs. (4.21 and 4.22) shows vary of (ϵ'_r) values with frequencies at (RT), within range from 50 Hz to 10⁶Hz. These figures refer to decreases gradually (nonlinear) in (ϵ'_r) values with increasing of frequencies of applied field. Also we note at high frequencies, the (ϵ'_r) values became approximately constant for all spaceman's, where due to the polarization effects.

Effects of BaFe₁₂O₁₉ and Ni_{0.7}Zn_{0.3}Fe₂O₄ add to the BaTiO₃ nominal composition on the (ϵ'_r) measurements were investigated. The results are (ϵ'_r) =39.605 for the BaTiO₃ nominal composition, while(AA1) and (AA2) equal (29.90132), (44.11444), and (BB1),(BB2) =(7.83247), (4.486934)at 1MHz. the

(ϵ'_r) values decrease with the increases of ratios (20% and 50%) . but at low frequency (50Hz) for the (ϵ'_r) values are increases with the increases of ratios (20% and 50%) for AA groups, while BB groups decrease and increases in the (ϵ'_r) values with the increases of ratios (20% and 50%).

From (50Hz-1MHz) the (ϵ'_r) values at for (AA1,AA2) and (BB1,BB2) specimens', decrease from (64.9532, 83.22725) and (18.50124, 76.06546) to (29.90132, 44.11444) and (7.83247, 4.48693) respectively, due to the increase the gradual crystallization at heat treatment, this means increase the level of a chemical reaction and the decrease in the total pores, which leads to getting better properties.

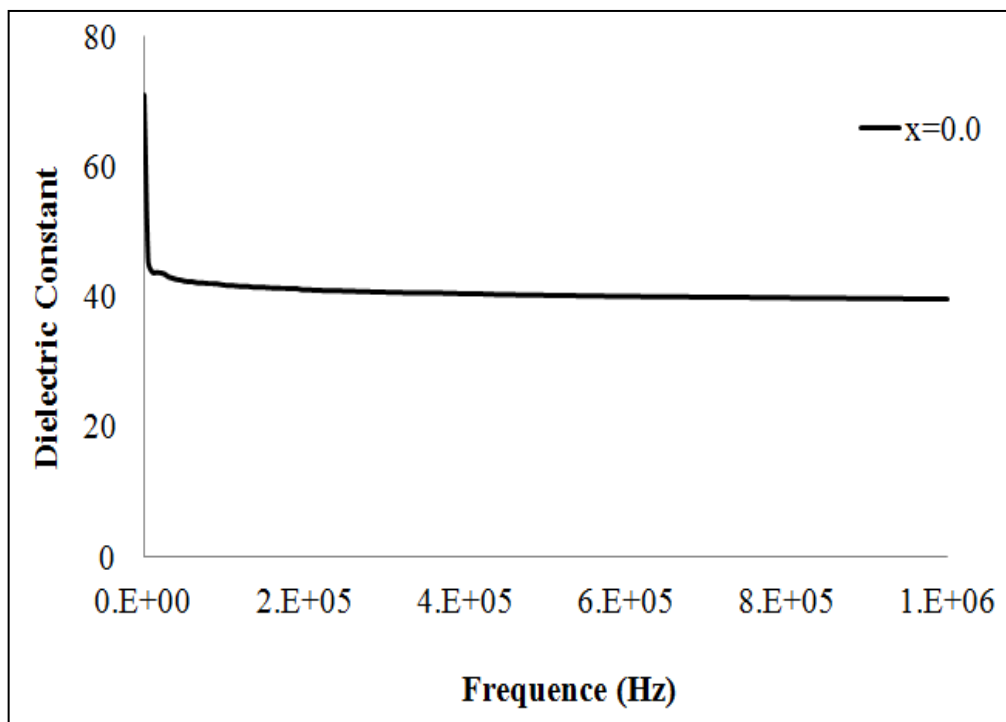


Fig. (4.19) (ϵ'_r) of BaTiO₃specimens.

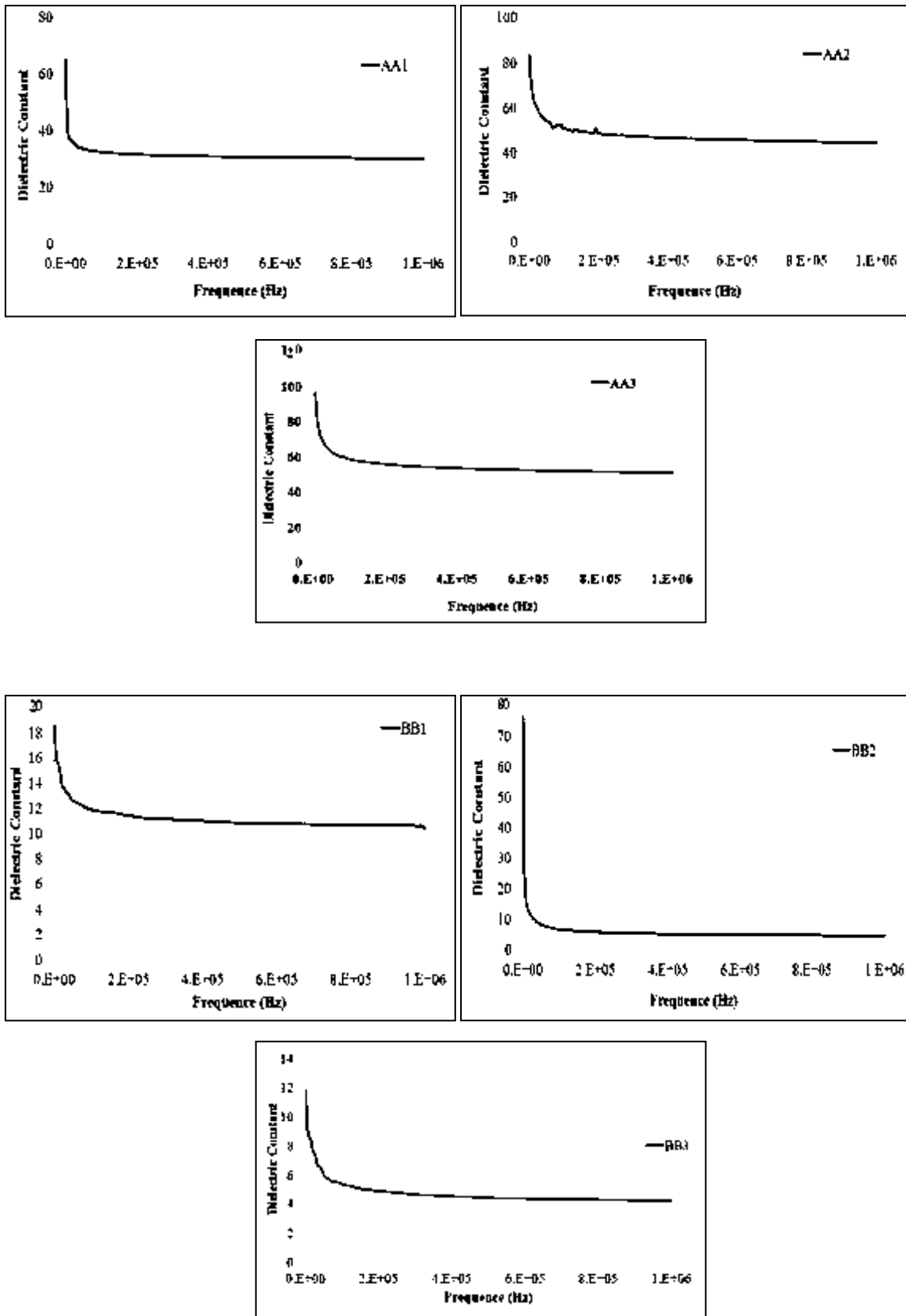


Fig. (4.20) (ϵ_r') for AA1, AA2, AA3, BB1, BB2 & BB3 specimens.

4.3.2 Dielectric loss factor (ϵ_r'')

In an insulator, the dielectric loss factor (ϵ_r'') is proportional to the power dissipation. So, it is a source of great concern for many applications of ceramic materials. The results of (ϵ_r'') are plotted in Figs. (4.23 and 4.24) as a function of applied frequency from (50-10⁶) Hz respectively for BaTiO₃ nominal composition, group AA and BB. The effect of (BaFe₁₂O₁₉ and Ni_{0.7}Zn_{0.3}Fe₂O₄) ratios to BaTiO₃ on the (ϵ_r'') values was investigated to determine the optimum ratios required to obtain the low (ϵ_r'') values for ceramics composites at groups BB1, (ϵ_r'') = 0.56609 at (1MHz), and this due to one of the main advantages of ceramics as dielectrics is that (ϵ_r'') is small compared with each materials [167]. The variation of the (ϵ_r'') values for samples compacted at (5.4)MPa compaction and treated at sintering temperature attribute to the decreasing and increasing the alternating electrical conductivity ($\sigma_{a.c}$), where (ϵ_r'') directly proportional to the ($\sigma_{a.c}$) as in Eqn. ($2\pi f \epsilon_r'' \epsilon_o$).

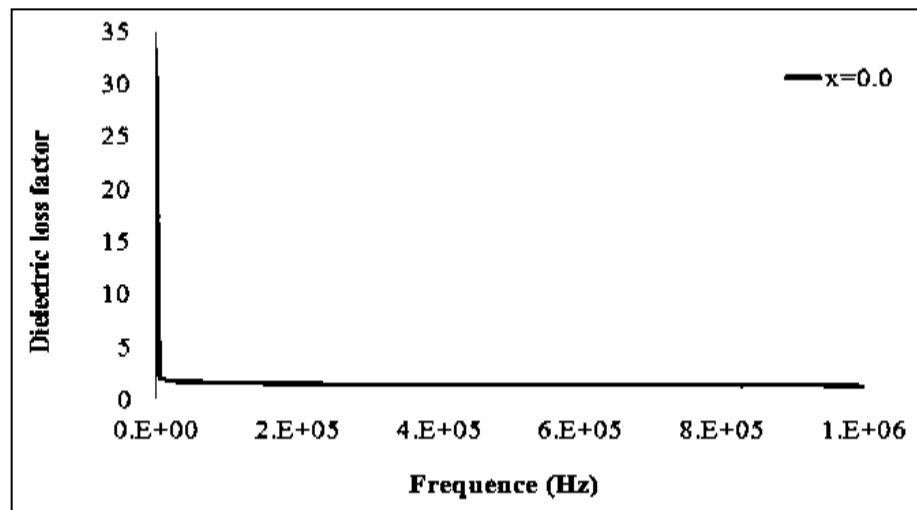


Fig. (4.21) Dielectric loss factor of the BaTiO₃ specimens.

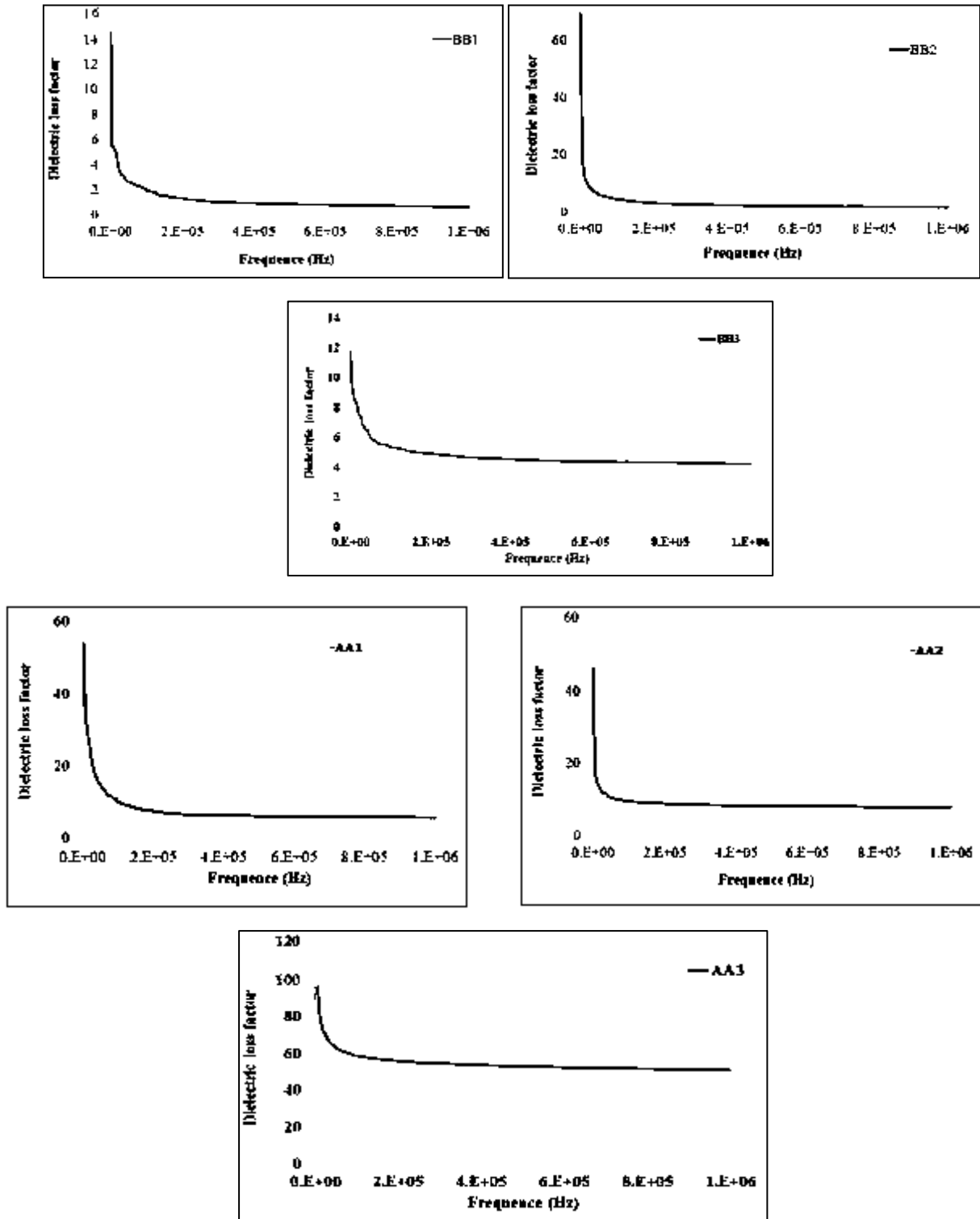


Fig. (4.22) Dielectric loss factor for AA1, AA2, AA3, BB1, BB2& BB3 specimens.

4.3.3 Tangent loss ($\tan\delta$)

The ($\tan\delta$), which is measured at (RT), is plotted as a function of frequency ($50\text{-}10^6$) Hz, for specimens as shown in Fig. (4.25 and 4.26), we noticed from the figures that, the loss tangent has a low value ($\tan\delta \leq 1$) for all specimens.

The shown figures exhibit that the maximum absorption energy values for (BaTiO_3)specimen decrease from 0.469 at $F=50\text{Hz}$ to 0.03028 at $F=1\text{MHz}$, then decreases to 0.06069 (for AA1 specimen at $F=1\text{MHz}$). The loss peak values at (1MHz) for AA2 sample increases to 0.1258, then decrease to 0.05473 at BB1 specimen and increases to 0.19647 for BB2 specimen compared with ($\tan\delta$) value, at (1MHz), for (BaTiO_3)specimen. The results of the (ϵ'_r), (ϵ''_r) and tangent at frequency (50 and 1M)Hz are compiled in [Table 4-17] for all specimens .

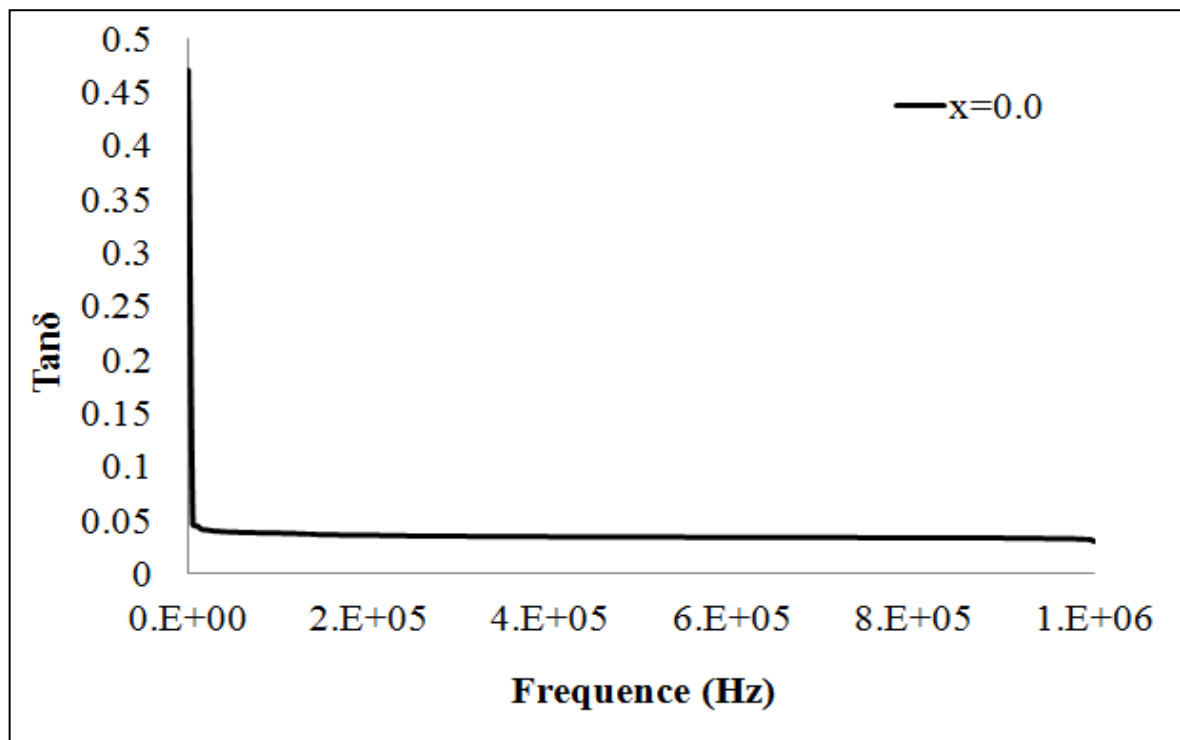


Fig. (4.23) $\tan\delta$ for BaTiO_3 specimen.

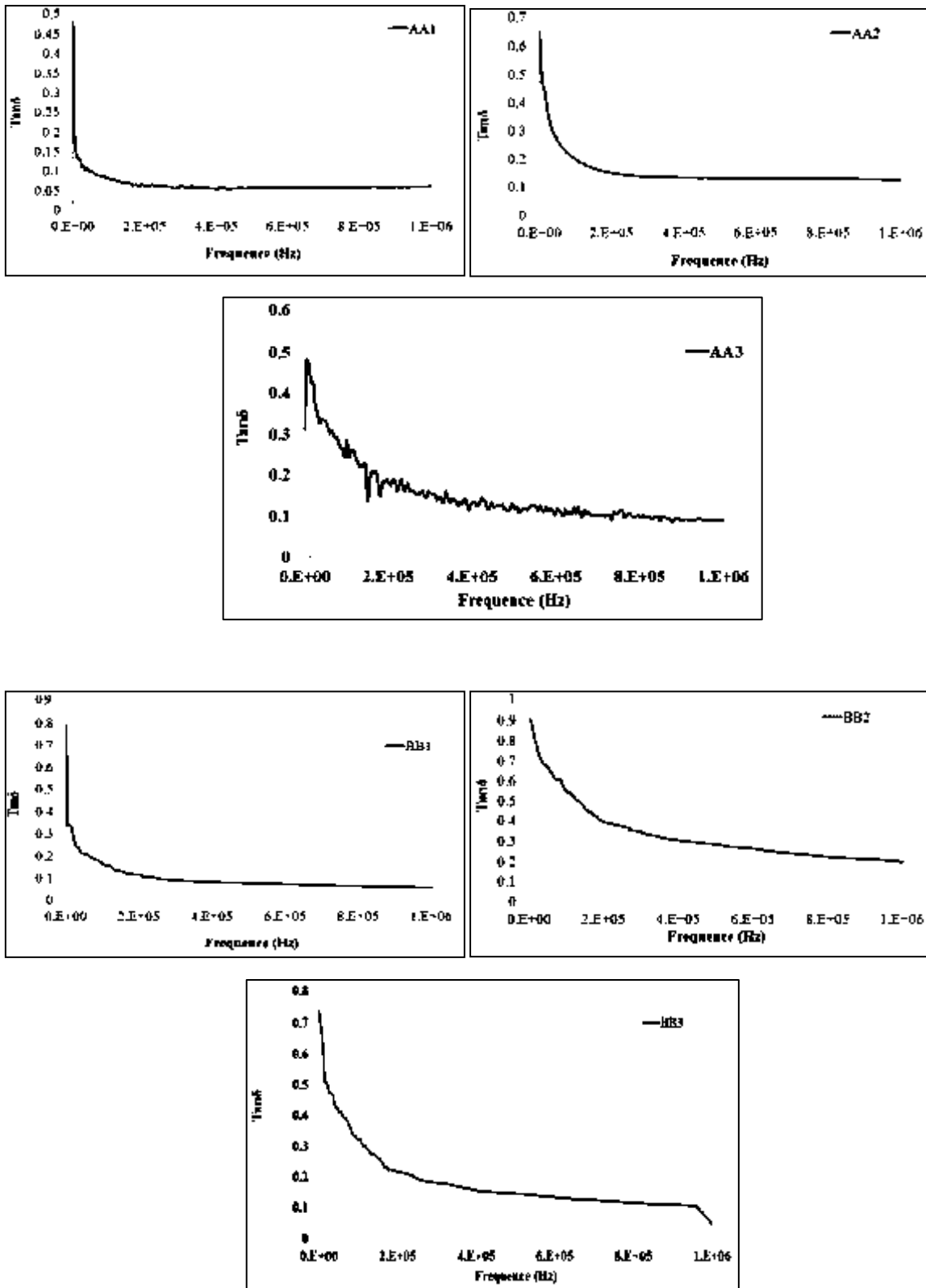


Fig. (4.24) $\tan\delta$ for AA1, AA2, AA3, BB1, BB2 & BB3 specimens.

Table (4-8): The (ϵ'_r) , (ϵ''_r) and $(\tan\delta)$ values at 50Hz and 1MHz for groups prepared at sintering temperature(1100°C), compaction(5.4 MPa) in room temperature

Samples	Dielectric constant (ϵ'_r) at		Dielectric loss factor (ϵ''_r) at		Tangent loss($\tan\delta$) at	
	50 Hz	1MHz	50 Hz	1MHz	50Hz	1MHz
BT	70.78	39.605	33.23	1.199262	0.469	0.03028
AA 1	64.9532	29.90132	30.85	1.81471	0.475	0.06069
AA 2	83.22725	44.11444	53.78228	5.549596	0.64621	0.1258
AA3	43.087	7.0384	13.452	0.6317	0.31222	0.0897
BB1	18.50124	7.83247	14.36	0.56609	0.7766	0.05473
BB 2	76.06546	4.486934	68.57	0.8815	0.901	0.19647
BB3	11.698	4.2123	8.6	0.19	0.735	0.0451

4.3.4 Alternating electrical conductivity ($\sigma_{a.c}$)

The results of the ($\sigma_{a.c}$) at room temperature for samples are plotted as a function of the applied frequency (50-10⁶) Hz, and defined by the Figs. (4.27 and 4.28).

We note from the figures that ($\sigma_{a.c}$) increases with the F (Hz). Increasing in Alternating electrical conductivity with the applied frequency, due to the direct relationship between ($\sigma_{a.c}$) and frequency ($\sigma_{a.c} = 2\pi f \epsilon''_r \epsilon_o$), and as a result of charge carriers polarization. As it is clear in the table, at 50Hz that the lower $\sigma_{a.c}$ results for all samples are ($1.30 \times 10^{-9} (\Omega.cm)^{-1}$) for BaTiO₃ sample than with(AA and BB) groups, while the higher ($\sigma_{a.c}$) values are ($3.08 \times 10^{-4} (\Omega.cm)^{-1}$) for sample AA2 at 1MHz compared with BaTiO₃, AA1, BB1, BB2 samples, this refers to the decrease in the vacancies concentration, which change in

composition in grain boundaries and crystal structure which has an effect on dielectrically properties .

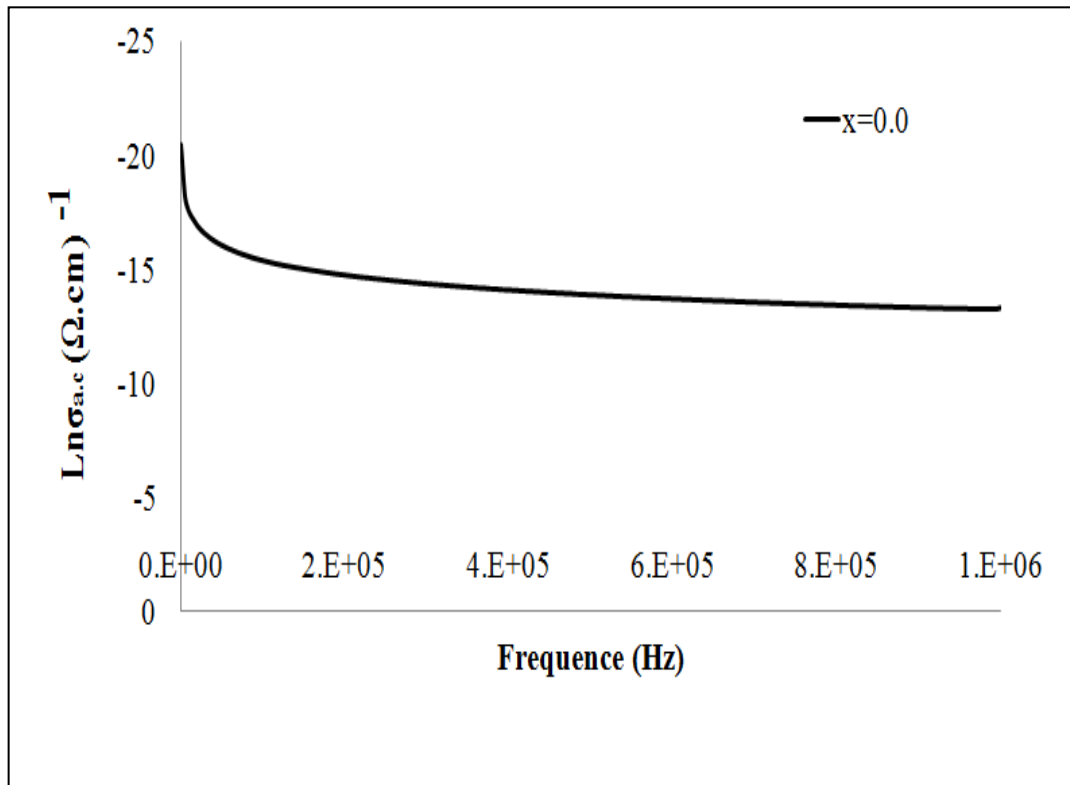


Fig. (4.25) $\sigma_{a.c}$ for BaTiO₃specimens.

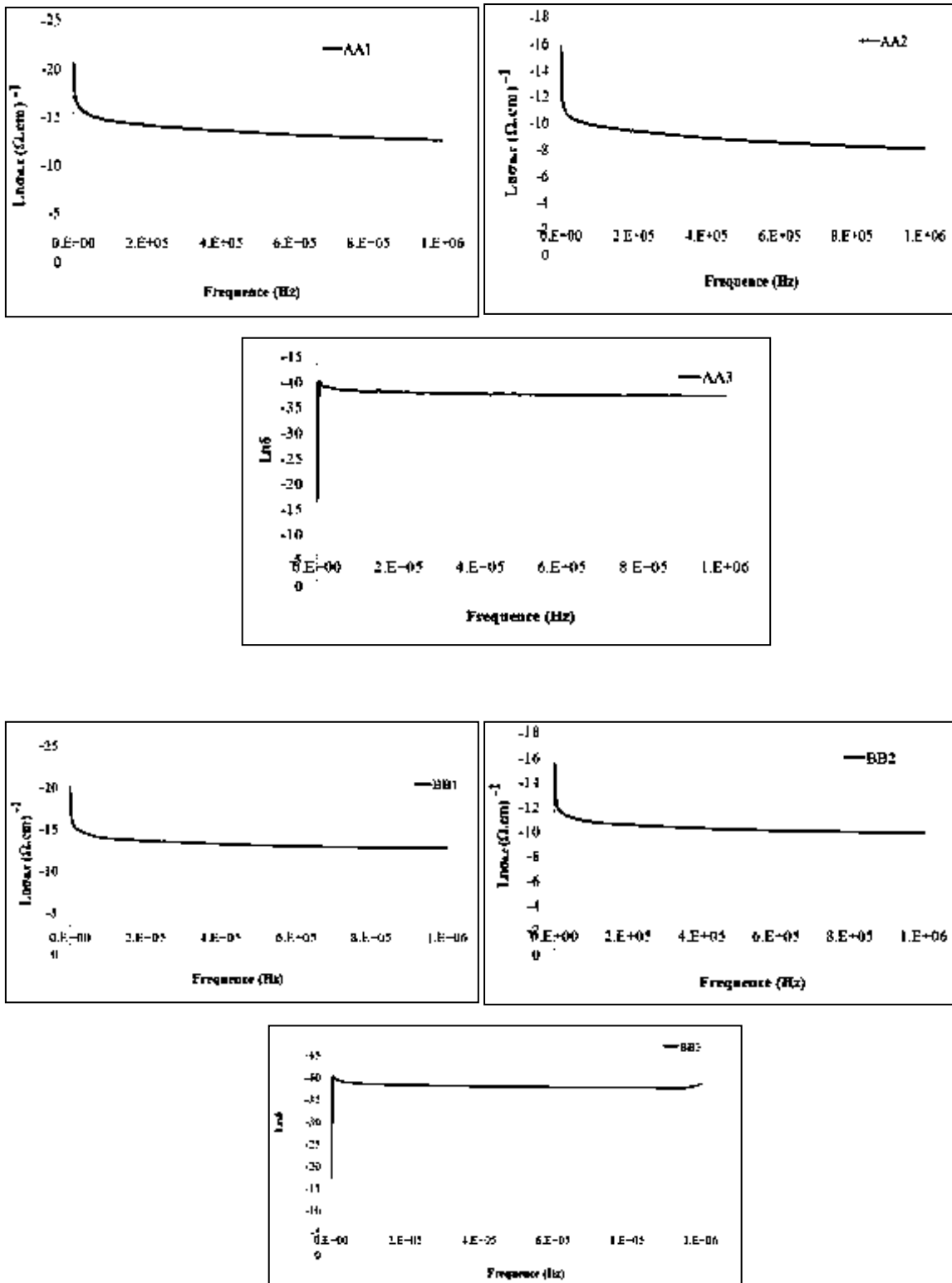


Fig. (4.26) σ_{ac} for AA1, AA2, BB1 & BB2 specimens

Table (4-9): The ($\sigma_{a.c}$) values at 50Hz and 1MHz for groups prepared at sintering temperature(1100°C), compaction(5.4 MPa) in room temperature

Samples	Alternating electrical conductivity ($\sigma_{a.c}$) ($\Omega.cm$) ⁻¹	
	50 Hz	1MHz
BT	92.342*10 ⁻⁹	6663.8*10 ⁻⁶
AA 1	85.729*10 ⁻⁹	10081.8*10 ⁻⁶
AA2	1.494*10 ⁻⁷	30840.2*10 ⁻⁶
AA3	3.738*10 ⁻⁸	3506.9*10 ⁻⁶
BB 1	39.905*10 ⁻⁹	3145.7*10 ⁻⁶
BB 2	1.905*10 ⁻⁷	4896.4*10 ⁻⁶
BB3	2.389*10 ⁻⁹	1055.9*10 ⁻⁶

4.3.5 Dielectric strength.

The break down voltage values of the prepared specimens is found to be in the range of (11.5 to 25.4) KV, as shown in figure (4.29). The break down voltage of the BaTiO₃ specimen is higher than the all specimens of (AA and BB)The decreasing in the dielectric strength values for samples referred to the porosity and ($\sigma_{a.c}$) values, where the increasing of porosity and electrical conductivity ($\sigma_{a.c}$) which leads to the decreasing of the dielectric strength [168]. This behavior was cleared in groups (AA and BB). Fig. (4.30) exhibits that the dielectric strength values for AA 1 and AA 2 samples decreases from (2.123 to 1.340) KV/mm and from (2.909 to 1.977)KV/mm for sample BB1 and BB2 than with dielectric strength value for BaTiO₃ specimen (3.476KV/mm), also Fig. (4-30) shows that AA groups has the lower dielectric strength values than BB groups due to the formation of porous structure.

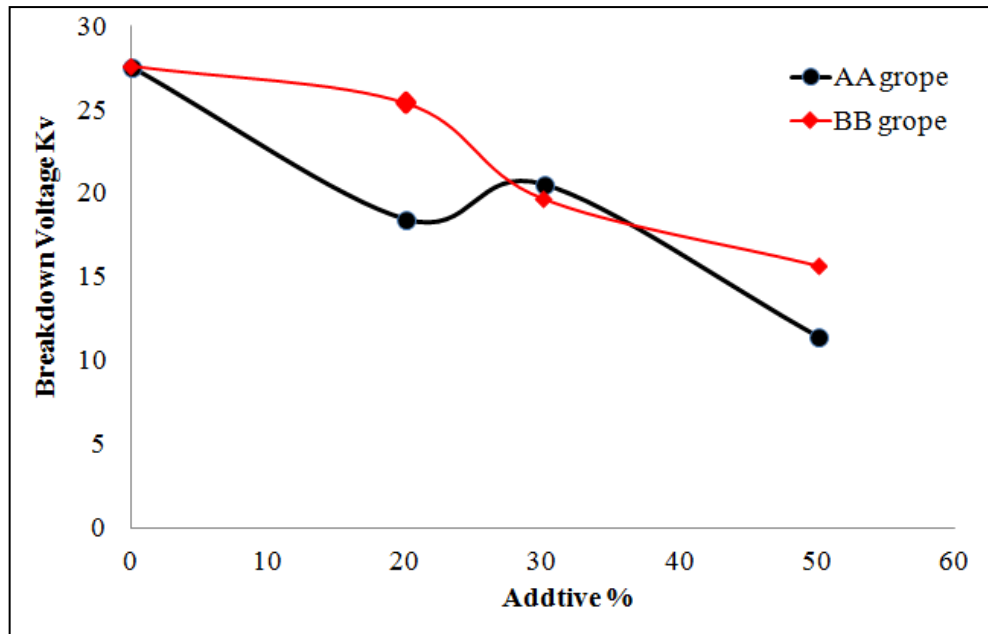


Fig. (4.27) Break down voltage for all specimens.

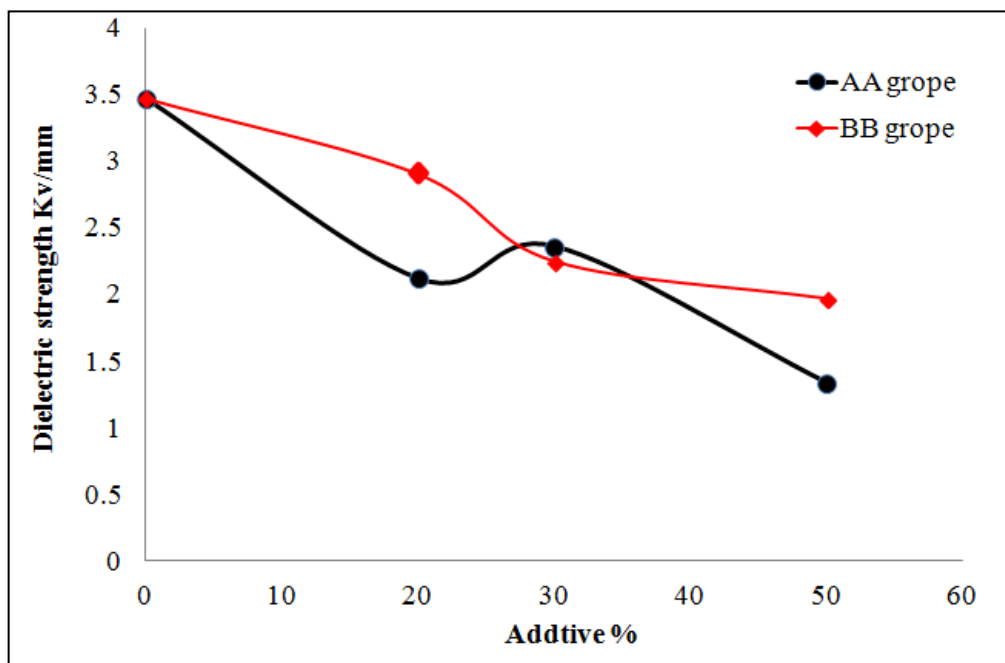


Fig. (4.28) Dielectric strength for all specimens.

Table (4-10): The Dielectric strength and breakdown voltage values for groups prepared at sintering temperature (1100°C), compaction(5.4 MPa) in room temperature

Samples	Breakdown voltage(KV)	Dielectric strength(KV/mm)
BaTiO₃	27.6	3.476071
AA 1	18.5	2.176470
AA2	11.5	1.352941
AA3	15.7	1.847058
BB 1	25.4	2.988235
BB 2	15.7	1.847058
BB3	11.5	1.352941

Chapter five
Conclusion,
References
and Future
work

Conclusions

1. The X-ray diffraction analysis of the (BaTiO₃),(BaF₁₂O₁₉), (Ni_{0.7} Zn_{0.3} Fe₂O₄) Nano-powder samples have shown a tetragonal crystal structure, and there is no other phases.
2. The microstructure shows granules with nearly spherical shape microstructure, with a conglomerate of granules for compounds (BaTiO₃),(BaF₁₂O₁₉),(Ni_{0.7} Zn_{0.3} Fe₂O₄) Nano-powder samples, as detect in the examination (EDX), also with the existance of all the elements of nanoparticles compounds in the samples examined.
3. The crystallized composite samples compacted to 5.4 MPa and fired at 1100°C, the dielectric constant at low frequency (50Hz) is increases with the increases of ratios(20and50) % for AA groups, while BB groups decrease and increases in the (ϵ'_r) values with the increases of ratios (20%and50%). The (ϵ'_r) values at 1MHz for (AA1,AA2) and (BB1, BB2) specimens', decrease from(64.9532, 83.22725) and (18.50124, 76.06546) to (29.90132, 44.11444)and (7.83247, 4.48693) respectively, the samples possess high dielectric constant especially AA composite groups of which to available use them as dielectrically materials
4. For the composites samples, the $\sigma_{a.c}$ has smaller values than that of the BaTiO₃sample, due to the porosity.
5. The results of the measurement of dielectric strength showthat the break down voltage of the BaTiO₃ specimen is higher than the all specimens of (AA and BB) . The decreasing in the dielectric strength values for samples referred to the ($\sigma_{a.c}$) values, and vice versa.
6. The best result is in the weight % of
(50% BaTiO₃ + 50% BaFe₁₂O₁₉, 50% BaTiO₃ + 50% Ni_{0.7} Zn_{0.3} Fe₂ O₄)

Future Work

- 1- Study the magnetic properties of the (BaTiO₃/BaF₁₂O₁₉) and (BaTiO₃/Ni_{0.7} Zn_{0.3} Fe₂O₄) composites such as the hysteric ring.
- 2- Study the electrical and magnetic properties of the (Ba_{1-x} Ca_x TiO₃/BaF₁₂O₁₉) and (Ba_{1-x} Ca_x TiO₃/Ni_{0.7} Zn_{0.3} Fe₂O₄) Nano composites and its applications.
- 3- Study the properties of the (Ba_{1-x} Sr_x TiO₃/BaF₁₂O₁₉) and (Ba_{1-x} Sr_x TiO₃/Ni_{0.7} Zn_{0.3} Fe₂O₄) Nano composites and its applications.

References

1. D. Makovec, Z. Samadmija and M. Drofenik, *J. Am. Ceram. Soc.* 87, 1324 (2004).
2. D. Maga, P. Igor and M. Sergei, *J. Mater. Chem.* 10, 941 (2000).
3. A. Jana, T. K. Kundu, S. K. pradhan and D. Chakravorty, *J. Appl. Phys.* 97 (4), 44311 (2005).
4. Z. Jin, C. Ang and Z. Yu, *J. Am. Ceram. Soc.* 82(5) 1345 (1999).
5. P. Yongping, Y. Wenhui and C. Shoutian, *J. Rare Earths.* 25, 154 (2005).
6. J. Smit, H.P.J. Wijn. *Ferrites*, Philips Technical Library, Eindhoven, (1959).
7. V.G. Harris, A. Geiler, Y. Chen, et al. Recent advances in processing and applications of microwave ferrites, *J. of Magnetism and Magnetic Materials*, 321(14) 2035–2047, (2009).
8. Y. Qu, H. Yang, N. Yang, et al. The effect of reaction temperature on the particle size, structure and magnetic properties of co-precipitated CoFe_2O_4 nanoparticles, *Materials Letters*, 60(29–30) 3548–3552,(2006).
9. N. Kasapoglu, B. Birsoz, A. Baykal, Y. Koseoglu, M.S. Toprak, Synthesis and magnetic properties of octahedral ferrite $\text{Ni}_x\text{Co}_{1-x}\text{Fe}_2\text{O}_4$ nanocrystals. *Central European J. of Chemistry*, 5(2) 570– 580,(2007).
- 10.S.W. Cao, Y.J. Zhu, G.F. Cheng, et al, ZnFe_2O_4 nanoparticles: microwave-hydrothermal ionic liquid synthesis and photocatalytic property over phenol, *J. of Hazardous Materials*, 171 (1–3) 431–435,(2009).
- 11.Y.L. Liu, Z.M. Liu, Y. Yang, et.al, Simple synthesis of MgFe_2O_4 nanoparticles as gas sensing materials. *Sensors and Actuators B: Chemical*, 107(2) 600–604,(2005).
- 12.H. Igarash, K. Okazaki, Effects of porosity and grain size on the magnetic properties of NiZn ferrites, *J. Am. Ceram. Soc.* 60 51-54,(1977).
13. K. Kulikowski, *Soft magnetic ferrites — Development or stagnation*, *J. Magn.Magn.Mater.* 41 56-62,(1984).

14. P. Ravindranathan, K.C. Patil, Novel solid solution precursor method for the preparation of ultrafine Ni-Zn ferrites, *J. Mater. Sci*, 22 3261-3264,(1987).
15. T. Abraham, Economics of ceramic magnets, *Am. Ceram. Soc. Bull.* 73 62-65,(1994).
16. P.I. Slick, in *Ferromagnetic Materials*, 2, ed. by E.P. Wohlforth North-Holland, Amsterdam, 196. , (1980).
17. B.V. Bhise, M.B. Dongare, S.A. Patil, S.R. Sawant, X-ray infrared and magnetization studies on Mn substituted Ni-Zn ferrites, *J. Mater. Sci. Lett.* 10 922-924,(1991).
18. Werner Känzig. "Ferroelectrics and Antiferroelectrics". In Frederick Seitz, T. P. Das, David Turnbull, E. L. Hahn. *Solid State Physics* 4. Academic Press.. 5. ISBN 0-12-607704-5,(1957).
19. M. Lines & A. Glass. *Principles and applications of ferroelectrics and related materials*. Clarendon Press, Oxford. ISBN 0-19-851286-4,(1979).
20. Chiang, Y. et al.: *Physical Ceramics*, John Wiley & Sons 1997, New York
Safari, Ahmad. Piezoelectric and acoustic materials for transducer applications. Springer Science & Business Media.p. 21. ISBN 0387765409,(2008)
21. M. Feder , "Microstructure and properties of Ni-Zn-Cu ferrite sintered at different temperature ", *Analele stiintifice Ale universitatii* ,(68),98-103,(2002).
22. R. V. Mangalaraja , "Magnetic ,Electrical and dielectric behavior of Ni_{0.8} Zn_{0.2} Fe₂O₄ prepared through flash combustion technique" *J. of Magnetism and Material* ,(253),56-64,(2002).
23. Kh. Khasawinaha, Y. A. Hamama, A. El Ali (AL- Dairy) and A. Rousanb, "Magnetic Properties of Barium Titanate – Barium Ferrite Composites, 1(2). 97-102,(2008).

- 24.**Liu Junliang, Zhang Wei, GuoCuijing, ZengYanwei,"Synthesis and magnetic properties of quasi-single domain M-type bariumhexaferrite powders via sol-gel auto-combustion: Effects of pH andthe ratio of citric acid to metal ions (CA/M)",*J. of Alloys and Compounds* 479 , 863–869,(2009).
- 25.**Mojtaba Nasr-EsfahaniandAzaliaAzlegini , "The Effect of Citric Acid and Ethylene Glycol Mole Ratios on theMicrostructure and Magnetic Properties of Z-Type Hexagonal FerriteNano Powder Prepared by Sol-Gel Method", 25 ,(2011).
- 26.**M. A. Ahmed,U. Seddik², N. G. Imam² , "First-Order Studies of NanometricBiferroic ",*World J. of Condensed Matter Physics*, 2, 66-74, (2012) .
- 27.**Ke Yu, Hong Wang, Yongcun Zhou, YuanyuanBai, and YujuanNiu,"Enhanced dielectric properties of BaTiO₃/poly(vinylidene fluoride)nanocomposites for energy storage applications", *J. Appl. Phys.* 113, 034105,(2013).
- 28.**H. Avila, L. A. Ramajo, M. S. Góes, M. M. Reboredo, M. S. Castro,and R. Parra, "Dielectric Behavior of Epoxy/BaTiO₃ Composites Using Nanostructured Ceramic Fibers Obtained by Electrospinning", *ACS Appl.Mater. Interfaces*, 5, 505–510,(2013).
- 29.** F. Bilge EMRE, Funda SAYILKAN, Can aÝM^aEK , "SYNTHESIS AND CHARACTERIZATION OF NANO-BaTiO₃ POWDER BY A HYDROTHERMALMETHOD", *International J. of Latest Research in Science and Technology ISSN (Online):2278-5299* , 3(3) , , 190-193,(2014).
- 30.**S.M.Ali Ridha , Mujahid , "Synthesis and study the dielectric properties of La-Doped Barium Titanate Nano powders ",*Eng& Tech J. Part (B)*, 33(2),(2015).
- 31.**A.S. Dzunuzovic, M.M. Vijatovic Petrovic¹, B.S. Stojadinovic² , N.I. Ilic ¹, J. D. Bobic¹ , C.R. Foschini³, M.A.Zaghet⁴, B.D. Stojanovic¹,"Multiferroic

- (NiZn) Fe₂O₄ - BaTiO₃ composites prepared fromnanopowders by auto-combustion method", (2015).
32. Aparna.A.R.a, Brahmajirao.Vb, & Kartikeyan.T.V, "Titanium doped barium ferrite powders (BaFe_(12-x)Ti_x O₁₉), prepared using sol gel method and characterised using XRD, SEM and FTIR techniques", IOSR J. of Electronics and Communication Engineering, p- ISSN: 2278-8735, 11(2), 06-11, (2016).
33. د. الراوي، صبحي سعيد، د. شاكر جابر شاكر، د. يوسف مولود حسن، "فيزياء الحالة الصلبة"، جامعة الموصل، (1988).
34. J.C. Anderson, "Dielectrics", Chapman and Hall LTD, London, (39-48, 121-149), (1964).
35. D. Halliday, R. Resnick, "Fundamentals of physics", John wiley and sons, Inc, NEW YORK, (489-499), (1974).
36. B. Tareev, "Physics of dielectric materials", Mir publishers, Moscow (101-145, 174-202), (1979).
37. احمد زيدان، شهاب، "تحضير العوازل الكهربائية من الكاولين العراقي"، رسالة ماجستير، جامعة بغداد، (1995).
38. J.R. Reitz, "Foundation of electromagnetic theory", 3rd ed, Addison-Wesely, pub-com. Inc, U.S.A, (75-113), (1979).
39. K.J. Pascoe, "Properties of materials for electrical engineers", John wiley and sons, London, (173-194), (1974).
40. L. H. Van Vlack, "Elements of materials Science and engineering", Fifth edition, Addison-Wesley, (1987).
41. W, D, Kingery, "Introduction to ceramics", John willy and sons, Newyork. (1-50, 155, 109, 448-507), (1976).
42. William D Callister Jr, "Materials Science and engineering An Introduction", Fifth edition, John Wiely & Sons, (2000).
43. J. Stanek, "Electric melting of glass", Elsevier Scientific Comp, LTD, Amsterdam, (28-31), (1977).
44. Jalle, "An outline of polymer chemistry", Oliver and Boyed, Ltd, (1974).
-

45. M.C. Lovell, A.J. Aery, and M.W. Vernon, "Physical properties of materials", New York (1976).
46. R.A. Levy, "Principle of solid state physics", 4th edition, Academic press (1976).
47. H. Frohlich, "Theory of dielectrics", 1st edition, Oxford University Press. (1958).
48. S. Borowitz, and A. Beiser, "Essentials of Physics", 2nd edition, Addison-Wesley publishing Company, (1971).
49. H.P. Myers, "Introduction solid state physics", Taylor and Francis (1990).
50. L.H. Vanvick, "Elements of materials science and engineering", 5th edition, Addison-Wesley Publishing company, Inc. (1987).
51. J.S. Blackemore, "Solid state physics", 2nd edition, W.B. Saunders Company (1974).
52. M.C. Lovell, A.J. Aery, and M.W. Vernon, "Physical properties of materials", New York (1976).
53. B. Mats. Ph.D. Thesis, "University Service US.AB", Stockholm, Sweden, (2005).
54. C. Kittel. "Introduction to solid state physics:", 6th edition, John Wiley and Sons, Inc. (1986).
55. R. Pampuch "Ceramic materials, An introduction to their properties", Publishers, Warszawa, Poland by DRP (1976).
56. R.Pampuch, "Ceramic materials an introduction to their properties", Elsevier scientific pub.com, Amsterdam, (263-296), (1976).
57. G.K. Thompson, B.J. Evans, The structure–property relationships in M-type hexaferrites: hyperfine interactions and bulk magnetic properties, J. Appl. Phys. 73 6295–6297, (1993).
58. M. Pardavi-Horvath, Microwave applications of soft ferrites, J. Magn. Mater. 171 215–216, (2000).
59. M. Fiebig, J. Phys. D: Appl. Phys. **38**, R123, (2005).

- 60.** L. Mitoseriu, V. Buscaglia, M. Viviani, M. T. Buscaglia, I. Pallecchi, C. Harnagea, A. Testino, V. Trefiletti, P. Nanni and A. S. Siri, *Journal of the European Ceramic Society*, **27**, 13-15 4379, (2007).
- 61.** G. Srinivasan, E. T. Rasmussen and R. Hayes, *Phys. Rev. B* **67**, 014418, (2003).
- 62.** Z. Yu and C. Ang, *J. Appl. Phys.* **91**, 794, (2002).
- 63.** X. Qi, J. Zhou, Z. Yue, Z. Gui, L. Li and S. Buddhudu, *Adv. Funct. Mater.* **9**, 920, (2004).
- 64.** R. Lebourgeois, J. Ageron, H. Vincent and J.P. Ganne, *Proceedings ICF-8, Kyoto and Tokyo*, 576, (2000).
- 65.** L. A. Dobrzanski, *Fundamentals of Materials Science and Physical Metallurgy* (in Polish), (WNT, Warsaw, 2002).
- 66.** K. H. Lachowicz, *Electrotechnical Review* **11**. (in Polish), (2002).
- 67.** M. Leonowicz, *Modern Hard Magnetic Materials* (in Polish), (Warsaw University of Technology, 1996).
- 68.** L.K. Templeton and J.A. Pask, *J. Am. Ceram. Soc.*, (42), 212, (**1959**).
- 69.** P. Hansen, D. Hennings, and H. Schreinemacher, *J. Am. Ceram. Soc.*, 81(5), 1369, (**1998**).
- 70.** D.F.K. Hennings, B.S. Schreinemacher, and H. Schreinemacher, *J. Am. Ceram. Soc.*, 84(12), 2777, (**2001**).
- 71.** M. Stockenhuber, H. Mayer, and J.A. Lercher, *J. Am. Ceram. Soc.*, 76(5), 1185, (**1993**).
- 72.** M.S.H. Chu and J. Bultitude, in *Dielectric Ceramics: Processing, Properties and Applications*, edited by K.M. Nair, J.P. Guha, and A. Okamoto The American Ceramic Society, Westerville, Ohio, 69, (**1993**).
- 73.** N. Kikuchi and T. Ogasawara, in *Dielectric Ceramics: Processing, Properties and Applications*, edited by K.M. Nair, J.P. Guha, and A. Okamoto (The American Ceramic Society, Westerville, Ohio, 191, (**1993**).

74. . K. Fukai, K. Hikada, M. Aoki, and K. Abe, *Ceram. Int.*, 16 (1990) 285.
75. M. Wu, J. Long, G. Wang, A. Huang, and Y. Luo, *J. Am. Ceram. Soc.*, 82(11), 3254,(1999).
76. M.P. Pechini, *U. S. Pat.* ,3 330 697, July 11 (1967).
- 77.F. Jona, G. Shirane, *Ferroelectric crystals*, Dover Publications, INC., New York, (1993) .
- 78.G.H. Haertling, *J. Am. Ceram. Soc.*, 82 797,(1999).
79. F.M. Filho, *FerroeletricidadeemCerâmicasPolicristalinas (perovskitas) ABO_3* , Seminario, Araraquara, (private communication), (2006).
- 80.R.C. Buchanan, *Ceramic Materials for Electronics*, University of Illinois at Urbana-Champaign, Urbana, Illinois , (2007).
- 81.Z. Lazarevic, B.D. Stojanovic, J.A. Varela, *Sci. Sintering*, 37 199,(2005).
- 82.P. Duran, D. Gutierrez, J. Tartaj, C. Moure, *Ceram. Int.* 28 283,(2002).
- 83.www.wikipedia.org
- 84.www.3dchem.com/inorganicmolecule.asp?id=1618
- 85.W.-S. Cho, *J. Phys. Chem. Solids* 59 659,(1998).
86. A. Koelzynski, K. Tkacz-Smiech, *Ferroelectrics*, 314 123,(2005).
- 87.B.I. Lee, M. Wang, D. Yoon, M. Hu, *J. Ceram. Proc. Research*, 4 17,(2003).
- 88.V. Vinothini, P. Singh, *Ceram. Int.* 32 99,(2006).
89. M. Boulos, S. Guillemet-Fritsch, F. Mathieu, B. Durand, T. Lebey, V. Bley, *Solid State Ionics* 176 1301,(2005).
- 90.H.S. Potdar, S.B. Deshpande, S.K. Date, *Mater. Chem. Phys.* 58 121,(1999).
91. L. Simon-Seveyrat, A. Hajjaji, Y. Emziane, B. Guiffard, D. Guyomar, *Ceram. Int.* 33 35,(2007).
- 92.H. Xu, L. Gao, *J. Am. Ceram. Soc.*, 86 203,(2003).
- 93.L. Wang, L. Liu, D. Xue, H. Kang, C. Liu, *J. Alloys Comp.* 440 78,(2007).
- 94.W.-S. Cho, E. Hamada, *J. Alloys Comp.* 266 118,(1998).
95. F. Guangneng, H. Lixia, H. Xueguang, *J. Cryst. Growth* 279 489,(2005).

96. W. Sun, J. Li, *Materials Letters* 60 1599,(2006).
97. S.-F. Liu, I. Robin Abothu, S. Komarneni, *Materials Letters* 38 344,(1999).
98. A.V. Prasadarao, M. Suresh, S. Komarneni, *Materials Letters* 39 359,(1999).
99. B.D. Stojanovic, *Ferroelectric Perovskite Materials: Barium Titanate Systems with PTCR behaviour*, Report CNPQ, Araraquara, , (private communication), (2000) .
100. Kumar, M.M., Palkar, V.R., Srinivas,K. and Suryanarayana, S.V., *J.Appl.Phys. Lett.*, 76 2764,(2000).
101. Matsui, T., Tanaka, H., Fujimura, N.,Ito, T., Mabuchi, H. and Morii, J.K.,*Appl. Phys. Lett.*, 81 2764,(2002).
102. Suryanarayana, S.V., *Bull. Mater. Sci.*,17 1259,(1994).
103. Gehring, G.A., *Ferroelectrics*, 161 275,(1994).
104. Siratori, K., Kohn, K. and Kita, E.,*Acta Phys. Pol. A*, 81 431,(1992).
105. Kashlinskii, A.I., Chechernikov, V.I.andVenvtsev, Yu.N., *Sov. Phys. SolidState*, 8 2074,(1976).
106. F. Soofivand, F. Mohandes, M. Salavati-Niasari, Silver chromate and silver dichromate nanostructures: sonochemical synthesis, characterization, and photocatalytic properties, *Mater. Res. Bull.* 48 2084–2094,(2013).
107. F. Motahari, M.R. Mozdianfard, F. Soofivand, M. Salavati-Niasari, NiO nanostructures: synthesis, characterization and photocatalyst application in dye pollution wastewater treatment, *RSC Adv.* 4 27654–27660,(2014).
108. A.R. Armstrong, P.G. Bruce, Synthesis of layered LiMnO₂ as an electrode for rechargeable lithium batteries, *Nature* 381 499–500,(1996).
109. M. Yousefi, F. Gholamian, D. Ghanbari, M. Salavati-Niasari, Polymeric nanocomposite materials: preparation and characterization of star-shaped PbSnanocrystals and their influence on the thermal stability of acrylonitrile–butadiene–styrene (ABS) copolymer, *Polyhedron* 30 1055–1060,(2011).

- 110.** G.K. Thompson, B.J. Evans, The structure–property relationships in M-type hexaferrites: hyperfine interactions and bulk magnetic properties, *J. Appl. Phys.* **73** 6295–6297,(1993).
- 111.** M. Pardavi-Horvath, Microwave applications of soft ferrites, *J. Magn. Mater.* **171** 215–216,(2000).
- 112.** T. G. Reynolds III, Ferrite Magnetic Ceramic,in: *Ceramics Materials for Electronics*, Ed. R.C. Buchanan (Marcel Dekker, Inc., NY,(1988).
- 113.** R. Lebourgeois, J. Ageron, H. Vincent and J.P. Ganne, *Proceedings ICF-8*, Kyoto and Tokyo, **576**,(2000).
- 114.** Z. Wang, D. Schiferl, Y. Zhao and H. St. C.O'Neill, *J. Phys. Chem. of Solids*, **64**(12),2517, (2003).
- 115.** H. Schmid, *Ferroelectrics* **162**, 317 ,(1994).
- 116.** V. E. Wood and A. E. Austin, in:*Magnetoelectric Interaction Phenomena in Crystals*, Eds. A. J. Freeman and H. Schmid(Gordon and Breach, (1975).
- 117.** M. Fiebig, *J. Phys. D: Appl. Phys.* **38**, R123,(2005).
- 118.** L. Mitoseriu, V. Buscaglia, M. Viviani, M. T.Buscaglia, I. Pallecchi, C. Harnagea, A.Testino, V. Trefiletti, P. Nanni and A. S. Siri,J. of the European Ceramic Society, **27**,13-15 4379 ,(2007).
- 119.** G. Srinivasan, E. T. Rasmussen and R. Hayes,*Phys. Rev. B* **67**, 014418, (2003).
- 120.** Z. Yu and C. Ang, *J. Appl. Phys.* **91**, 794,(2002).
- 121.** X. Qi, J. Zhou, Z. Yue, Z. Gui, L. Li and S.Buddhudu, *Adv. Funct. Mater.* **9**, 920, (2004).
- 122.** L. A. Dobrzanski, *Fundamentals of Materials Science and Physical Metallurgy*. (in Polish), (WNT, Warsaw, 2002)
- 123.** K. H. Lachowicz, *Electrotechnical Review* **11**. (in Polish), (2002)
- 124.** M. Leonowicz, *Modern Hard Magnetic Materials*. (in Polish), (Warsaw University of Technology, 1996)

- 125.** J. Ding, W. F. Miao, P. G. McCormick and R. Street, *J. of Alloys and Compounds* **281**, 32, (1998).
- 126.** M. H. Makled, T. Matsui, H. Tsuda, H. Mabuchi and M. K. El- Mansy, *J. of Materials Processing Technology* **160**, 229 ,(2005).
- 127.** J. Qiu and M. Gu, *Applied Surface Science* **252**, 888, (2005).
- 128.** Silvaa, J., Britoa, W., Mohallem, N., Influence of heat treatment on cobalt ferrite ceramic powders. *Mater. Sci. Eng. B*, 112: 182–187,(2004).
- 129.** L. Nalbandian, A. Delimitis, V.T. Zaspalis, E.A. Deliyanni, D.N. Bakoyannakis, E.N. Peleka, , Hydrothermally prepared nanocrystallineMn–Zn ferrites: Synthesis and characterization. *Microp. Mesopor. Mat.*, 114: 465–473,(2008).
- 130.** Venkataraju, C., Sathishkumar, G., Sivakumar,K, Effect of cation distribution on the structural and magnetic properties of nickel substituted nanosizedMn– Zn ferrites prepared by co-precipitation method. *J. Magn. Mater.*, 322: 230–233, (2010).
- 131.** Heer, W.A., *Nanomagnetism characterization of nanophase materials.* Wiley-VCH,(2000).
- 132.** Nalwa, H.S., *Magnetic nanostructure.* American Cientific Publishers, USA, (chapter 1–4), (2002).
- 133.** Masala, O., Hoffman, D., Sundaram, N., Page, K., Proffen, T., Lawes, G., Seshadri, R, Preparation of magnetic spinel ferrite core/shell nanoparticles: Soft ferrites on hard ferrites and vice versa. *Solid State Sci.*, 8:1015., (2006).
- 134.** Tzeng S. S. , and Chang F. Y . , EM1 shielding effectiveness of metal-coated carbon fiber-reinforcedABS composites. *Materials Science andEngineering A*, 302(2) : 258, (2001).
- 135.** Zhong W., Jiang Y. M . , Zhang N . , et al.,Preparation and magnetic properties of bariumhexaferrite nanoparticles produced by the citrateprocess. *J. of the American Ceramic Society*, 80(12): 3258, (1997).

136. Pinho M. S., Gregori M. L., Nunes R. C. R. , et al . , Performance of radar absorbing materials by wave guide measurements for X- and Ku-band frequencies. *European Polymer J o m l*,38(11): 2321, (2002).
137. KimD.H., LeeS.H., KimK.N., e t a l . , Cytotoxicityoffemte particles by MTT and agar diffusionmethods for hyperthermic application .*J. of Magnetism and Magnetic Materials*. 293(1) : 287,(2005).
138. Guo R.Q., Chen Y. I . , and Gu M .Y., Synthesisand characterization of gadolinium doping Mtypehexagonal barium femteultratinepowders.*J. of Rare Earths*, 21(5) : 543, (2003).
139. Meshrama M.R., Agrawala N . K . , and SinhaB. , Characterization of M-type barium hexagonalfemte-based wide band microwave absorber.*Jownal of Magnetism and Magnetic Materials*, 271(2/3): 207,(2004).
140. Singh P. , Razdan A. , Srivastava S. L. , et al . , Microwave absorption studies of Ca-NiTi hexaferritecomposites in X-band. *Materials Science andEngineering B*, 78(2/3): 70, (2000).
141. Synthesis and characterization of nanocrystallineBaFe_{9.6} c_{0.8} Ti_{0.8} M_{0.8} O₁₉ particles. *MaterialsChemistry and Physics*, 64(3) : 256, (2000).
142. pullar R . C . , Appleton S. G . , and BhattacharyaA. K . , The manufacture, characterisationandmicrowave properties of aligned M ferrite fibres.*J. o m l of Magnetism and Magnetic Materials*, 186(3): 326,(1998).
143. Xu J . F . , Guo F.F., and Xu Z . , Synthesis andcharacterization of hexagonal Ba-femtenanocrysta.*Jownal of Tong Ji University (Natural Science)*, 320): 929,(2004).
144. Abo El Ata A.M., El NimrM.K., and El KonyD., Dielectric and magnetic permeability behaviorofBaCo_z - Ni,Fe₁₆ O₂₇ W-type hexafemtes.*Journal of Magnetism and Magnetic Materials*, u)4(1): 36,(1999).
145. Zuang H. J., Wu M.Z., and Yao X., Complexpermittivity, permeability, and microwave absorptionofbariumferrite by citrate sol-gel process.*Rare Metals*, 22(2): 125, (2003).

146. Kojima H. In: Wohlfarth EP, editor. Ferromagnetic materials. Amsterdam: North Holland;. 305,(1982).
147. Benito G, Morales MP, Requena J, Raposo V, Vazquez M, MoyaJS. J. MagnMagn Mater;234:65,(2001).
148. Stablin H. In: Wohlfarth EP, editor. Ferromagnetic materials. Amsterdam: North Holland;. 441,(1982).
149. Ataie A, Heshmati-Manesh S, Kazempour H. J Mater Sci;37:2125,(2002).
150. Liu X, Wang J, Gan LM, Ng SC. J. MagnMagn Mater;195:452,(1999).
151. Zhong W, Ding W, Zhang N, Hong J, Yan Q, Du Y. J. MagnMagn Mater;168:196,(1997).
152. Surig C, Hempel KA, Bonnenberg D. IEEE Trans Magn;30:4092,(1994).
153. Rezlescu L, Rezlescu E, Popar PD, Rezlescu N. J. MagnMagnMater;193:288,(1993).
154. Liu X, Wang J, Gan LM, Ng SC, Ding J. J. MagnMagn Mater;184:344,(1998).
155. Sankaranarayanan VK, Khan DC. J. MagnMagn Mater;153:337,(1996).
156. Chin TS, Hsu SL, Deng MC. J. MagnMagn Mater;120:64,(1993).
157. D.S.Su , "scan electron microscopy (SEM)", Max .planck .cesellschaft ,7_30 ,(2010).
158. T.Ferreira , "Image J user Guide",8-22,(2012).
159. M.Santiago , "Introduct to X-ray Differaction meter university of Puerto Rico ,24 -29 ,(2006).
160. "Solutions for measuring permittivity and permeability with LCR meter and Impedance Analyzer" ,Agilent Technolgies ,(2014).
161. سامر ، عبدالكاظم صبيح، "دراسة التاثيرات الكهروميكانيكية لانواع مختلفة م الزجاج" رسالة ماجستير، جامعة بغداد،(2010)م.
162. Intrenationl Center for Diffiraction Data-PCPDFWIN-ICDD .(1996).

- 163.** S. Wada, T. Suzuki, and T. Noma, "Preparation of Barium Titanate Fine Particles by Hydrothermal Method and Their Characterization," *J. Ceram. Soc. Jpn.*, 103 [12], 1220–1227,(1995).
- 164.** Kim Y -II, Jung JK, Ryu KS. "Structural study of nano BaTiO₃ powder by Rietveld refinement." *Mater Res Bull* ,39, 1045 -1053,(2004).
- 165.** B. D. Cullity and S. R. Stock, "Elements of X-Ray Diffraction", Prentice Hall,third edition, 170, (2001).
- 166.** Michael Tinkhan " Introduction to Superconductivity" Second Edition ,Harvard University ,(1996).
- 167.** w.d.kingery.h.k.bowen,andd.r.uhlmann,introduction to ceramic,2ndwileynewyork 197.
- 168.** B.tarrev,physics of dielectric material,mir publishes Moscow,translated from the Russian ,(1979).

الخلاصة

في عملنا هذا قمنا بتحضير مركب الباريوم تيتانيت ($BaTiO_3$) ومركب الباريوم فرايت ($BaFe_{12}O_{19}$) والنيكل زنك فرايت ($Ni_{0.7} Zn_{0.3} FeO_4$) ذات التراكيب النانوية وذلك بطريقة السول-جل للاحتراق التلقائي (sol-gel auto-comustion) وقد تم اخذ فحص (XRD) حيود الاشعة السينية لجميع المركبات المذكورة اعلاه من اجل الحصول على معلومات الشبيكة والتركيبة الهندسي والحجم البلوري وذلك باستعمال معادلة (شيرر) وتم حساب كثافة الاشعة السينية للعينات التي تم تحضيرها وذلك لتحسين الخواص الكهربائية للمركب الباريوم تيتانيت مع الباريوم فرايت ($BaTiO_3$ - $BaFe_{12}O_{19}$) بالاوزان الاتية

80% $BaTiO_3$ + 20% $BaFe_{12}O_{19}$, 70% $BaTiO_3$ + 30% $BaFe_{12}O_{19}$, 50%
 $BaTiO_3$ + 50% $BaFe_{12}O_{19}$.

ومركب النيكل زنك فرايت مع الباريوم فرايت مع الباريوم فرايت

$BaTiO_3$ + $Ni_{0.7} Zn_{0.3} Fe_2O_4$

بالاوزان الاتية

80% $BaTiO_3$ + 20% $Ni_{0.7} Zn_{0.3} Fe_2O_4$, 70% $BaTiO_3$ + 30% $Ni_{0.7} Zn_{0.3}$
 Fe_2O_4 , 50% $BaTiO_3$ + 50% $Ni_{0.7} Zn_{0.3} Fe_2O_4$.

حيث تم دراسة الخصائص الكهربائية باستخدام جهاز (LCR meter) واطافة لذلك قمنا باخذ الفحوصات (SEM , EDX and AFM) للمركبات الثلاث ($BaTiO_3$, $BaFe_{12}O_{19}$, $Ni_{0.7}$) ($Zn_{0.3} Fe_2O_4$) واستنتجنا بعد الفحص ان المركبات ذات حجم نانوي وضمن الحدود النانوية (20-30 nm)

وقمنا باخذ فحص انهيار الفولتية (breakdown V) ووجدنا بعد الاختيارات ان متانة العزل تتناقض مع الاضافات مقارنة مع الباريوم تيتانيت، واستنتجنا ايضا من هذا العمل ان افضل الخصائص الكهربائية تم الحصول عليها من المتراكبات

50% $BaTiO_3$ + 50% $BaFe_{12}O_{19}$, 50% $BaTiO_3$ + 50% $Ni_{0.7} Zn_{0.3} Fe_2O_4$



جمهورية العراق
وزارة التعليم العالي والبحث العلمي
جامعة بغداد
كلية التربية (ابن الهيثم)
للعلوم الصرفة / قسم الفيزياء

تحضير متراكبات باريوم تيتانيت النانوي $BaTiO_3$

ودراسة بعض خصائصها العزلية

رسالة تقدمت بها الطالبة

هالة حسين علي قاسم

(بكالوريوس علوم الفيزياء 2012)

الى قسم

الفيزياء / كلية التربية (ابن الهيثم) / جامعة بغداد

وهي جزء من متطلبات نيل درجة الماجستير في علوم الفيزياء

بإشراف

أ. م. د. فاروق ابراهيم حسين

أستاذ مساعد

٢٠١٧ هـ

١٤٣٩ هـ